Dynamics and Phenomenology of Scalar Field Dark Matter through the Higgs Portal

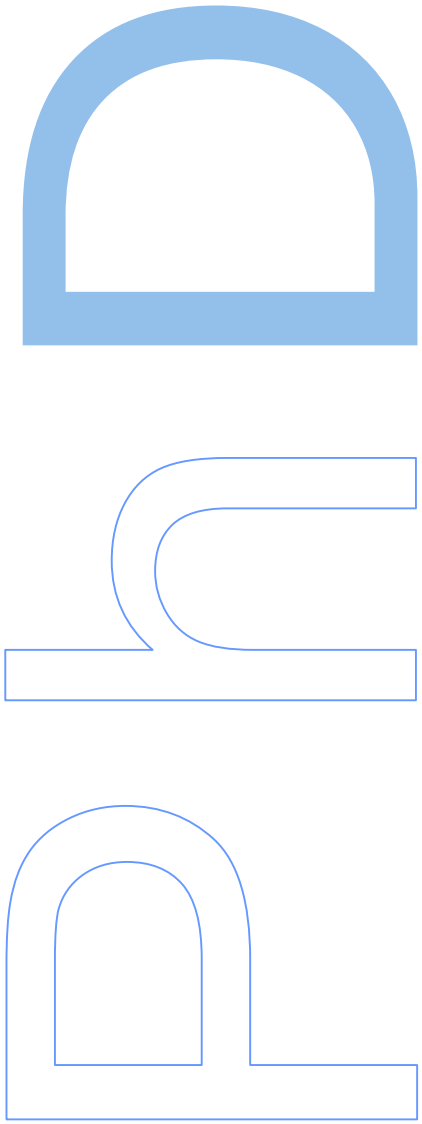

Catarina Martins Cosme
Programa Doutoral em Física
Departamento de Física e Astronomia
2018

Orientador
Orfeu Bertolami, Professor Catedrático, Faculdade de Ciências da Universidade do Porto

Coorientador
João G. Rosa, Investigador FCT, Universidade de Aveiro

This thesis is dedicated to
my parents, Quintino and Luísa, and my sister, Inês
for all their love and care;
and to my grandmother Nanda (1933-2012):
I wish you were here to celebrate this with me.

Para ser grande, sê inteiro: nada
Teu exagera ou exclui.
Sê todo em cada coisa.
Põe quanto és
No mínimo que fazes.
Assim em cada lago a lua toda
Brilha, porque alta vive.

Fernando Pessoa, in *Odes de Ricardo Reis*

Acknowledgements

First of all, my most sincere thanks to my supervisors: João Rosa and Orfeu Bertolami. I feel so fortunate for having enrolled a PhD in Physics under their guidance, and there are no words to express my gratitude to them for their support and infinite patience for my questions. Thank you for teaching me how to be a theoretical physicist, and for always motivating me to go further.

For financial support, I thank Fundação para a Ciência e Tecnologia for the research grants PD/BI/106012/2014 and PD/BD/114453/2016 and Centro de Física do Porto for other expenses, under the project UID/FIS/04650/2013.

I am grateful for the opportunity to work with great collaborators: Tommi Tenkanen, Nicolás Bernal and Ville Vaskonen. Thank you for the interesting and stimulating discussions we had together, from which I learned a lot.

All this work would not be possible without very good professors. I would like to thank all my PhD professors, in particular, Nuno Castro.

I must thank all my colleagues and administrative staff at the Department of Physics of the University of Porto, and my office mates: Artur Amorim, Cláudio Gomes, Daniel Passos, Emilio Trevisani, Gonçalo Ventura, Lauren Greenspan, Pedro Leal and, especially, Robert Carcassés, Paula Quitério, Niaz Ali Khan and André Guerra, who became my personal friends. Thank you for the great moments we have shared together.

A word of gratitude to Gr@V members of the University of Aveiro for their hospitality during my weekly visits to Aveiro. Thank you for making me feel welcome and for sharing interesting discussions with me.

A big thank you to all my friends but, especially, Ana, Ivo, Vasco, and Zé. I feel fortunate for having such amazing friends with whom I can share not only laughter and good moments, but also my worries and sorrows. Thank you for always being there for me.

Last but not least, a special word of gratitude to my parents, Quintino and Luísa, and to my sister, Inês, for supporting my choices, for hearing my grumbling when I was not satisfied with my work but, primarily, for their care and love. Thank you for reminding me everyday that life has many obstacles but, if we fight hard, we can overcome them. After all, what really matters is not giving up on our dreams.

Abstract

In this thesis, we discuss the dynamics and phenomenology of an oscillating scalar field coupled to the Higgs boson and which may account for the dark matter in the Universe.

First, we study the case where the field has negligible self-interactions. We argue that the initial field amplitude should generically be of the order of the Hubble parameter during inflation, as a result of its quasi-de Sitter fluctuations. This implies that such a field may account for the present dark matter abundance for masses in the range $10^{-6} - 10^{-4}$ eV, if the tensor-to-scalar ratio is within the range of planned Cosmic Microwave Background experiments. We show that such mass values can naturally be obtained through either Planck-suppressed non-renormalizable interactions with the Higgs boson or, alternatively, through renormalizable interactions within the Randall-Sundrum scenario.

Then, we consider the case where the field's potential has a quartic coupling accounting for the dark scalar self-interactions. The model assumes an underlying scale invariance such that the scalar field only acquires mass after the electroweak phase transition, behaving as dark radiation before the latter takes place. While for a positive coupling to the Higgs field the dark scalar is stable, for a negative coupling it acquires a vacuum expectation value after the electroweak phase transition and may decay into photon pairs, albeit with a mean lifetime much larger than the age of the Universe. We explore possible astrophysical and laboratory signatures of such a dark matter candidate in both cases and we find that dark matter within this scenario will be generically difficult to detect in the near future, except for the promising case of a 7 keV dark scalar decaying into photons, which may naturally explain the observed galactic and extra-galactic 3.5 keV X-ray line.

Finally, we study the case where an oscillating scalar field coupled to the Higgs field drives a non-thermal electroweak symmetry breaking. We show that this possibility may be achieved with a late inflaton decay and, consequently, an early-matter era. We find that the dark matter candidate within this scenario is heavier than the ones considered above, making it more likely to be detected in the laboratory.

Resumo

Nesta tese, discutimos a dinâmica e fenomenologia de um campo escalar a oscilar acoplado ao bosão de Higgs e que pode constituir toda a matéria escura no Universo.

Primeiramente, estudamos o caso em que o campo tem auto-interacções desprezáveis. A sua amplitude inicial é da ordem do parâmetro de Hubble durante a inflação, devido às suas flutuações quasi-de Sitter, o que implica que o campo pode explicar a abundância observável de matéria escura para massas na ordem dos $10^{-6} - 10^{-4}$ eV, se o rácio tensor-escalar não for muito suprimido. Além disso, mostramos que, embora estas massas sejam pequenas, podem ser naturalmente obtidas através de interacções não-renormalizáveis com o bosão de Higgs que sejam suprimidas pela escala de Planck ou através de interacções renormalizáveis no contexto do cenário de Randall-Sundrum.

Em seguida, consideramos o caso em que o potencial do campo de matéria escura tem uma interacção quártica, representando as auto-interacções do campo. O modelo assume uma invariância de escala subjacente tal que o campo apenas adquire massa após a transição electrofraca, comportando-se como radiação escura antes de a transição ocorrer. Enquanto que para um acoplamento positivo ao Higgs o campo de matéria escura é estável, para um acoplamento negativo o campo de matéria escura adquire um valor esperado no vácuo após a transição electrofraca e pode decair em pares de fotões, sendo o tempo de vida médio deste processo superior à idade do Universo. Assim, exploramos possíveis assinaturas astrofísicas e no laboratório que possam advir deste candidato a matéria escura, e constatamos que, embora a sua detecção num futuro próximo seja muito difícil, há um caso promissor: o decaimento do nosso candidato, com uma massa de 7 keV, em fotões, o que poderia explicar a linha de 3.5 keV, na gama dos raios-X, observada na nossa galáxia e em sistemas fora dela.

Finalmente, estudamos o caso em que o campo escalar a oscilar acoplado ao bosão de Higgs controla uma transição de fase electrofraca não térmica. Mostramos que esta possibilidade pode ser concretizada se o inflatão decair tardiamente, o que conduz a uma era de matéria logo após a inflação. Neste cenário, o candidato de matéria escura é mais pesado que os candidatos acima mencionados, o que o torna mais provável de ser detectado em laboratório.

List of included papers

This thesis is based on the following publications [1–4]:

- **Scalar field dark matter and the Higgs field**,
  Orfeu Bertolami, Catarina Cosme and João G. Rosa
  Phys. Lett. B **759** (2016) 1-8

- **Scalar field dark matter with spontaneous symmetry breaking and the 3.5 keV line**,
  Catarina Cosme, João G. Rosa and Orfeu Bertolami
  Phys. Lett. B **781** (2018) 639-644

- **Scale-invariant scalar field dark matter through the Higgs portal**
  Catarina Cosme, João G. Rosa and Orfeu Bertolami
  JHEP **05** (2018) 129

- **Can Dark Matter drive electroweak symmetry breaking?**
  Catarina Cosme, João G. Rosa and Orfeu Bertolami
  submitted to JHEP

In addition, during the course of my PhD studies, I have co-authored the following articles, which have not been included in the present thesis [5, 6]:

- **Phenomenology of Self-Interacting Dark Matter in a Matter-Dominated Universe**,
  Nicolás Bernal, Catarina Cosme and Tommi Tenkanen
  submitted to EPJ C

- **Scalar singlet dark matter in non-standard cosmologies**,
  Nicolás Bernal, Catarina Cosme, Tommi Tenkanen and Ville Vaskonen
  submitted to EPJ C

Contents

List of Figures

1 | Introduction

1.1 Motivation

The existence of a significantly undetected non-relativistic matter component in the Universe is widely accepted, with plenty of evidence arising from different sources. In particular, the flatness of the rotational curves of galaxies requires a significant dark matter component to account for the inferred dynamical galactic mass. In addition, the invisible mass of galaxy clusters and the temperature and polarization anisotropies of the Cosmic Microwave Background (CMB) radiation indicate a dark matter component that accounts for about 27% of the present energy balance in the Universe. The origin and the composition of dark matter remain, however, unknown, despite the large number of candidates that arise in theories beyond the Standard Model of Particle Physics (see e.g. Ref. [15] for a review).

Although a particle explanation seems to be favoured by observational data, as opposed to e.g. modified gravity theories, such putative new particles have so far evaded detection, with a wide range of masses and couplings to the Standard Model fields being still allowed. Weakly Interacting Massive Particles (WIMPs) are certainly the most popular dark matter candidates in the literature, corresponding to particles with masses typically within the GeV-TeV range that attained thermal equilibrium with the cosmic plasma in the early Universe and later decoupled to yield a frozen-out abundance. The so-called “WIMP miracle", where the relic WIMP abundance matches the present dark matter abundance for weak-scale cross sections, makes such scenarios quite appealing, with a plethora of candidates within extensions of the Standard Model at the TeV scale. However, the lack of experimental evidence for such WIMPs and, in particular, the absence of novel particles at the LHC, strongly motivates looking for alternative scenarios. Hence, in this work, we intend to provide an alternative to the WIMP paradigm.

An interesting candidate for dark matter is a dynamical homogeneous scalar field that is oscillating about the minimum of its (quadratic) potential, and which can be seen as a condensate of low-momentum particles acting coherently as non-relativistic matter. Scalar fields are ubiquitous in extensions of the Standard Model including, for instance, the QCD axion in the Peccei-Quinn scenario to address the strong CP problem, supersymmetric theories and theories with extra compact spatial dimensions. Establishing the form of the interactions between such scalars and the Standard Model particles is of the utmost importance to detect dark matter either directly or indirectly, and an obvious possibility is the Higgs portal, where dark matter only interacts directly with the Higgs field, $\mathcal{H}$. A coupling of the form $g^2|\Phi|^2|\mathcal{H}|^2$ should generically appear for any complex or real scalar field, since it is not forbidden by any symmetries, except for the QCD axion and analogous pseudo-scalars where such an interaction is forbidden by a shift symmetry.

The Higgs portal for dark matter has been thoroughly explored in the context of scalar WIMP-like candidates [16–29], but only a few proposals in the literature discuss the case of an oscillating scalar condensate [1, 2, 30–32]. In this work, we aim to fill in this gap and consider a generic model for scalar field dark matter where, like all other known particles, the dark scalar acquires mass exclusively through the Higgs mechanism, i.e. no bare scalar mass term in the Lagrangian is introduced for dark matter. While the Standard Model gauge symmetries forbid bare masses for chiral fermions and gauge bosons, this is not so for scalars, since $|\Phi|^2$ is always a gauge-invariant operator. Scalar mass terms are, however, forbidden if the theory is scale-invariant (or exhibits a conformal invariance). This has arisen some interest in the recent literature, with the possibility of dynamically generating both the Planck scale and the electroweak scale through a spontaneous breaking of scale-invariance. In fact, with the inclusion of non-minimal couplings to gravity allowed by scale-invariance, one can generate large hierarchies between mass scales from hierarchies between dimensionless couplings and naturally obtain an inflationary period in the early Universe, as shown in Refs. [33–36]. For other scenarios with scale-invariance and viable dark matter candidates, see also Refs. [37–42].

This thesis is organized as follows: in chapter 1 we review the basics of the Standard Model of Particle Physics, Cosmology and the present status of dark matter. In chapter 2, we focus on the dynamics of an oscillating scalar field without significant self-interactions as a dark matter candidate, considering that it only acquires mass

through the Higgs mechanism, at the electroweak phase transition. We determine, in particular, the relation between the field's mass and initial amplitude required in order to explain the observed dark matter abundance. In chapter 3, our starting point is the idea of chapter 2, introducing, this time, dark matter self-interactions and investigating their implications on the dynamics of this dark matter candidate. In chapter 4, we explore the scenario where an oscillating scalar field accounting for dark matter drives a non-thermal electroweak phase transition, which can be accomplished by considering a late decay of the inflaton field and, consequently, an early-matter era. We summarize our conclusions and future prospects in chapter 5. For the sake of simplicity, throughout this thesis we use natural units, $c = \hbar = k_B = 1$.

1.2 The Standard Model of Particle Physics

1.2.1 A historical overview

The Universe is made of small building blocks, which we call particles, and governed by four fundamental forces: gravity, electromagnetism, weak and strong interactions. Over the years, physicists tried to unravel these particles, how they interact with each other and with the fundamental interactions. All this work culminated in the Standard Model of Particle Physics, a mathematical description of the elementary particles and all forces except gravity. Since its development, the Standard Model has proven to be very successful, since it has predicted the existence of particles that were found later, for example, the vector bosons $W^{\pm}$ and Z^0, the top quark, the tau neutrino or, more recently, the Higgs boson. The building of the Standard Model began in 1961, when Sheldon Glashow discovered a way of combining the electromagnetic and weak interactions [43]. This work was complemented by Abdus Salam and John Ward who proposed, in 1964, a similar theory [44]. In 1967, Steven Weinberg introduced the Higgs mechanism in order to give rise to the masses of gauge particles and fermions, shaping the Standard Model in its modern form [45] and later, in 1971, 't Hooft, using tools developed by his supervisor, Veltman, proved that the electroweak theory is renormalizable [46]. Although many contributed to the development of the theory of strong interactions, we highlight two physicists, Murray Gell-Mann and George Zweig, who independently proposed that the properties of the strongly interacting particles, the hadrons, could be explained if these particles could be divided into small pieces - the quarks [47, 48].

In the next subsection, we will describe the contents of the Standard Model. We intend to provide a brief introduction to the Standard Model, with useful concepts that will be needed ahead; however, we do not intend to provide an extensive study of the Standard Model, since it is not the focus of this thesis.

1.2.2 The Standard Model as a gauge group $SU(3)_C \times SU(2)_L \times U(1)_{\mathrm{Y}}$

In this subsection, we review the main aspects of the Standard Model. It includes fermions, gauge bosons, the Higgs boson and it is well-established for three of the four fundamental forces: electromagnetic, weak and strong interactions, assigning carriers for each one.

Fermions are particles of spin 1/2 which respect the Pauli exclusion principle. There are six quarks - up, down, charm, strange, bottom and top - and six leptons - electron, electron neutrino, muon, muon neutrino, tau and tau neutrino. Quarks interact via strong, electromagnetic and weak forces, while the electron, the muon and the tau interact through weak and electromagnetic interactions and neutrinos interact only through the weak force.

Gauge bosons are force carriers, with spin 1, mediating strong, electromagnetic and weak interactions. This category includes photons, W^+, W^- and Z^0 bosons and gluons.

From a mathematical point of view, the Standard Model is based on the gauge group $SU(3)_C \times SU(2)_L \times U(1)_{\mathrm{Y}}$, which includes the groups describing the electromagnetic, weak and strong interactions. The electromagnetic interaction corresponds to a gauge invariance under local phase rotations of spinor fields ψ with electric charges: $\psi \rightarrow \psi' = e^{-i\alpha}\,\psi$. The associated gauge symmetry is $U(1)_{\mathrm{EM}}$ and the corresponding gauge boson is the photon. This is an exact symmetry, that is, it is not spontaneously broken, otherwise the photon would acquire mass. $U(1)_{\mathrm{EM}}$ is a subgroup of the electroweak gauge group, $SU(2)_L \times U(1)_{\mathrm{Y}}$.

In turn, the weak interaction arises from $SU(2)$ local transformations, $\psi \rightarrow \psi' = e^{-i\alpha I}\,\psi$, where I are the generators of the group: $I_i = \frac{1}{2}\,\tau_i$ and τ_i, $i = 1, 2, 3$, are the Pauli matrices. I constitutes the weak isospin, with $I^2 \equiv I_1^2 + I_2^2 + I_3^2$. The weak gauge bosons only couple to the left-handed spinor part of a Dirac-spinor, which means that the left-handed fermions form $SU(2)$ doublets, while the right-handed fields are isospin singlets. Therefore, we represent the group of weak interactions by $SU(2)_L$, where the

subscript L stands for "left".

The electroweak interaction is described by the group $SU(2)_L \times U(1)_{\mathrm{Y}}$ where the subscript Y refers to "weak hypercharge", which relates the electric charge Q and the third component of the weak isospin, I_3: $Y = 2\,(Q - \mathrm{I}_3)$. This group encompasses the four gauge bosons: the photon, the two $\mathrm{W}^{\pm}$ bosons, which mediate charged-current weak interactions, and the neutral Z^0 boson which mediates neutral-current weak interactions. $SU(2)_L \times U(1)_{\mathrm{Y}}$ is spontaneously broken into $U(1)_{\mathrm{EM}}$, yielding the masses of $\mathrm{W}^{\pm}$ and Z^0.

The gauge group behind the strong interaction is $SU(3)_C$ (here the subscript "C" stands for "color"), which has eight generators: the Gell-Mann matrices, the $SU(3)$ analog of the Pauli matrices in $SU(2)$. There are eight spin-1 particles, the gluons, and any particle that couples to them carries color charge. Quarks have strong interactions and are color triplets, while the colorless particles, like baryons, are $SU(3)_C$ singlets.

The Higgs boson is the only scalar boson of the Standard model. This massive particle has no spin, electric or color charge and is responsible for providing mass to the Standard Model particles. It was found in 2012, at the Large Hadron Collider (LHC) in CERN, confirming the predictions of the Standard Model, and has a mass $m_h = 124.97 \pm 0.24$ GeV [49]. In the next subsection, we will briefly explain the Higgs mechanism, showing how it generates masses to all known elementary particles.

1.2.3 The Higgs mechanism

In the Standard Model of Particle Physics, the Higgs mechanism is responsible for assigning mass to the particles and its explanation resulted from combined efforts of many physicists: Anderson [50], R. Brout and F. Englert [51], P. Higgs [52] and G. Guralnik, C. R. Hagen and T. Kibble [53]. In this section, we will discuss the Higgs mechanism, considering a simple model that contains all the important features of the process - the Higgs mechanism in the $U(1)$ gauge theory. This can be generalized to the case of the electroweak theory of the Standard Model, but we will not include this treatment here, for the sake of simplicity.

Consider a complex scalar field, ϕ, which is the combination of two real fields, ϕ_1 and ϕ_2:

$$\phi = \frac{\phi_1 + i\phi_2}{\sqrt{2}}. \tag{1.1}$$

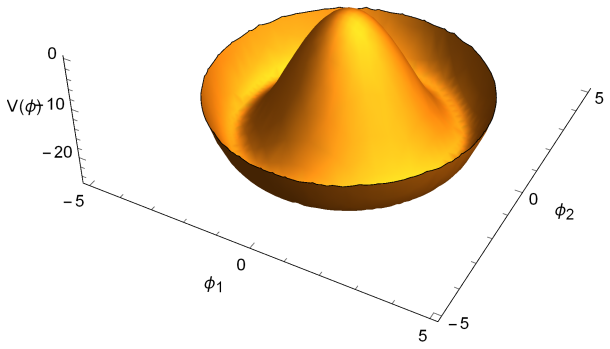

Figure 1.1: The "mexican hat" Higgs potential.

The Lagrangian density for a scalar complex field and a gauge field A^μ reads

$$\mathcal{L} = -\frac{1}{4}F_{\mu\nu}F^{\mu\nu} + D_\mu\phi^* D^\mu\phi - V(\phi), \tag{1.2}$$

where the potential of the scalar complex is $V(\phi) = \pm\mu^2\phi^*\phi + \lambda(\phi^*\phi)^2$ and μ and λ are positive constants. The gauge invariance is ensured by introducing the covariant derivative, D_μ, defined as $D_\mu = \partial_\mu + i\,q\,A_\mu$, and the strength tensor is defined by $F_{\mu\nu} = \partial_\mu A_\nu - \partial_\nu A_\mu$, as usual. Taking a look at the ϕ potential, if the term $\mu^2\phi^*\phi$ has a positive sign, the field's potential has a minimum at $|\phi| = 0$, which corresponds to the lowest energy state in this configuration, and the system is completely symmetric. However, if $\mu^2\phi^*\phi$ has a negative sign, the potential of the field has a "mexican hat shape" and acquires minima for $|\phi| \neq 0$, as illustrated in Fig. 1.1. In this case, $|\phi| = 0$ is no longer a stable point provided that there are other values for $|\phi|$ with lower energy. The field rolls to one of those states and, since it "chooses" a particular spot, the system is not symmetric anymore - it underwent a spontaneous symmetry breaking. Moreover, since the point of lower energy is different from zero, we say that the field acquired a non-zero vacuum expectation value (vev), v:

$$|\phi|_{min} = \sqrt{\frac{\mu^2}{\lambda}} \equiv \mathrm{v}. \tag{1.3}$$

Note that the new potential's minimum is infinitely degenerate, because any point that satisfies Eq. (1.3) is the lowest energy state of the model. For simplicity, we will consider a coordinate system where the new vacuum state occurs at $\phi_1 = \mathrm{v}$ and $\phi_2 = 0$. Now, we can expand the fields ϕ_1 and ϕ_2 around the vacuum, writing them

in terms of the classic value - the vev - and fields accounting for fluctuations around the vev, ϕ_1' and ϕ_2'. Hence, $\phi_1 = \mathrm{v} + \phi_1'$ and $\phi_2 = \phi_2'$ and the complex scalar field (Eq. (1.1)) reads, after the spontaneous symmetry breaking:

$$\phi = \frac{1}{\sqrt{2}} \left(\phi_1' + \mathrm{v} + i\phi_2'\right). \tag{1.4}$$

Inserting Eq. (1.4) into the Lagrangian density Eq. (1.2), we obtain the following:

$$\begin{aligned} \mathcal{L} &= -\frac{1}{4} F_{\mu\nu} F^{\mu\nu} + \frac{1}{2} q^2 \mathrm{v}^2 A_\mu A^\mu + \frac{1}{2} \partial_\mu \phi_1' \partial^\mu \phi_1' \\ &+ \frac{1}{2} \partial_\mu \phi_2' \partial^\mu \phi_2' + \mu^2 \left(\phi_1'\right)^2 + \mathcal{O}\left(fields^3\right), \end{aligned} \tag{1.5}$$

where the last term refers to powers of the fields higher than two. Here, it is possible to identify a massive real scalar field, ϕ_1', a massless scalar field, ϕ_2', and a massive vector field, A_μ. The existence of a massless scalar field is not surprising, giving the Goldstone theorem: for any generator of a broken symmetry in the ground state, there is always a massless scalar Goldstone boson.

Comparing Eqs. (1.2) and (1.5), we notice that the Lagrangian density Eq. (1.2) has four degrees of freedom: two of them come from the field ϕ and the other two from the field A_μ (corresponding to the transverse polarizations of the photon). In turn, the Lagrangian density Eq. (1.5) has five degrees of freedom: one coming from ϕ_1', one from the Goldstone boson, ϕ_2', and three from A_μ, since the latter is a massive field now. There is one more degree of freedom in the Lagrangian density of Eq. (1.5), which means that the Goldstone boson degree of freedom is not physical. Hence, we can eliminate it by choosing an appropriate gauge. In fact, given that ϕ_1', $\phi_2' \ll \mathrm{v}$, the field ϕ can be conveniently rewritten as:

$$\phi = \frac{1}{\sqrt{2}} \left(\phi_1' + \mathrm{v}\right) e^{\left(i\frac{\phi_2'}{\mathrm{v}}\right)}, \tag{1.6}$$

and, choosing a particular gauge, $A_\mu \to A_\mu - \frac{1}{q\,\mathrm{v}} \partial_\mu \phi_2'$, the Lagrangian density becomes:

$$\begin{aligned} \mathcal{L} &= -\frac{1}{4} F_{\mu\nu} F^{\mu\nu} + \frac{1}{2} \partial_\mu \phi_1' \partial^\mu \phi_1' + \frac{1}{2} q^2 \mathrm{v}^2 A_\mu A^\mu + q^2 \mathrm{v} A_\mu A^\mu \phi_1' \\ &+ \frac{1}{2} q^2 A_\mu A^\mu \left(\phi_1'\right)^2 - \frac{\mu^2}{2} \left(\phi_1' + \mathrm{v}\right)^2 + \frac{\lambda}{4} \left(\phi_1' + \mathrm{v}\right)^4. \end{aligned} \tag{1.7}$$

Thus, we have a theory with a real scalar field, the Higgs field ϕ_1', whose mass is $m_h \equiv m_{\phi_1'} = \sqrt{2\lambda}\,\mathrm{v}$, and a vector field, A_μ, with mass $m_A = q\,\mathrm{v}$. We can conclude that, when A_μ acquires mass, it gets a third degree of freedom, corresponding

to the longitudinal polarization, that comes from the Goldstone boson, which has disappeared. As a matter of fact, the field $\phi_2^{'}$ is not really gone, since the degree of freedom associated to the Goldstone boson was absorbed into the longitudinal polarization of the massive gauge field. In other words, the gauge field "has eaten" the Goldstone boson and obtained mass and another degree of freedom. This process is called the Higgs mechanism. In the Standard Model, the Higgs field is an isospin doublet, with four real degrees of freedom. The spontaneous symmetry breaking $SU(2)_L \times U(1)_{\rm Y} \to U(1)_Q$ occurs when one of the components acquires a vev, when the temperature of the Universe falls below $T \sim 100$ GeV - this is the electroweak phase transition (EWPT). The other three components give rise to three Goldstone bosons that are "eaten" by three gauge bosons which become massive (they are the $\rm W^+$, $\rm W^-$ and the Z^0 bosons), while the photon remains massless. The Higgs mechanism will be crucial to provide mass to our dark matter candidate, as we discuss in chapters 2, 3 and 4.

1.2.4 Electroweak vacuum stability

The Higgs vacuum is stable if its self-coupling, λ_h, is positive for any scale of energy μ where the minimum of its potential is a global minimum. Actually, for the observed Higgs mass $m_h \simeq 125$ GeV, λ_h becomes negative around $\mu \sim 10^{10} - 10^{12}$ GeV [7, 54], as illustrated in Fig. 1.2, which is well below the GUT or the Planck scales. The fact of λ_h becoming negative could constitute a problem because it can lead to a possible instability in the Higgs potential (see, for e.g., Refs. [7, 55, 56] and references therein).

Usually, the value of the couplings may vary with the energy scale. The running of a coupling parameter, λ, is encoded in the beta function, defined as

$$\beta\left(\lambda\right) = \frac{\delta\lambda}{\delta \ln \mu}. \tag{1.8}$$

In the case of the Higgs boson, the beta function of λ_h is given, at one-loop, by [56]:

$$\beta_{\lambda_h} = \frac{1}{16\,\pi^2}\left(-6y_t^4 + 12y_t^2\lambda_h + \frac{3}{8}\left(2g^4 + \left(g^2 + g'^2\right)^2\right) - 3\lambda_h\left(3g^2 + g'^2\right) + 24\lambda_h^2\right), \tag{1.9}$$

where y_t corresponds to the top Yukawa coupling, g is the $SU\left(2\right)_L$ coupling and g' is the $U\left(1\right)_Y$ coupling. From the last equation, we can conclude that the behaviour of λ_h is mostly driven by the large contribution of the top Yukawa coupling at one-loop, i.e, strongly depends on the top quark mass. When the coupling constant becomes

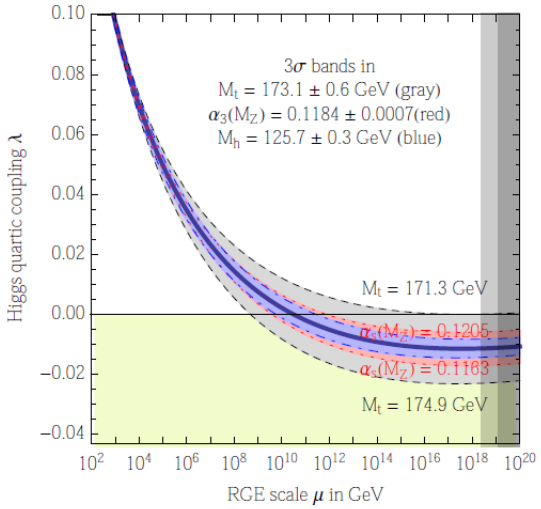

Figure 1.2: The running of the Higgs quartic coupling, $\lambda \equiv \lambda_h$, for the Higgs mass $M_h \simeq 125$ GeV. The uncertainties in the top mass (M_t), strong coupling (α_3) and the Higgs mass are also indicated. We can see that λ_h becomes negative for an energy scale, μ, around $\mu \sim 10^{10} - 10^{12}$ GeV. This plot is taken from [7].

negative, $V(h) = \lambda_h \frac{h^4}{4} < 0$ and, therefore, the Higgs minimum could be only a local minimum, instead of a global minimum. However, if the lifetime of the quantum tunneling to this true minimum is higher than the age of the Universe, the Higgs vacuum is metastable. In fact, Ref. [56] shows that the lifetime for the quantum tunneling is extremely long: about the fourth power of the age of the Universe.

There are some attempts to cure the (in)stability problem of the electroweak vacuum. For instance, Ref. [7] shows that a shift in the top quark mass of about $\delta m_t = -2$ GeV would suffice to keep $\lambda_h > 0$ at the Planck scale (this could also be a good reason to motivate more precise measurements of the top quark mass). Other ways include introducing physics beyond the Standard Model. In particular, coupling a scalar singlet with non-zero expectation value to the Higgs may stabilize the electroweak vacuum, provided that the contribution of the coupling between the Higgs and the singlet scalar maintains the Higgs self-coupling positive. This idea has been explored in the literature, and some of them promote this singlet scalar to a dark matter candidate, such as illustrated in Refs. [23, 57, 58].

In addition, we should worry about the stabilization of the Higgs field during inflation. If the Higgs field is light during inflation, de Sitter quantum fluctuations could drive the field to the true global minimum of the potential. However, the

introduction of scalar field dark matter can avoid this scenario. We will explore this possibility in chapter 4.

As a final note of this section, the Standard Model is one of the most successful theories ever constructed, but it has some loose ends. In particular, it does not predict dark matter. In the next sections we will discuss the topic of dark matter but, before that, we will comment on the cosmological framework, introducing the status of the Standard Cosmological model.

1.3 Standard Cosmology

Cosmology, defined as the study of the dynamics and evolution of the Universe, seeks to understand the long path from the origin of time until the Universe's final fate. It is based on a very basic postulate, the cosmological principle: we do not occuppy a special place in the Universe, since it is essentially homogeneous and isotropic on large scales. The standard model of cosmology, furnished with this principle, is able to describe the geometry of the Universe, its contents and features along this journey of 13.8 billion years, although it is not free from problems. In this section, we intend to describe summarily the main aspects of the standard cosmological model, also known as ΛCDM model, and show how cosmic inflation can complement this paradigm.

1.3.1 Geometry of the Universe

Einstein's General Theory of Relativity showed us that gravity is just a consequence of the curvature of space-time. Defining the Einstein-Hilbert action,

$$S = \int d^4x \sqrt{-g} \left(\frac{R}{16\,\pi\,G} + \mathcal{L}_{matt} \right), \tag{1.10}$$

where g is the determinant of the metric, R is the Ricci scalar, G is the gravitational constant and $\mathcal{L}_{matt}$ is the Lagrangian density of the matter in the Universe, and varying it with respect to the metric, $g_{\mu\nu}$, Einstein obtained a set of equations that describe the relation between the curvature of space-time and the local matter content:

$$R_{\mu\nu} - \frac{1}{2}\, g_{\mu\nu}\, R = 8\pi\, G\, T_{\mu\nu}, \tag{1.11}$$

where $R_{\mu\nu}$ is the Ricci tensor and $T_{\mu\nu}$ the energy-momentum tensor.

At large scales, the most general metric that takes into account the Universe's spatial homogeneity and isotropy is the Friedmann-Robertson-Walker metric (FRW),

which reads, assuming a metric signature $(-,+,+,+)$:

$$ds^2 = -dt^2 + a^2(t)\left[\frac{dr^2}{1-k\,r^2} + r^2\left(d\theta^2 + \sin^2(\theta)\,d\phi^2\right)\right], \tag{1.12}$$

where t refers to time, r is a radial coordinate, θ and ϕ are angular coordinates, $a(t)$ is the scale factor and k is a parameter representing the spatial curvature of the Universe and can be normalized to -1, 0 or 1, depending on whether the Universe is closed, flat or open, respectively. Assuming that the Universe is filled with a homogeneous and isotropic perfect fluid, the energy-momentum tensor is just $T^{\mu\nu} = diag(\rho, p, p, p)$, where ρ is the perfect fluid energy density and p its pressure. Using the energy-momentum tensor, and introducing the metric Eq.(1.12) into the Einstein field equations Eq. (1.11), we get the Friedmann equation:

$$H^2 \equiv \left(\frac{\dot{a}}{a}\right)^2 = \frac{8\pi G}{3}\rho - \frac{k}{a^2} \tag{1.13}$$

and the Raychaudhuri equation:

$$\frac{\ddot{a}}{a} = -\frac{4\pi G}{3}(\rho + 3p), \tag{1.14}$$

where $H \equiv \frac{\dot{a}}{a}$ is the Hubble parameter, which characterizes the expansion rate of the Universe, and the dot denotes differentiation with respect to time.

The covariant conservation of the energy-momentum tensor, $\nabla^\mu T_{\mu\nu} = 0$, corresponds to energy and momentum conservation in an expanding Universe, implying that:

$$\frac{\dot{\rho}}{\rho} = -3\,(1+w)\,H. \tag{1.15}$$

The last equation is the continuity equation for a perfect fluid, where $w \equiv \frac{p}{\rho}$ defines its equation of state. The three relevant forms of cosmological fluids are non-relativistic matter (dust), radiation and vacuum energy. Non-relativistic matter consists of cold and heavy particles ($T \ll m$) with negligible pressure, $w = 0$, whose energy density falls off in an expanding Universe as $\rho_m \propto a^{-3}$, according to Eq. (1.15). This includes baryons and cold dark matter. In turn, radiation describes relativistic particles ($T \gg m$) , such as photons and all particles in the early Universe, when temperatures were high. Its equation of state is $w = 1/3$ and the corresponding energy density drops as $\rho_{rad} \propto a^{-4}$. Finally, vacuum energy (also known as "cosmological constant") has an equation of sate $w = -1$, corresponding to a fluid with a negative pressure that is responsible for accelerating the expansion of the Universe. In this case, the energy density is constant, $\rho_\Lambda \propto a^0$.

In fact, since the Universe is composed by those three forms of fluids (dust, radiation and vacuum energy), we can rewrite Eq. (1.13) as a function of the abundance of each component, Ω_i:

$$\sum_i \Omega_i - 1 = \frac{k}{H^2\, a^2}, \tag{1.16}$$

where $\Omega_i \equiv \frac{\rho_i}{\rho_c}$ and $\rho_c = \frac{3H^2}{8\pi G}$ is the critical energy density of the Universe, i.e., the energy density for $k = 0$. According to Planck data, $\Omega_m = 0.3166 \pm 0.0084$ (this includes baryonic and cold dark matter), $\Omega_{rad} \simeq 9{\times}10^{-5}$ and $\Omega_\Lambda = 0.6834{\pm}0.0084$ [10], hence $\sum_i \Omega_i$ is very close to 1, which means that the Universe is practically flat ($k \simeq 0$).

In this subsection, we have studied the geometry of the Universe, the equations that govern its evolution (Eqs. (1.13) and (1.14)) and how the fluid components, non-relativistic matter, radiation and vacuum energy evolve with the expansion of the Universe, which is parameterized by a dimensionless quantity, the scale factor, $a(t)$. We have found that the curvature k of the Universe is almost zero, which means that the Universe is essentially flat. The scenario where we have a flat Universe, described by the FRW metric and presently filled mainly with vacuum energy and non-relativistic matter constitutes the ΛCDM model. We will briefly comment on this model in the next subsection.

1.3.2 ΛCDM model

The ΛCDM model is the simplest model that encompasses a flat, homogeneous and isotropic Universe filled with a cosmological constant, radiation and matter, which can account for current cosmological observations [10]. In addition, it describes the Universe's evolution since its very early stages until its final fate and, for this reason, it is commonly dubbed "the Standard Model of Cosmology". The letter Λ represents the cosmological constant/vacuum energy which is the simplest example of dark energy, while CDM corresponds to the cold dark matter model. The ΛCDM model requires six parameters to model the evolution of the Universe: the Hubble parameter today, H_0, the density parameters of baryonic and dark matter, Ω_b and Ω_{CDM}, respectively, the spectral amplitude $\mathcal{A}_s$, the spectral index n_s and the optical depth τ [59]. In this subsection, we will briefly discuss each of these parameters.

The Hubble parameter at the present time assumes the value $H_0 = 67.36 \pm 0.54\,\mathrm{km\,s^{-1}\,Mpc^{-1}}$, while the baryonic and dark matter density parameters are $\Omega_b h^2 = 0.0224 \pm 0.0001$ and $\Omega_{CDM} h^2 = 0.120 \pm 0.001$, respectively [10]. The remainder of

the Universe's content is mainly dark energy, Λ, an unknown form of energy that is responsible for the late acceleration of the expansion of the Universe (see, for instance, Ref. [60]).

The spectral amplitude and the spectral index are intimately related, since both characterize the primordial curvature power spectrum behind CMB perturbations, putatively induced by the inflaton field (see, for instance, Ref. [61]). The curvature power spectrum is defined by

$$\mathcal{P}(k) \equiv \mathcal{A}_s \left(\frac{k}{k_*}\right)^{n_s(k)-1}, \tag{1.17}$$

where $\mathcal{A}_s$ is the amplitude of the power spectrum at the pivot scale k_* and the spectral index $n_s(k)$ is defined as $n_s(k) - 1 \equiv d\ln[\mathcal{P}(k)]/d\ln k$. According to Planck data, $\mathcal{A}_s \simeq 2.1 \times 10^{-9}$ and $n_s = 0.965 \pm 0.004$ at pivot scale $k = 0.05\,\mathrm{Mpc}^{-1}$ [10]. A detailed analysis of the spectrum of CMB temperature fluctuations is outside the scope of this work, although more details are given in chapers 2 and 3, when we describe the dynamics of our dark matter model during inflation.

In turn, the optical depth τ is related to the reionization process and it is defined such that $e^{-\tau}$ corresponds to the probability that a photon emitted after decoupling, but before reionization, is scattered [62].

According to the ΛCDM scenario, the Universe emerged from an initial singularity, where all the known Physics does not apply. Then, the Universe underwent a period of accelerated expansion - cosmic inflation - before being dominated by hot radiation. At some point, the matter content of the Universe overcomes radiation, ruling most of its history, until very recent times, when dark energy takes over and dominates the expansion of the Universe. In the next subsections we will address briefly the topics of cosmic inflation and the subsequent thermal history of the Universe.

1.3.3 Cosmic Inflation

The standard model of Cosmology describes an expanding Universe that is homogeneous and isotropic on large scales; however, it does not provide a satisfactory explanation for some questions. For instance, we mentioned that the Universe is essentially flat, since $\sum_i \Omega_i$ is presently very close to 1 and k, the parameter related to the curvature of the Universe (see Eq. (1.12)), is approximately null. Therefore, it seems that the model requires fine-tuned initial conditions, but the cosmological paradigm as we have described in the last section does not provide any. In addition,

the model does not explain the homogeneity problem (also called the horizon problem), that is the fact that the Universe has regions with nearly the same density and temperature, even though they have never been in causal contact since the Big Bang, nor explain the absence of unwanted relics, such as magnetic monopoles, that could be produced in the early Universe but whose existence is in conflict with current observations [62].

In fact, Alan Guth, in 1980, was concerned about the magnetic monopoles that could be produced during the GUT (Grand Unified Theory) transition when he came up with the idea of inflation, which could solve the above-mentioned problems [63]. During inflation, the Universe grows by a factor of $\sim e^{60}$, diluting the number density of unwanted relics and flattening the Universe. In its original proposal, Guth considered the case where a scalar field is in a false minimum of its potential, where its kinetic energy vanishes and, therefore, the field mimics a cosmological constant. Inflation ends when the scalar field performs a quantum tunneling to the true minimum of the potential. This could solve the problems arisen, but since the probability of quantum tunneling is small, it turns out that the transition to a radiation-dominated era would be very unlikely.

In new versions of inflation (see, for e. g., Ref. [64]), there is an additional scalar field, the inflaton, χ, with equation of state $w \simeq -1$, which drives inflation. The inflaton field rolls slowly down its potential until it reaches a minimum and begins to oscillate around it.

In fact, the simplest model for inflation admits a scalar field, since it can provide all the necessary ingredients for inflation to occur: a period of accelerated expansion that erases unwanted relics and solves the horizon and flatness problems and, at the end of this period, recovers standard Cosmology. The action for the inflaton field χ is:

$$S_\chi = \int d^4x \sqrt{-g} \left[-\frac{1}{2} \partial_\mu \chi \partial^\mu \chi - V(\chi) \right], \tag{1.18}$$

where $V(\chi)$ corresponds to the inflaton potential. The energy-momentum tensor is computed varying the last expression with respect to the metric tensor:

$$T^{\mu\nu}_\chi = \frac{2}{\sqrt{-g}} \frac{\delta S_\chi}{\delta g_{\mu\nu}} = -\left(\frac{1}{2} \partial_\alpha \chi \partial^\alpha \chi + V(\chi) \right) g^{\mu\nu} + \partial^\mu \chi \partial^\nu \chi. \tag{1.19}$$

Analogously with a perfect fluid, the energy density of the inflaton and its pressure, ρ_χ and p_χ, respectively, for a FRW metric, are:

$$\rho_\chi = T_{00} \simeq \frac{1}{2} \dot{\chi}^2 + \frac{1}{2} \frac{(\nabla \chi)^2}{a^2} + V(\chi), \tag{1.20}$$

$$p_\chi = \frac{g^{ij}\,T_{ij}}{3} \simeq \frac{1}{2}\,\dot{\chi}^2 - \frac{1}{6}\frac{(\nabla\chi)^2}{a^2} - V(\chi)\,, \tag{1.21}$$

where the gradients are given by $(\nabla\chi)^2 = \gamma^{ij}\partial_i\chi\partial_j\,\chi$ and γ^{ij} is defined as $\gamma^{ij}dx_i dx_j = \frac{dr^2}{1-k\,r^2} + r^2 d\Omega^2$, which follows from the FRW metric (see subsection 1.3.1) with curvature k. Hence, from Eqs. (1.20) and (1.21), we can see that it is possible to have different equations of state depending on whether $\dot{\chi}^2$, $(\nabla\chi)^2$ or $V(\chi)$ dominate. If the inflaton's kinetic energy dominates, $p_\chi \simeq \rho_\chi$, and $w \simeq 1$; on the other hand, if gradient energy dominates, $p_\chi \simeq -\frac{1}{3}\rho_\chi \Rightarrow w = -\frac{1}{3}$. Finally, if the potential energy dominates, $p_\chi \simeq -\rho_\chi \Rightarrow w = -1$, which mimics the behavior of a cosmological constant and allows for the accelerated expansion, required for solving the problems mentioned above.

The dynamics of the inflaton field is described by its equation of motion, which can be obtained by minimizing the variation of the action in Eq. (1.18) for small field variations, that is:

$$\delta S_\chi = \int d^4x\,\sqrt{-g}\left[\frac{1}{\sqrt{-g}}\,\partial_\nu\left(\sqrt{-g}\,g^{\mu\nu}\,\partial_\mu\chi\right) - V'(\chi)\right]\delta\chi = 0. \tag{1.22}$$

Considering the flat FRW metric, $g_{\mu\nu} = diag\,(-1,\,a^2(t)\,,\,a^2(t)\,,\,a^2(t))$ and $\sqrt{-g} = a^3(t)$, and neglecting the gradient contributions ($(\nabla\chi)^2$), since they will be exponentially diluted, the equation of motion is:

$$\ddot{\chi} + 3H\dot{\chi} + V'(\chi) = 0. \tag{1.23}$$

Notice that the potential of the inflaton acts like a force, while the expansion of the Universe works as a friction term. Since in chapters 2, 3 and 4 we discuss scalar fields that behave like dark matter candidates, whose potential is dominated by a quadratic term, it is worth checking what the equation of motion Eq. (1.23) tells us for a quadratic inflaton potential, $V(\chi) = \frac{1}{2}\,m_\chi^2\,\chi^2$. Introducing this into Eq. (1.23), we are left with:

$$\ddot{\chi} + 3H\dot{\chi} + m_\chi^2\chi = 0, \tag{1.24}$$

which is the equation of motion of a damped harmonic oscillator. Thus, if $m_\chi \gg H$, the friction term can be neglected and the inflaton field is in an underdamped regime, behaving like a harmonic oscillator. On the other hand, if $m_\chi \ll H$, the friction term is more important - the field is overdamped in this regime and does not oscillate. For successful inflation, the last condition must be satisfied, i.e, the inflaton field has to be in an overdamped regime, which mimics the effect of the cosmological constant. Other inflaton field potentials are just generalizations of the quadratic inflation case, and the results we have referred to here can apply to those cases too.

Hence, there are two requirements for having a successful inflation, which are known as the slow-roll conditions. One of them states that

$$\frac{1}{2}\dot{\chi}^2 \ll V(\chi), \tag{1.25}$$

that is, the kinetic energy of the inflaton has to be smaller than its potential energy, $V(\chi)$, to ensure an equation of state close to a cosmological constant, $w = -1$. The other slow-roll condition reads:

$$\ddot{\chi} \ll 3\,H\,\dot{\chi}, \tag{1.26}$$

meaning that the acceleration of the field has to be small so that the first condition is fulfilled for a sufficiently long period. These slow-roll conditions are usually expressed in terms of the following quantities, the slow-roll parameters:

$$\epsilon_\chi = \frac{1}{2}\,M_{Pl}^2\,\left(\frac{V'(\chi)}{V(\chi)}\right)^2 \tag{1.27}$$

$$\eta_\chi = M_{Pl}^2\,\left(\frac{V''(\chi)}{V(\chi)}\right). \tag{1.28}$$

A successful inflation requires $\epsilon_\chi \ll 1$ and $\eta_\chi \ll 1$, and will last until $\epsilon_\chi \sim 1$ and $\eta_\chi \sim 1$. The duration of inflation is usually measured in e-folds, N_e, which is the amount of time that the Universe takes to expand its original size by a factor e. The number of e-folds of inflation is defined by:

$$N_e = \log\left(\frac{a_e}{a_i}\right), \tag{1.29}$$

where a_i is the scale factor at the beginning of inflation and a_e the scale factor at the end of inflation. Noting that

$$\log\left(\frac{a_e}{a_i}\right) = \int_{a_i}^{a_e}\frac{da}{a} = \int_{t_i}^{t_e} H(t)\,dt, \tag{1.30}$$

and using the slow-roll conditions Eqs. (1.25) and (1.26), the Friedmann equation (1.13) and the Raychaudhuri Eq. (1.14), the number of e-folds reads:

$$N_e \simeq -\frac{1}{M_{Pl}^2}\int_{\chi_i}^{\chi_e}\frac{V(\chi)}{V'(\chi)}\,d\chi. \tag{1.31}$$

The horizon problem is solved if $N_e \sim 50 - 60$.

When the slow-roll equations are no longer valid, inflation ends and the inflaton transfers all its energy into Standard Model degrees of freedom, via a period called reheating, starting the radiation era. At the end of inflation, the kinetic term of the

inflaton's potential dominates over the potential term, and the inflaton energy density decays quickly. To study the reheating period we must take into account the decay of the inflaton into other particles, which leads to an additional friction term in its equation of motion:

$$\ddot{\chi} + 3H\dot{\chi} + V'(\chi) + \Gamma_\chi \dot{\chi} = 0, \tag{1.32}$$

where Γ_χ corresponds to the inflaton decay width. Multiplying both sides of Eq. (1.32) by $\dot{\chi}$, we obtain the continuity equation for this scenario:

$$\dot{\rho}_\chi + 3\,H\,(\rho_\chi + p_\chi) = -\Gamma_\chi \dot{\chi}^2. \tag{1.33}$$

Hence, the energy stored in the inflaton is transferred mainly into relativistic Standard Model degrees of freedom and the particles produced by the inflaton's decay interact with each other and, eventually, reach a state of thermal equilibrium with a temperature T_R. This reheating temperature, T_R, can be estimated by equating the Hubble parameter during the radiation era,

$$H_{rad} = \sqrt{\frac{\pi^2\, g_*}{90}}\,\frac{T^2}{M_{Pl}}, \tag{1.34}$$

where g_* stands for the number of relativistic degrees of freedom, and the inflaton decay width:

$$H_{rad} \sim \Gamma_\chi \Rightarrow T_R \sim \left(\frac{90}{\pi^2 g_*}\right)^{1/4} \sqrt{M_{Pl}\,\Gamma_\chi}. \tag{1.35}$$

Notice that the reheating temperature is determined by the duration of the inflaton decay, whose lifetime is $\tau_\chi = \Gamma_\chi^{-1}$. This means that a long decay time leads to lower reheating temperature. However, T_R cannot be arbitrarily small: $T_R \gtrsim 10$ MeV, as the Universe must be radiation dominated during the synthesis of light elements (Big Bang nucleosynthesis).

In addition to solving the horizon and flatness problems, as well as erasing any unwanted relics, inflation can also explain the Universe's structure that we observe today. In fact, quantum fluctuations of the inflaton field get stretched and amplified during inflation, that later will give origin to the large scale structure that we observe in the Universe and also the small perturbations in the temperature and polarization of the CMB. We can split the inflaton field into a homogeneous value, $\bar{\chi}$, and its fluctuations, $\delta\chi$:

$$\chi = \bar{\chi} + \delta\chi, \tag{1.36}$$

with $\delta\chi \ll \bar{\chi}$ and $\bar{\chi}$ obeys the classical equations of motion. During the slow-roll regime, $m_\chi^2 \ll H^2$, so we are considering the case of a light field during inflation[1]. In turn, the quantum fluctuations satisfy the following equation of motion:

$$\delta\ddot{\chi} + 3\,H\,\delta\dot{\chi} - \frac{1}{a^2}\nabla^2\delta\chi = 0, \tag{1.37}$$

which, in the Fourier modes basis, $\delta\chi_k = A_k\, e^{i\mathbf{k}.\mathbf{x}}$, reads:

$$\delta\chi_k'' + 2\,\frac{a'}{a}\,\delta\chi_k' + k^2\delta\chi_k = 0, \tag{1.38}$$

where primes $'$ denote derivatives with respect to the conformal time, τ, defined by $d\tau = \frac{dt}{a(t)}$ and, during inflation,

$$\tau = -\frac{1}{a\,H}, \tag{1.39}$$

as the scale factor evolves like $a \sim e^{H\,t}$. Notice that the Hubble parameter is approximately constant during inflation. The wavelength of each mode is given by

$$\lambda_k = \frac{2\pi}{k}\,a. \tag{1.40}$$

If λ_k is larger than the Hubble horizon H^{-1}, i.e, $\lambda_k > H^{-1}$, the mode is outside the horizon. In particular, from Eqs. (1.39) and (1.40) we can state that:

$$\lambda_k \gg H^{-1} \Rightarrow |k\tau| \ll 1 \Leftrightarrow k \ll a\,H. \tag{1.41}$$

Consequently, the mode is inside the horizon if $|k\tau| \gg 1$ ($k \gg a\,H$) and crosses the horizon when $|k\tau| \sim 1$ ($k \sim a\,H$).

The solutions of Eq. (1.38) are:

$$\delta\chi_k^{\pm}(\tau) = \frac{1}{a\,(t)}\left(1 \mp \frac{i}{k\tau}\right) e^{\mp ik\tau}. \tag{1.42}$$

Hence, when $|k\tau| \ll 1$, i.e., the mode is super-horizon, its amplitude is $\left|\delta\chi_k^{\pm}(\tau)\right| \simeq H/k$, which is approximately a constant value. This means that, when a mode becomes larger than the horizon, its amplitude becomes frozen, and all modes with the same wavenumber k are frozen in phase. In contrast, the amplitude of the sub-horizon modes is suppressed relatively to the previous one: since $|k\tau| \gg 1$ and $\left|\delta\chi_k^{\pm}(\tau)\right| \simeq 1/a \simeq e^{-H\tau}$. Thus, although the average fluctuations of the inflaton field vanishes, its

[1]This can be seen taking the example, for instance, of the quadratic potential for the inflaton. Since the slow-roll parameter Eq. (1.28) must be smaller than 1 for inflation to occur, we get that $m_\chi^2 \ll H^2$.

variance, $\left\langle (\delta\chi)^2 \right\rangle$, does not, and only the super-horizon modes contribute significantly to its value. Integrating over all superhorizon modes, the variance reads:

$$\left\langle (\delta\chi)^2 \right\rangle = \int_{k_{min}}^{k_{max}} \frac{d^3k}{(2\pi)^3} \mathcal{P}_\chi(k) = \left(\frac{H}{2\pi}\right)^2 \log\left(\frac{k_{max}}{k_{min}}\right), \tag{1.43}$$

where $k_{max} \sim a_e\, H$ is the last mode to leave the horizon during inflation and $k_{min} \sim a_i\, H$ correspond to the first mode to exit the horizon and

$$\mathcal{P}_\chi(k) = \frac{H^2}{2\,k^3}. \tag{1.44}$$

Using the definition of number of e-folds, Eq. (1.31) , it is easy to see that the variance of the inflaton's fluctuations grows with the number of e-folds during inflation:

$$\left\langle (\delta\chi)^2 \right\rangle = \left(\frac{H}{2\pi}\right)^2 N_e. \tag{1.45}$$

During inflation, it is possible that other fields coexist with the inflaton field. These fields could be dark matter fields, for example, and they may also exhibit quantum fluctuations. However, as we will see, if they are massive during inflation, i.e, $m_\phi \gtrsim H_{inf}$ (where ϕ is not the inflaton), its quantum fluctuations are more suppressed than the ones corresponding to light fields during inflation. The procedure to obtain the amplitude of each Fourier mode and the corresponding variance of fluctuations is the same as briefly described above. This case will be explored in subsections 2.2 and 3.1.1, where we study the behavior of an oscillating scalar field dark matter during inflation.

1.3.4 Brief thermal history of the Universe

In the previous section, we described how the Universe evolved during inflation. After inflation and a period of reheating, where the inflaton transfers all its energy into Standard Model particles, the Universe enters a radiation-dominated epoch. We have seen that the Universe contains non-relativistic matter, whose energy density follows $\rho_{mat} \sim a^{-3}$, radiation, $\rho_{rad} \sim a^{-4}$ and vacuum energy, $\rho_\Lambda = const.$ From here, we can see that radiation dilutes faster, implying the early Universe was dominated by relativistic particles. At some point, the matter component starts to dominate the Universe, followed, finally, by dark energy.

In the very early Universe, the different particles that constitute the Standard Model were relativistic and in thermal equilibrium, obeying the phase-space momentum

distribution function:

$$f_i(p) = \frac{1}{e^{\frac{E_i-\mu}{T}} \pm 1}, \tag{1.46}$$

where $E_i^2 = |p|^2 + m^2$ is the energy of the particle species i, p its momentum, $+$ refers to bosons, $-$ to fermions, T is the temperature and μ is the chemical potential. The number and energy densities read, respectively

$$n_i = \frac{g_i}{(2\pi)^3} \int d^3p \, f_i(p) \tag{1.47}$$

and

$$\rho_i = \frac{g_i}{(2\pi)^3} \int d^3p \, E_i(p) \; f_i(p), \tag{1.48}$$

where g_i corresponds to the number of degrees of freedom of the particle species i. Considering the case where $|\mu| \ll T$ (which, in general, is a good approximation, see, e.g., [65]) and writing the effective number of degrees of freedom at a temperature T as

$$g_*(T) \equiv \sum_{bosons} g_i + \frac{7}{8} \sum_{fermions} g_i, \tag{1.49}$$

the total energy density of radiation is given by:

$$\rho_{rad} = \frac{\pi^2}{30} g_* T^4. \tag{1.50}$$

The radiation era ends when $\rho_{rad}(a_{eq}) = \rho_m(a_{eq})$. Defining the redshift, z, as

$$z + 1 = \frac{a_0}{a(t)}, \tag{1.51}$$

where a_0 refers to the present value of scale-factor, matter-radiation equality takes place at z_{eq}:

$$1 + z_{eq} = \frac{\Omega_{m,0}}{\Omega_{rad,0}} \simeq 3400, \tag{1.52}$$

where $\Omega_{i,0}$ refers to the today's density parameter of the component i. In turn, following the same reasoning, the matter era ends at

$$1 + z_\Lambda = \left(\frac{1 - \Omega_{m,0}}{\Omega_{m,0}} \right)^{1/3} \simeq 1.3. \tag{1.53}$$

Another useful quantity, when it comes to thermal history, is entropy. Entropy conservation states that $S = a^3 s$ is constant as the Universe expands, where S is the entropy and s is the total entropy density, given by

$$s = \frac{\rho + p}{T}, \tag{1.54}$$

which follows from thermodynamic relations. As we have seen in subsection 1.3.1, the equation of state for relativistic species is $p = \rho/3$, implying that

$$s_i = \frac{4}{3}\frac{\rho_i}{T_i}. \tag{1.55}$$

Summing over all relativistic species, and using Eq. (1.50), the entropy density of radiation in the early Universe is:

$$s = \frac{2\,\pi^2}{45}\, g_{*S}\,(T)\; T^3. \tag{1.56}$$

Since $d\,(a^3\,s) = 0$, we can get a relation between T and a from Eq. (1.56):

$$T \propto g_{*S}^{-1/3}\, a^{-1}, \tag{1.57}$$

implying that $s \sim a^{-3}$. The number of particles of a given species i in a comoving volume, N_i, is defined as:

$$N_i \equiv \frac{n_i}{s}. \tag{1.58}$$

If particles are neither produced nor destroyed in a comoving volume, $n_i \sim a^{-3}$ and N_i becomes constant. This quantity will be useful in the next chapters to compute the present dark matter abundance. But, before going through these computations, let us discuss briefly the present dark matter status.

1.4 Dark matter

One of the most intriguing and challenging mysteries of Cosmology and Particle Physics is the existence of non-baryonic matter, which makes up almost 27% of the mass-energy content of the Universe and may explain the missing mass of galaxies, the so-called dark matter [10].

Dark matter was first predicted by the Swiss astronomer Fritz Zwicky, in 1933, to explain the missing mass accounting for the orbital velocities of galaxies in clusters [66]. Back then, Zwicky intended to measure the Coma cluster's mass and used two different methods. One method consisted in counting the total number of galaxies within the cluster, adding up all luminosity and converting this into mass using a mass-to-light relation. The other method took advantage of the virial theorem and measurements of galaxy velocities to estimate the gravitational potential and infer the cluster's mass. Then, Zwicky noticed that the gravitational mass that he got using the second method was about 400 times greater than expected from luminosity (method

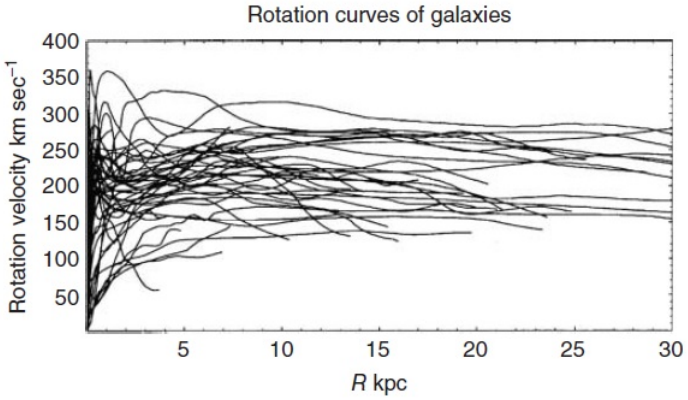

Figure 1.3: This figure illustrates the rotation curves of spiral galaxies [8]. The orbital velocity becomes almost constant beyond the boundary of the galactic disk. Typically, the disk's radius is about 10 kpc and we can see that the rotation velocity is constant up to 30 kpc, showing no evidence of decreasing.

one) and concluded that there must be some unseen mass component accounting for the total mass of the cluster, which he dubbed dark matter[2]. In fact, there are several phenomena that point towards the existence of dark matter, as we present in the next subsection.

1.4.1 Observational motivation for dark matter

Evidence for dark matter comes from several sources. At galactic scales, we have the example of galaxy rotation curves, which are plots of the orbital velocity of stars or gas within the galaxy as a function of their radial distance from the galactic center [67], as illustrated in Fig. 1.3. Using Newtonian mechanics, the orbital velocity is $v(r) = \sqrt{\frac{2GM(r)}{r}}$, where G is the gravitational constant and M is the mass within the radius r. Therefore, we would expect that the velocity would decay as it goes far away from the galactic center. However, what we really observe is that the curves do not decay with distance - they become almost constant instead, as shown in Fig. 1.3. Hence, the flattening of the rotation curves, i.e, $v(r)$ being approximately constant, indicates that $M(r) \propto r$ and that there should exist a dark matter halo surrounding galaxies.

The Bullet Cluster, a system that was formed after the collision of two large clusters

[2]Nowadays, the same calculation shows a factor smaller than 400, but it is clear that most of the non-relativistic matter in the Universe is dark.

Figure 1.4: The Bullet Cluster [9]. The pink region corresponds to the baryonic matter, while the blue areas show where most of the mass of the system is localized. Since these two regions do not overlap, we may conclude that most of the mass of the system is invisible.

of galaxies, provides one of the most convincing evidence for the existence of dark matter [68]. Using X-rays and weak-lensing observations, astronomers were able to find where the baryonic matter and most of the mass of the system were located, as illustrated in Fig. 1.4. Fig. 1.4 is a composite image, i.e, uses information from different telescopes. The two pink clumps in the image correspond to the hot gas detected by the Chandra telescope in X-rays, which constitutes most of the baryonic matter in the system. In addition to the Chandra observation, the Hubble Space Telescope, the European Southern Observatory's Very Large Telescope and the Magellan Optical Telescopes were used to determine the location of the mass in the clusters. The blue areas in this image show where most of the mass in the clusters was found, and were determined using the effect of gravitational lensing. Hence, we may conclude that baryonic matter (pink) of this system is clearly separated from the spot where the major part of the mass is localized (blue). This gives direct evidence that nearly all of the mass in the clusters must arise from an invisible form of matter - dark matter. In addition, theories without dark matter cannot explain this effect, since they predict that the lensing would follow the baryonic matter, which is not what is observed.

Moreover, the angular fluctuations of the CMB spectrum can be used to infer the existence of dark matter. These fluctuations are acoustic oscillations in the photon-

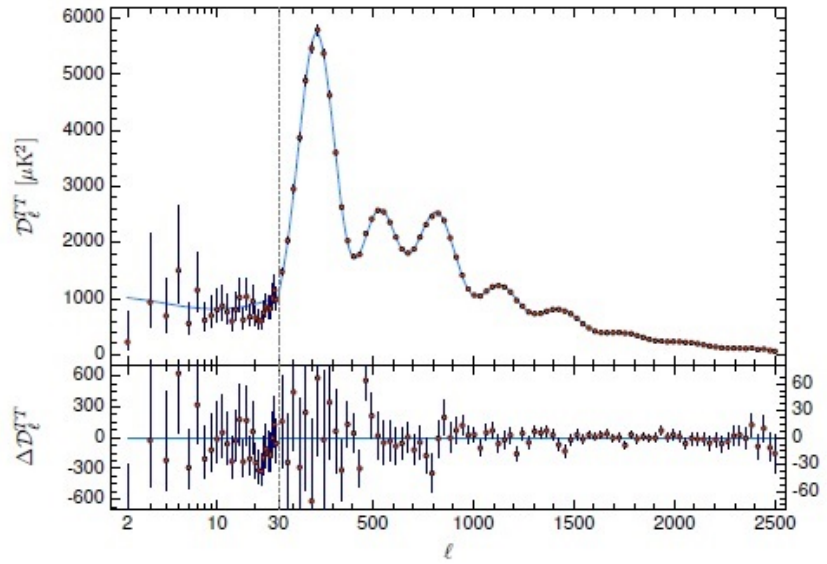

Figure 1.5: The Planck 2018 temperature power spectrum [10]. The Planck 2018 data is in red, with error bars, and the base-ΛCDM theoretical spectrum best fit to the Planck data is the blue curve in the upper panel. Residuals with respect to ΛCDM model are shown in the lower panel. The error bars show $\pm 1\sigma$ uncertainties.

baryon plasma and, although both dark and baryonic matter affect the oscillations through gravity, their effects are different. The power spectrum of anisotropies depicts the typical angular scales of the CMB and show the different effects of baryonic matter and dark matter. In particular, the shape of this power spectrum is determined by the oscillations in the hot gas in the primordial Universe and exhibits a large first peak and smaller successive peaks [10], as shown in Fig. 1.5.

The physics of the hot gas is well-studied and we can compute the properties of the oscillating gas by studying the position and the relative size of these peaks. In fewer words, the first peak contains information about the curvature of the Universe, whereas the second peak tells us the baryonic mass abundance in the Universe. In turn, the difference between the second and third peaks give us the dark matter density in the early Universe [69], telling us that $\Omega_{CDM} \sim 5\,\Omega_b$.

1.4.2 What is dark matter made of?

Despite all evidence suggesting that there must exist a dark non-baryonic component in the Universe, its constituents remain unknown. Nevertheless, we have some hints about what a dark matter candidate should look like. For instance, the study of

large scale structure tells us that most dark matter is "cold", i.e., non-relativistic, whereas the current fits to the Planck data indicates that its abundance has to be $\Omega_{CDM}\, h^2 = 0.120 \pm 0.001$ [10]. In addition, the dark matter candidate must be stable at cosmological scales, meaning that its lifetime must exceed the age of the Universe, $\tau_{Universe} \sim 10^{17}$ sec, and the interaction with the electromagnetic field must be null or very small [3]. From this description, it is clear that nothing in the Standard Model fits in, and its discovery would lead to new Physics. In fact, there is already a wide range of candidates beyond the Standard Model, which we briefly review.

1.4.2.1 Freeze-out mechanism and WIMPs

Several models assume that dark matter is produced thermally in the early Universe through the "freeze-out" mechanism. According to this mechanism, dark matter particles were in thermal equilibrium with the Standard Model particles at early times. While the dark matter interaction rate, Γ_{DM}, is larger than the Hubble parameter, H, particles are created and destroyed within a Hubble time, and equilibrium is maintained. As soon as $\Gamma_{DM} \lesssim H$, interactions can no longer keep up with expansion and, virtually, no particles are created or destroyed within a Hubble time. Thus, dark matter decouples from the thermal bath and its abundance becomes constant - or, in other words, "freezes-out". This mechanism is illustrated in Fig. 1.6.

To understand this dark matter production mechanism, let us assume that, in the early Universe, there are dark matter particles X and antiparticles $\overline{X}$ that may annihilate and produce Standard Model particles. Thus, the dark matter abundance will depend on annihilation and inverse annihilation processes, $X\overline{X} \leftrightarrow SM$, given that they may change the number of dark matter particles in a comoving volume. Assuming that there is no initial asymmetry between X and antiparticles $\overline{X}$, i.e, the number density of X is equal to the number density of $\overline{X}$, $n_X = n_{\overline{X}}$, the evolution of the dark matter number density is given by the Boltzmann equation [65]:

$$\frac{dn_X}{dt} + 3\,H\,n_X = -\,\langle\sigma v\rangle \left(n_X^2 - (n_X^{eq})^2\right), \tag{1.59}$$

where $\langle\sigma v\rangle$ is the thermally averaged annihilation cross-section times interaction velocity of the particles and n_X^{eq} denotes the equilibrium dark matter number density. As stated in the beginning of this subsection, interactions freeze-out when $\Gamma_X =$

[3] In chapter 3 we present a dark matter model whose interaction with the electromagnetic field is not zero, which can lead to interesting astrophysical signatures.

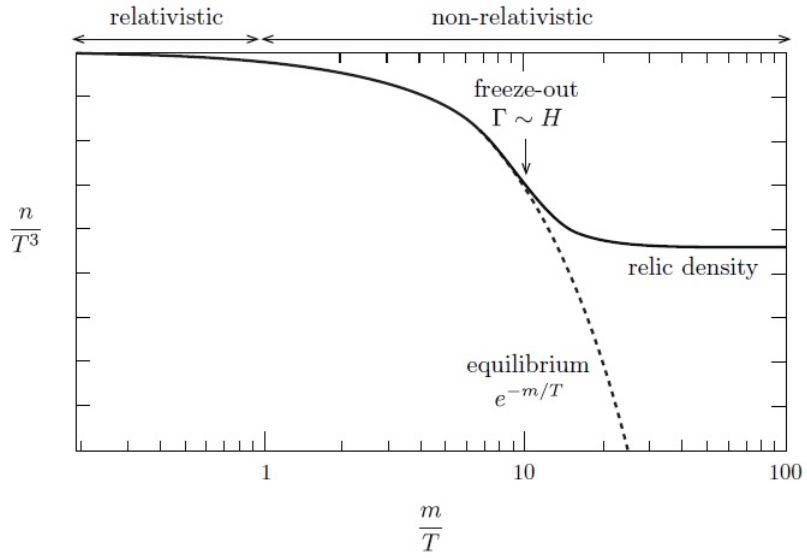

Figure 1.6: Schematic representation of the freeze-out mechanism (this picture is taken from [11]). When $\Gamma_{DM} > H$, the particle abundance follows its equilibrium value. However, as soon as $\Gamma_{DM} < H$, dark matter decouples from the thermal bath and its abundance becomes constant.

$n_X \langle \sigma v \rangle \lesssim H$. Assuming that dark matter particles are non-relativistic at freeze-out, its number density is given by

$$n_X (T_F) = g_X \left(\frac{m_X T_F}{2\pi} \right)^{3/2} e^{-\frac{m_X}{T_F}}, \tag{1.60}$$

where T_F is the freeze-out temperature, and since the Hubble parameter during the radiation era is given by Eq. (1.34), the freeze-out condition, $\Gamma_X (T_F) = H (T_F)$, reads

$$x_F^{1/2} e^{-x_F} = \sqrt{\frac{\pi^2 g_{F*}}{90}} \frac{(2\pi)^{3/2}}{g_X} \frac{1}{M_{pl}} \frac{1}{m_X} \frac{1}{\langle \sigma v \rangle}. \tag{1.61}$$

where we define $x_F = m_X / T_F$. From this point onwards, the interactions between dark matter and the heath bath, made of Standard Model particles, become rare and the dark matter particles number density in a comoving volume, n_X/s, becomes constant. Therefore, the dark matter number density today, $n_{X,0}$, can be written at the expense of the dark matter number density at freeze-out:

$$n_{X,0} = n_X (T_F) \frac{s_0}{s_F}, \tag{1.62}$$

where $s = \frac{2\pi^2}{45} g_{*S} T^3$ as defined in subsection 1.3.4. Hence, we may compute the

present dark matter relic abundance, $\Omega_{X,0}$:

$$\Omega_{X,0} \equiv \frac{\rho_{X,0}}{\rho_{crit}} = \frac{m_X}{3\,H_0^2\,M_{Pl}^2}\,n_X\left(T_F\right)\,\frac{g_{*0}\,T_0^3}{g_{*F}\,T_F^3}, \tag{1.63}$$

where $H_0 \simeq 10^{-42}\,h^2$ GeV is the today's Hubble parameter, $T_0 \simeq 2.4 \times 10^{-13}$ GeV is the present value of the CMB temperature and g_* is the number of relativistic degrees of freedom, with $g_{*0} \simeq 3.91$. Using these values, and noting that $n_X\left(T_F\right) = H\left(T_F\right) / \langle\sigma v\rangle$, the dark matter relic density yields:

$$\Omega_{X,0}\,h^2 \simeq 0.12\,\left(\frac{x_F}{10}\right)\,\left(\frac{g_{*F}}{10}\right)^{-1/2}\,\frac{10^{-8}\,\mathrm{GeV}^{-2}}{\langle\sigma v\rangle}. \tag{1.64}$$

So, if $\langle\sigma v\rangle \sim 10^{-8}\,\mathrm{GeV}^{-2}$, $\Omega_{X,0}\,h^2 \simeq 0.12$, which is the observed dark matter abundance [10]. A cross section of this order corresponds to the characteristic values for processes that occur at the electroweak scale. For this reason, the dark matter candidates produced by this freeze-out mechanism are known as "Weakly Interacting Massive Particles" (WIMPs), whose masses range from GeV to TeV scale (see e.g. Ref. [70] for a review). WIMPs examples include supersymmetric candidates, such as the lightest neutralino, "Little Higgs" models, "Two Higgs doublet" models, Kaluza-Klein states, among many others. There are many experiments designed to detect WIMPs (e.g. LUX [71], XENON1T [72], DAMA/LIBRA [73]) but, so far, they have evaded experimental detection. Nevertheless, the non-detection of WIMPs in these experiments places strong constraints on the properties of these dark matter candidates, such as masses and scattering cross-sections.

1.4.2.2 Freeze-in mechanism and FIMPs

Notwithstanding, non-thermally produced dark matter has been increasing in interest in the literature, in particular, models that incorporate the "freeze-in" mechanism [74]. In this case, dark matter was never in thermal equilibrium with the Standard Model sector since the interactions between them are very feeble. The initial number density of these dark matter particles is negligible, but it increases due to Standard Model particle decays and annihilations, lasting until the number density of the Standard Model particles becomes Boltzmann-suppressed. At this point, the dark matter abundance becomes constant and "freezes-in". This is shown in Fig. 1.7. Let us analyze the simplest case of the freeze-in mechanism, where the initial dark matter abundance is zero and increases due to decays of a Standard Model particle, σ, only:

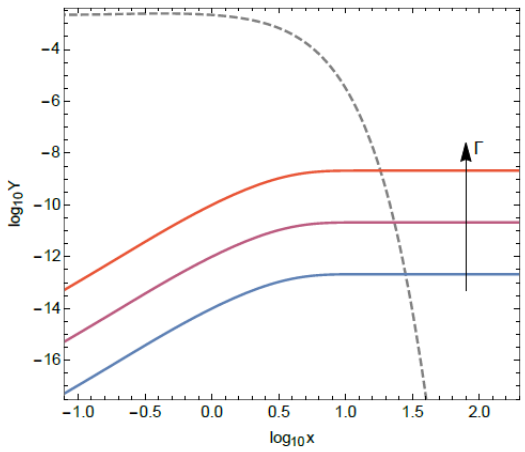

Figure 1.7: Schematic representation of the freeze-in mechanism [12]. $Y = n_{DM}/s$ and $x = m_{DM}/T$. Initially, the dark matter abundance is negligible, increasing due to decays and annihilations of the heat bath particles. When the heath bath particles number density becomes Boltzmann suppressed, the dark matter abundance becomes constant, "freezing-in".

$\sigma \to X\overline{X}$. Once again, we can analyze the evolution of the dark matter number density using the Boltzmann equation which, in this case, assumes the following form [12]:

$$\frac{dn_X}{dt} + 3\,H\,n_X = 2\,\Gamma_{\sigma\to XX}\,\frac{K_1\left(m_\sigma/T\right)}{K_2\left(m_\sigma/T\right)}\,n_\sigma^{eq}, \tag{1.65}$$

where m_σ is the σ particle mass, K_j are the modified Bessel functions of the second kind, $\Gamma_{\sigma\to XX}$ is the decay width of σ particles into dark matter, and n_σ^{eq} equilibrium number density of σ. By defining dimensionless parameters $Y = n_X/s$ and $x = m_X/T$, Eq. (1.65) becomes

$$\frac{x}{Y_\sigma^{eq}}\,\frac{dY}{dx} = 2\,\frac{\Gamma_{\sigma\to XX}}{H}\,\frac{K_1\left(x\right)}{K_2\left(x\right)}, \tag{1.66}$$

which can be used to compute the present dark matter abundance [74]:

$$\Omega_X\,h^2 \simeq 4.48\times 10^8\,\frac{g_\sigma}{g_{*S}\,\sqrt{g_*}}\,\left(\frac{m_X}{\mathrm{GeV}}\right)\,M_{Pl}\,\frac{\Gamma_{\sigma\to XX}}{m_\sigma^2}. \tag{1.67}$$

If we assume that $m_X \ll m_\sigma$ and $\Gamma_{\sigma\to XX} = \lambda_X^2\,\frac{m_\sigma}{8\pi}$, where λ_X is the coupling between X and σ, the coupling needed to produce a sizable dark matter abundance is [12]:

$$\lambda_X \simeq 10^{-12}\,\left(\frac{\Omega_X\,h^2}{0.12}\right)^{1/2}\,\left(\frac{g_*}{10^2}\right)^{3/4}\,\left(\frac{m_\sigma}{m_X}\right)^{1/2}. \tag{1.68}$$

Such dark matter candidates are known as "Feebly Interacting Massive Particles" (FIMPs). Besides FIMPs, other non-thermal candidates are axions, axion-like particles and sterile neutrinos.

1.4.2.3 Other examples of non-thermal candidates

The models that we develop in this thesis present an oscillating scalar field as a dark matter candidate, which was never in thermal equilibrium during its all cosmic history and acquires mass through the Higgs field. This could constitute an alternative to thermally produced dark matter, which has yet to be fully explored and for which we give a detailed study in chapters 2, 3 and 4. However, before going through a detailed study of those models, let us start by reviewing why a homogeneous oscillating field, ϕ, with a potential dominated by a quadratic term, $V(\phi) = \frac{1}{2}m_\phi^2\phi^2$, behaves as non-relativistic matter.

In a generic cosmological epoch where the scale factor evolves as $a(t) = (t/t_i)^p$, with $p > 0$ and $a(t_i) = 1$, the Hubble parameter is simply $H = p/t$. The field ϕ then satisfies the Klein-Gordon equation:

$$\ddot{\phi} + 3\frac{p}{t}\dot{\phi} + m_\phi^2\phi = 0 \ . \tag{1.69}$$

For $m_\phi t \gg 1$, the solution of this equation is then approximately given by:

$$\phi(t) \simeq \frac{\phi_{inf}}{a(t)^{3/2}}\cos(m_\phi t + \delta_\phi) \ , \tag{1.70}$$

where we have defined the initial field amplitude, ϕ_{inf}, and phase, δ_ϕ. According to the virial theorem for an oscillating scalar field with a quadratic potential,

$$\left\langle \dot{\phi}^2 \right\rangle = 2\,V(\phi)\,, \tag{1.71}$$

which can be inferred directly from the solution Eq. (1.70) taking into account that the field oscillations are much faster than expansion. Hence, from Eqs. (1.20) and (1.21), and ignoring the gradients because they are negligible, the energy density and the pressure of the field ϕ are, respectively:

$$\rho_\phi \sim V(\phi) \sim a^{-3} \tag{1.72}$$

and

$$p_\phi \sim 0\,, \tag{1.73}$$

which corresponds to the behavior of non-relativistic matter.

One of the best known examples of an oscillating scalar field that can account for dark matter is the axion (see, e.g., Ref. [75] for a review). Axions were introduced to solve the strong-CP (charge conjugation and parity) problem in Quantum Chromodynamics (QCD). This arises from the QCD term:

$$\mathcal{L}_{QCD} = \frac{\Theta}{32\,\pi^2}\,\mathrm{Tr}\,G_{\mu\nu}\tilde{G}^{\mu\nu}, \tag{1.74}$$

where Θ is a parameter, $G_{\mu\nu}$ is the gluon field strength tensor, $\tilde{G}^{\mu\nu} = \epsilon^{\alpha\beta\mu\nu}\,G_{\alpha\beta}$ its dual and the trace runs over the color indices. Since this term violates CP, it originates an electric dipole moment for the neutron [76]:

$$d_n \simeq 3.6 \times 10^{-16}\,\Theta\,e\,\mathrm{cm}, \tag{1.75}$$

where e is the electron's charge. The dipole moment of the neutron is constrained to $|d_n| < 3 \times 10^{-26}\,e\,\mathrm{cm}$ [77], which imposes an upper bound on Θ:

$$\Theta \lesssim 10^{-10}. \tag{1.76}$$

It is not clear why the value of Θ is so close to zero, and this constitutes the strong-CP problem.

In 1977, Peccei and Quinn proposed a mechanism to solve the strong-CP problem [78]. This proposal introduces a pseudoscalar field, the QCD axion, coupled to the term $G\tilde{G}$, which will set $\Theta = 0$ through QCD non-perturbative effects. According to the Peccei-Quinn theory, there is an additional global $U(1)_{PQ}$ symmetry - the Peccei-Quinn symmetry - which is spontaneously broken. The axion, a, is the Goldstone boson of the broken symmetry and has a shift symmetry, $a \to a + const.$ This shift symmetry is responsible for making the axion massless at all orders in perturbation theory and only non-perturbative effects, the QCD instantons, can break the shift symmetry and provide a periodic potential for the axion, of the form [75]:

$$V(a) = \Lambda_a^4\left(1 - \cos\left(\frac{n\,a}{f_a}\right)\right), \tag{1.77}$$

where Λ_a is the scale of non-perturbative Physics, n is an integer and f_a is the scale at which the Peccei-Quinn symmetry is broken. Considering the case $a \ll f_a$, the dominant term of the potential is

$$V(a) \simeq \frac{1}{2}\,m_a^2\,a^2, \tag{1.78}$$

where the axion mass is given by $m_a^2 = \Lambda_a^4/f_a^2$. Given that the axion field may be displaced from the origin in the early Universe, this leads to an oscillating scalar field whose potential is dominated by a quadratic term. Thus, the axion can be a viable dark matter candidate, if it is stable and provides the correct dark matter abundance, as we have seen above. In the case of the QCD axion, $\Lambda_a^4 = \Lambda_{QCD}^3\, m_u$, where $\Lambda_{QCD} = 200$ MeV is the QCD scale and m_u the up quark mass, and $10^9\,\text{GeV} < f_a < 10^{17}\,\text{GeV}$ [79]. This leads to:

$$4 \times 10^{-10}\,\text{eV} \lesssim m_a \lesssim 4 \times 10^{-2}\,\text{eV}. \tag{1.79}$$

Therefore, the QCD axion, in addition to solve the strong-CP problem, can constitute the dark matter in the Universe. In chapter 2, we present another non-thermal dark matter candidate, ϕ, with some similarities with this axion candidate - in particular, in the range of masses, since $m_\phi \sim 10^{-5}$ eV.

As a final note of this section, we would like to point out that there are some theories which assume that dark matter does not exist and that the graviational anomalies that we observe, such as the missing mass in galaxies, are a product of the incompleteness of the General Relativity theory. There are some examples of modified gravity theories, such as MOND ("Modified Newtonian Mechanics") [80], $f(R)$ theories (see for instance Ref. [81] for a review) and theories with non-minimal coupling between curvature and matter (see, for instance, [82]). However, those models are in some tension with some phenomena, in particular, they fail to explain the separation between visible and dark component that occurred in the Bullet Cluster and cannot provide an interpretation for the baryon acoustic oscillations in the CMB [83].

2 | Ultra-light Higgs portal scalar field dark matter

The discovery of the Higgs boson at the Large Hadron Collider (LHC) [84, 85] has opened up new possibilities for understanding the nature of dark matter. In fact, several works in the literature have already considered the possibility that dark matter interacts with the Higgs field in a variety of forms. The first models [17, 18, 86–88] considered an extension of the Standard Model with an additional singlet scalar field, ϕ, with renormalizable interactions with the Higgs field, $\mathcal{H}$, of the form:

$$V(\phi, h) = \frac{m_\phi^2}{2}\phi^2 + \frac{\lambda_\phi}{4}\phi^4 + g^2\phi^2|\mathcal{H}|^2 \ , \tag{2.1}$$

where m_ϕ is the field mass, λ_ϕ its self-coupling term, g the coupling term between the "phion" and the Higgs field and $\mathcal{H} = h/\sqrt{2}$. Several analyses of this and related models have been performed in the literature [16, 19–29, 31, 32] and this possibility has become widely known as "Higgs portal" dark matter. A connection to dark energy has also been suggested in [89, 90].

Most of the works in the literature focus, however, on dark matter candidates whose abundance is set by the standard decoupling and freeze-out mechanism, with masses in the GeV-TeV range. In this chapter, we consider an alternative possibility in which the scalar field ϕ acquires a large expectation value during inflation and begins oscillating after the electroweak phase transition, behaving as non-relativistic matter. Although a related scenario was considered e.g. in Ref. [31], in the latter case interactions are sufficiently large to lead to the decay of the scalar condensate and thermalization of the ϕ-particles, so that the present-day dark matter abundance also corresponds to a GeV-TeV WIMP thermal relic.

In this chapter, we start by considering a scenario where the dark matter field is part of a hidden/sequestered sector with an inherent conformal symmetry/scale invariance, which is broken only by feeble interactions with the Higgs boson. This implies that

the field's mass and self-couplings are extremely small, which in particular leads to a long-lived oscillating scalar condensate that is never in thermal equilibrium in the cosmic history. We will consider particular models where this generic idea can be realized, and show that such a field can naturally account for the present dark matter abundance. This chapter is based on Ref. [1].

2.1 Oscillating scalar field as dark matter

As we have seen in subsection 1.4.2.3, an oscillating scalar field is a plausible dark matter candidate, provided that it is stable and yields the correct present abundance. In general, the field will begin to oscillate after inflation when $m_\phi \simeq H$. If we consider that the field only acquires mass through the Higgs mechanism, its mass vanishes before electroweak symmetry breaking and, consequently, $H > m_\phi$ and the field is overdamped, such that its amplitude remains approximately constant. After the electroweak phase transition at temperatures around 100 GeV, the field acquires a mass that eventually becomes larger than the Hubble parameter. The field then becomes underdamped and begins to oscillate as discussed above. This will generically occur during the radiation-dominated epoch, where the Hubble expansion rate is given by:

$$H = \frac{\pi}{\sqrt{90}}\sqrt{g_*}\frac{T^2}{M_{Pl}} \ , \tag{2.2}$$

where M_{Pl} is the reduced mass Planck, $M_{Pl} = 1/\sqrt{8\pi G}$, T is the cosmic temperature and $g_* = N_B + (7/8)N_F$ is the total number of relativistic degrees of freedom, including N_B and N_F bosonic and fermionic degrees of freedom, respectively.

As we have shown, the field behaves like cold dark matter (CDM) and its energy density scales as $\rho_\phi \sim a^{-3}$. Therefore, the field's amplitude evolves with the scale factor as $\phi \sim a^{-3/2}$ and, by entropy conservation ($a \sim T^{-1}$), we can write it in the following way:

$$\phi\,(T) = \phi_{inf}\left(\frac{T}{T_{osc}}\right)^{3/2} \ , \tag{2.3}$$

where T_{osc} is the temperature at which the field starts to oscillate and ϕ_{inf} is its initial amplitude of oscillations. From Eq. (2.3), we may define an effective number density of ϕ particles in the oscillating scalar condensate:

$$n_\phi = \frac{\rho_\phi}{m_\phi} = \frac{1}{2}\,m_\phi\,\phi_{inf}^2\,\left(\frac{T}{T_{osc}}\right)^3 \ . \tag{2.4}$$

The total entropy density of radiation in the early Universe is given by:

$$s = \frac{2\pi^2}{45} g_{*S} T^3 \ , \tag{2.5}$$

where $g_{*S} = N_B + \frac{3}{4} N_F$ is the effective number of relativistic degrees of freedom contributing to the entropy. Using Eqs. (2.4) and (2.5), it is easy to see that the number of particles in a comoving volume is:

$$\frac{n_\phi}{s} = \frac{m_\phi \phi_{inf}^2 / (2\, T_{osc}^3)}{\frac{2\pi^2}{45}\, g_{*S}} = \text{const}, \tag{2.6}$$

which is a conserved quantity.

We consider now two separate cases, since the field only acquires its mass after the electroweak phase transition at $T_{EW} \sim 100$ GeV. If, on the one hand, the field mass is smaller than the Hubble rate $H_{EW} = \pi/\sqrt{90} g_* T_{EW}^2 / M_P \sim 10^{-5}$ eV, with $g_* \sim 100$ [4], the field will only start to oscillate after the phase transition. If, on the other hand, $m_\phi \gtrsim H_{EW}$, oscillations start as soon as the Higgs field acquires its vacuum expectation value, which we take approximately to be at T_{EW}.

In the first case, for $m_\phi \lesssim H_{EW}$, the temperature at which $m_\phi = H$ and the field starts to oscillate is given by:

$$T_{osc} = \left(\frac{90}{\pi^2}\right)^{1/4} g_*^{-1/4} \sqrt{M_{Pl}\, m_\phi} \ , \tag{2.7}$$

which is valid for temperatures below T_{EW}. Introducing this temperature into Eq. (2.6), we get:

$$\frac{n_\phi}{s} = \frac{1}{8} \left(\frac{90}{\pi^2}\right)^{1/4} g_*^{-1/4} \frac{\phi_{inf}^2}{\sqrt{m_\phi\, M_{Pl}^3}} \ , \tag{2.8}$$

where we have taken $g_* = g_{*S}$ when field oscillations begin. We may then use this to compute the present dark matter abundance, $\Omega_{\phi,0}$, defined as:

$$\begin{aligned} \Omega_{\phi,0} &\equiv \frac{\rho_{\phi,0}}{\rho_{c,0}} = \frac{m_\phi}{3 H_0^2 M_{Pl}^2} \left(\frac{n_\phi}{s}\right) s_0 \\ &\simeq \frac{1}{6} \left(\frac{\pi^2}{90}\right)^{3/4} \frac{g_{*S0}}{g_*^{1/4}} \frac{T_0^3\, m_\phi^{1/2}\, \phi_{inf}^2}{H_0^2\, M_{Pl}^{7/2}} \ , \qquad m_\phi < H_{EW} \ , \end{aligned} \tag{2.9}$$

[4] Note that the electroweak phase transition is not instantaneous, and both the temperature and the number of relativistic species vary during the phase transition. This simplified approach to consider a given temperature and g_* gives nevertheless a sufficiently good approximation for determining the main properties of the dark matter field.

where $H_0 \simeq 1.45 \times 10^{-33}$ eV is the present Hubble parameter, $T_0 \simeq 2.58 \times 10^{-4}$ eV is the present CMB temperature and $g_{*S0} \simeq 3.91$.

For the case where the field starts oscillating immediately after the electroweak phase transition, for $m_\phi \gtrsim H_{EW}$, we take the temperature at the beginning of the field oscillations to be $T_{osc} = T_{EW}$ and, following the same steps as for the previous case, we obtain:

$$\Omega_{\phi,0} \simeq \frac{1}{6} \frac{g_{*S0}}{g_*} \left(\frac{T_0}{T_{EW}} \right)^3 \frac{m_\phi^2 \, \phi_{inf}^2}{H_0^2 \, M_{Pl}^2} \ , \qquad m_\phi > H_{EW} \ . \tag{2.10}$$

Then, assuming that the field accounts for all of the present dark matter abundance, $\Omega_{\phi,0} \simeq 0.26$ [10], we obtain the following relations between the field mass and its initial amplitude:

$$m_\phi \simeq \begin{cases} 3 \times 10^{-5} \left(\frac{g_*}{100} \right)^{1/2} \left(\frac{\phi_{inf}}{10^{13} \text{ GeV}} \right)^{-4} \text{ eV} \ , & m_\phi < H_{EW} \\ 2 \times 10^{-5} \left(\frac{g_*}{100} \right)^{1/2} \left(\frac{\phi_{inf}}{10^{13} \text{ GeV}} \right)^{-1} \text{ eV} \ , & m_\phi > H_{EW} \end{cases} . \tag{2.11}$$

2.2 Inflation and initial conditions for the scalar field

In the previous section we have determined the values of the field mass that may account for the present dark matter abundance as a function of its initial oscillation amplitude. As has been previously observed in the literature [24], the initial conditions for scalar field oscillations in the post-inflationary Universe are set by the inflationary dynamics itself, depending on whether the field mass is greater or smaller than the inflationary Hubble parameter, H_{inf}.

We have assumed above that the dark matter field ϕ acquires mass through the Higgs mechanism, such that its mass during inflation would depend on the inflationary dynamics of the Higgs field itself. As we will see below, we will be interested in extremely small couplings between ϕ and the Higgs field of order $\text{v}/M_{Pl} \sim 10^{-16}$, where $\text{v} = 246$ GeV is the Higgs vacuum expectation value (vev). This implies that the field mass during inflation will be at most of the order of the electroweak scale unless the Higgs field acquires super-planckian values. The dark matter field would thus be light during inflation, and consequently exhibit de-Sitter fluctuations of order $H_{inf}/2\pi$ on super-horizon scales. This would be phenomenologically unacceptable, since this would lead to large inhomogeneities in the dark matter density that would

lead to sizeable cold dark matter isocurvature modes in the CMB spectrum as e.g. for the case of axions (see e.g. Ref. [91]).

The Higgs field need not, however, be the unique source of mass for the dark matter field. In fact, in most extensions of the Standard Model with additional scalar fields, the latter typically acquire masses of the order of the Hubble parameter during inflation. This is, for example, the case of supergravity models, where the scalar potential involves terms of the form $V(\phi) \sim e^{K(\phi)/M_{Pl}^2}\mu^4 + \cdots \sim \mu^4 + \mu^4|\phi|^2/M_{Pl}^2 + \ldots$, where μ^4 is the inflationary energy density, for canonical forms of the Kähler potential, $K(\phi)$. This results in field masses of order $\mu^2/M_{Pl} \sim H_{inf}$, which is the origin of the so-called "eta-problem" found in supergravity/string inflationary scenarios (see e.g. Ref. [92]).

From a more general effective field theory point of view, we may argue that, even if there are no direct renormalizable interactions between the dark matter and the inflaton scalar fields, gravitational interactions may induce non-renormalizable terms of the form:

$$\mathcal{L}_{int} = \frac{c}{2}\frac{\phi^2\, V(\chi)}{M_{Pl}^2} \ , \tag{2.12}$$

where χ is the inflaton field and c is a dimensionless parameter. This leads to a contribution to the field mass $m_\phi \sim c\, H_{inf}$ during inflation that vanishes in the post-inflationary era, assuming that $V(\chi) = 0$ in the ground state. The magnitude (and sign) of this mass cannot be determined in the absence of a UV-complete description of the theory, but in the absence of fine-tuning we expect $|c| \sim \mathcal{O}(1)$, and we will focus, in this chapter, on the case $c > 0$ where the minimum of the ϕ potential lies at the origin. Note that the reheating period may have some effects on the dynamics of the fields, but it does not affect our scenario, as shown in appendix A.

A massive field with $m_\phi \sim H_{inf}$ will nevertheless exhibit quantum fluctuations that get stretched and amplified by expansion during the quasi-de Sitter inflationary phase. For $m_\phi/H_{inf} < 3/2$, the amplitude of each Fourier mode with comoving momentum k is given by [93]:

$$|\delta\phi_k| \simeq \frac{H_{inf}}{\sqrt{2k^3}}\left(\frac{k}{aH_{inf}}\right)^{\frac{3}{2}-\nu_\phi} \ , \tag{2.13}$$

where $\nu_\phi = \left(\frac{9}{4} - \frac{m_\phi^2}{H_{inf}^2}\right)^{1/2}$. Notice that fluctuations do not "freeze" on super-horizon scales, for $k < aH_{inf}$, unless $\nu_\phi \simeq 3/2$, i.e. unless the field is very light. Instead, for a massive field, fluctuations are exponentially damped as inflation proceeds. The homogeneous field component can be obtained by integrating over all super-horizon

modes, yielding for the variance of the scalar field:

$$\left\langle \phi^2 \right\rangle = \left(\frac{H_{inf}}{2\pi}\right)^2 \frac{\left(1-\left(e^{-N_e}\right)^{3-2\nu_\phi}\right)}{3-2\nu_\phi} \simeq \frac{1}{3-2\nu_\phi}\left(\frac{H_{inf}}{2\pi}\right)^2 , \tag{2.14}$$

where, in the last step, we have taken $e^{-N_e} \ll 1$ for $N_e = 50-60$ e-folds of inflation. Notice that the field variance becomes constant, even though each super-horizon Fourier mode is continuously damped. This is associated with the fact that there are always modes $k \sim aH_{inf}$ that give a significant contribution to the variance.

As mentioned above, fluctuations in the dark matter scalar field will lead to isocurvature perturbations in the CMB spectrum, which are then given by [93]:

$$\mathcal{P}_I(k) \equiv \left\langle \left(2\frac{\delta\phi_i}{\phi_i}\right)^2 \right\rangle \simeq \frac{2\pi^2}{k^3}\left(\frac{k}{aH_{inf}}\right)^{3-2\nu_\phi}(3-2\nu_\phi) \ . \tag{2.15}$$

For $m_\phi/H_{inf} > 3/2$, the fluctuations are more suppressed, as we will see in subsection 3.1.1.

Let us focus on the case $m_\phi \sim H_{inf}$ (with real values of ν_ϕ), and determine the minimum field mass during inflation that leads to cold dark matter isocurvature perturbations compatible with observations. For this we consider the dimensionless power spectrum:

$$\Delta_I^2 \equiv \frac{k^3}{2\pi^2}\mathcal{P}_I(k) = (3-2\nu_\phi)\left(\frac{k}{aH_{inf}}\right)^{3-2\nu_\phi} . \tag{2.16}$$

Notice that the comoving scales that are relevant for CMB perturbations have left the horizon 50-60 e-folds before the end of inflation, such that at the end of inflation $k/aH_{inf} \simeq e^{-N_e} \ll 1$. Isocurvature modes are then measured in terms of the ratio:

$$\beta_{iso}(k) = \frac{\Delta_I^2(k)}{\Delta_{\mathcal{R}}^2(k)+\Delta_I^2(k)}, \tag{2.17}$$

where $\Delta_{\mathcal{R}}^2 \simeq 2.2\times10^{-9}$ is the amplitude of the adiabatic curvature perturbation spectrum generated by the inflaton field χ. Note that the dark matter field is sub-dominant during inflation, so that its fluctuations do not induce perturbations in the space-time curvature. CDM isocurvature modes and adiabatic modes will be uncorrelated, since fluctuations in ϕ and χ are independent. The Planck collaboration data places an upper bound on uncorrelated CDM isocurvature perturbations $\beta_{iso}(k_{mid}) < 0.037$ for $k_{mid} = 0.050$ Mpc^{-1} [13]. Using the above results, this yields $\nu_\phi \lesssim 1.3$ for 55 e-folds of inflation, implying $m_\phi \gtrsim 0.75 H_{inf}$.[5]

[5]Although there are more recent bounds (Ref. [94]), our results remain unchanged.

This lower bound on the dark matter field mass during inflation allows us to place an upper bound on the variance of the field at the end of inflation of $\langle\phi^2\rangle \lesssim 0.25^2\, H_{inf}^2$, and for masses of the order of the Hubble parameter during inflation we have $\langle\phi^2\rangle = \alpha^2 H_{inf}^2$, with $\alpha \simeq 0.1 - 0.25$, where $\alpha = 0.1$ corresponds to $m_\phi = 1.5\, H_{inf}$. This variance will set the average amplitude of the field at the end of inflation, and since the field remains overdamped until after the electroweak phase transition, we take the initial amplitude for field oscillations in the post-inflationary era to be in this range, i.e.:

$$\phi_{inf} \simeq \alpha H_{inf} \ , \qquad \alpha \simeq 0.1 - 0.25 \ . \tag{2.18}$$

We may express the Hubble parameter during inflation in terms of the tensor-to-scalar ratio, $r = \Delta_t^2/\Delta_{\mathcal{R}}^2$, since the amplitude of the primordial gravitational wave spectrum is a direct probe of the inflationary energy scale, with:

$$H_{inf} = \frac{\pi}{\sqrt{2}}\sqrt{\Delta_{\mathcal{R}}^2} M_{Pl}\sqrt{r} \simeq 2.5 \times 10^{13} \left(\frac{r}{0.01}\right)^{1/2} \text{ GeV} \ . \tag{2.19}$$

Replacing this into Eq. (2.11), we can obtain a relation between the dark matter field mass and the tensor-to-scalar ratio:

$$m_\phi \simeq 2 \times 10^{-5} \left(\frac{g_*}{100}\right)^{1/2} \times \begin{cases} (\alpha/0.25)^{-4}(r/0.03)^{-2} \ , & m_\phi < H_{EW} \\ (\alpha/0.25)^{-1}(r/0.03)^{-1/2} \ , & m_\phi > H_{EW} \end{cases} \text{ eV} \ . \tag{2.20}$$

This relation is illustrated in Fig. 2.1, where one can see that the upper bound $r < 0.11$ set by the Planck collaboration at 95% C.L. [13] leads to a lower bound on the field mass $m_\phi \gtrsim 10^{-6} - 10^{-5}$ eV for $\alpha \simeq 0.1 - 0.25$.

In the next sections we discuss possible scenarios that may lead to field masses of this order through the electroweak Higgs mechanism.

2.3 Non-renormalizable interactions between the dark matter and Higgs fields

The present dark matter abundance and the initial conditions set by the inflationary dynamics require very small scalar field masses, unless the tensor-to-scalar ratio is very suppressed. If the dark matter field were to couple directly to the Higgs field, via renormalizable operators, we would expect a mass not much below e.g. the electron mass, unless the coupling is unnaturally small. However, we may envisage theories

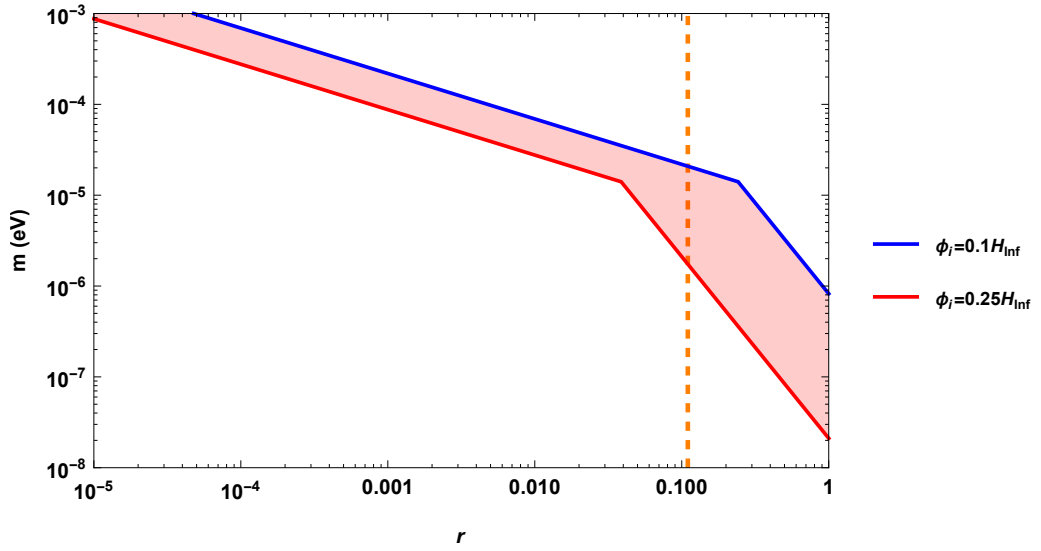

Figure 2.1: Relation between the dark matter field mass and the tensor-to-scalar ratio for an initial field amplitude $\phi_{inf} = \alpha\, H_{inf}$ set by inflationary de Sitter fluctuations, with $\alpha = 0.1 - 0.25$, corresponding to field masses during inflation $m_\phi \simeq (0.75 - 1.5)\, H_{inf}$. The dashed line gives the upper bound on the tensor-to-scalar ratio set by the Planck collaboration at 95% C.L. [13].

where such couplings are not present and, for instance, the dark matter field belongs to a *hidden* sector that is sequestered from the *visible* sector, which contains the Standard Model fields and in particular the Higgs boson. The absence of bare mass for the dark matter field could, for example, be motivated by a conformal symmetry or scale invariance in the hidden sector. The two sectors may, nevertheless, be indirectly coupled through heavy messenger fields that are e.g. charged under the gauge symmetries of both sectors. Even in the absence of such messengers, the two sectors will be coupled through gravity. Taking a strictly effective field theory point of view, we may consider that the conformal symmetry/scale invariance in the hidden sector is broken only by non-renormalizable terms suppressed by a mass scale M that corresponds to the messenger mass, or M_{Pl} in the case of gravity-mediated interactions.

Imposing a $\mathbb{Z}_2$ reflection symmetry on the dark matter field, i.e. the invariance of the Lagrangian under $\phi \to -\phi$, we can ensure the stability of the field, since linear terms that allow for its decay are thus forbidden. In this case, the lowest-order non-renormalizable operator involving the dark matter and the Higgs field is of dimension-6

and takes the form:

$$\mathcal{L}_{int} = a_6^2 |\mathcal{H}|^4 \frac{\phi^2}{M^2} \ , \tag{2.21}$$

where a_6 is a dimensionless parameter, which we expect to be $\mathcal{O}(1)$. It is then easy to see that, after electroweak symmetry breaking when the Higgs field acquires its vev, the dark matter field acquires a mass:

$$m_\phi = \frac{a_6}{2} \frac{v^2}{M} \sim 10^{-5}\, a_6 \left(\frac{M}{M_{Pl}}\right)^{-1} \quad \text{eV} \ . \tag{2.22}$$

This implies that one obtains a dark matter field mass in the range required by the observed abundance for Planck-suppressed interactions, assuming inflation occurs close to the GUT scale and the tensor-to-scalar ratio is not too suppressed ($r \gtrsim 10^{-3}$). If inflation occurs at an energy scale somewhat below the GUT scale, leading to lower values of the tensor-to-scalar ratio, the observed dark matter abundance would require larger values of m_ϕ, and these could equally be motivated e.g. by messenger masses at or below the GUT scale.

The case of Planck-suppressed interactions seems, however, rather special, since the hierarchy between the electroweak and Planck scales leads to a similar hierarchy between the dark matter and Higgs masses. This motivates going beyond the effective field theory perspective and finding a concrete and well-motivated scenario where this hierarchy is naturally obtained, as we describe in the next section.

2.4 Scalar field dark matter in warped extra dimensions

A concrete realization of the hierarchy mentioned in the previous section in the context of an effective field theory can be found in the Randall-Sundrum (RS) scenario for warped extra-dimensions [95]. The RS construction considers a model with one additional spatial dimension with a warped geometry, and which is compactified in an orbifold $S^1/\mathbb{Z}_2$. This geometry can be viewed as an effective dimensional reduction of brane-models in 10/11-dimensional string/M-theory, where brane tensions are responsible for warping the geometry in the directions transverse to their world-volume.

The bulk geometry is a slice of anti-de Sitter space (AdS_5), where the metric

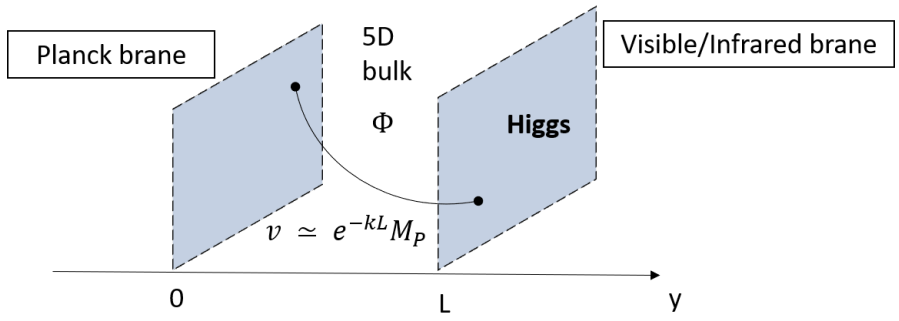

Figure 2.2: The Randall-Sundrum scenario. The Higgs boson is confined to the brane at $y = L$, and its mass and expectation value are exponentially suppressed with respect to the fundamental mass scale in the construction, which is taken to be the Planck scale. This explains the large hierarchy $e^{-kL} \simeq v/M_P \simeq 10^{-16}$ between the electroweak and gravitational scales and a solution to the hierarchy problem.

corresponds to the warped product:

$$ds^2 = e^{-2\sigma(y)} g_{\mu\nu} dx^\mu dx^\nu + dy^2, \tag{2.23}$$

where $y \in [-L, L]$ is the radial coordinate along the extra-dimension, for $L = \pi r_c$ with r_c denoting the compactification radius, and $\mu, \nu = 0, 1, 2, 3$. The warp factor is given in terms of the linear function $\sigma(y) = k|y|$, where k is the bulk AdS curvature. The orbifold symmetry has two fixed points at $y = 0$ and $y = L$, where branes of opposite tension reside. Einstein's equations then require a particular relation between the brane tensions and the (negative) bulk cosmological constant.

In their original proposal, Randall and Sundrum observed that if the Standard Model fields, in particular the Higgs boson, were confined to the brane at $y = L$, the Higgs mass and its expectation value would be exponentially suppressed with respect to the fundamental mass scale in the construction, which is taken to be the Planck scale. One then naturally obtains a large hierarchy $e^{-kL} \simeq v/M_P \simeq 10^{-16}$ between the electroweak and gravitational scales for a relatively small extra-dimension, providing a simple solution to the well-known gauge hierarchy problem. This scenario is illustrated in Fig. (2.2). The Randall-Sundrum model has, since its original proposal, been the object of several analyses and extensions, including e.g. scenarios where the Standard Model gauge and fermion fields reside in the bulk [96, 97], which could explain e.g. the measured fermion mass hierarchy.

Here we will show that the required hierarchy between the dark matter and Higgs

field masses can also be naturally obtained within the RS construction, if the dark matter field corresponds to the zero-mode of a bulk scalar field that is coupled to the Higgs field on the "visible" or "infrared" brane at $y = L$. We start with the following five-dimensional action for the Higgs and dark matter sectors:

$$\begin{aligned} S &= \int d^4x \int dy \sqrt{-G} \left[\frac{1}{2} G^{MN} \partial_M \Phi \partial_N \Phi - \frac{1}{2} M_\Phi^2 \Phi^2 \right. \\ &+ \left. \delta(y - L) \left(G^{MN} \partial_M h^\dagger \partial_N h - V(h) + \frac{1}{2} g_5^2 \Phi^2 h^2 \right) \right] , \end{aligned} \tag{2.24}$$

where G_{MN} is the five dimensional metric, Φ is the 5-dimensional scalar field that includes the dark matter field as its zero-mode and g_5 is the five-dimensional coupling between the Higgs and bulk scalars on the visible brane. In general, we may include a bare mass term for the scalar field, that is even under the $\mathbb{Z}_2$ orbifold symmetry and can be parametrized as [96]:

$$M_\Phi^2 = ak^2 + b\sigma'' , \tag{2.25}$$

where a and b are dimensionless parameters yielding the bulk and boundary contributions to the field mass, such that:

$$\sigma' = \frac{d\sigma}{dy} = k \, \mathrm{sgn}(\mathrm{y}) , \qquad \sigma'' = \frac{d^2\sigma}{dy^2} = 2k \left[\delta(y) - \delta(y - L) \right] . \tag{2.26}$$

From the five-dimensional action we may derive the equation of motion for the bulk scalar. Assuming that a perturbative approach is valid, we may first neglect the brane-localized interactions with the Higgs field, to obtain:

$$\frac{1}{\sqrt{-G}} \partial_M \left(\sqrt{-G} \, G^{MN} \partial_N \Phi \right) - M_\Phi^2 \Phi = 0 . \tag{2.27}$$

Using the metric Eq. (2.23), this can be written in the form:

$$\left[e^{2\sigma} g^{\mu\nu} \partial_\mu \partial_\nu + e^{4\sigma} \partial_y \left(e^{-4\sigma} \partial_y \right) - M_\Phi^2 \right] \Phi(x^\mu, y) = 0 . \tag{2.28}$$

We can then decompose the bulk scalar into a tower of Kaluza-Klein (KK) modes:

$$\Phi(x^\mu, y) = \frac{1}{\sqrt{2L}} \sum_{n=0}^{\infty} \phi_n(x^\mu) \, f_n(y) , \tag{2.29}$$

where the mode functions $f_n(y)$ satisfy the orthonormality condition:

$$\frac{1}{2L} \int_{-L}^{L} dy \, e^{-2\sigma} \, f_n(y) \, f_m(y) = \delta_{nm} . \tag{2.30}$$

Substituting into Eq. (2.28), we get:

$$\left[-e^{4\sigma} \partial_y \left(e^{-4\sigma} \partial_y \right) + M_\Phi^2 \right] f_n = e^{2\sigma} \, m_n^2 \, f_n, \tag{2.31}$$

where m_n is the mass of the Kaluza-Klein mode n. This equation admits, in particular, a massless solution $f_0(y)$ with $m_n = 0$ of the form:

$$f_0(y) = c_1^0 \, e^{\left(2-\sqrt{4+a}\right)ky} + c_2^0 \, e^{\left(2+\sqrt{4+a}\right)ky} \ , \tag{2.32}$$

where c_1^0 and c_2^0 are constants, and the orbifold symmetry allows us to focus on the interval $y \in [0, L]$. This solution only exists for fields that are even under the orbifold $\mathbb{Z}_2$ symmetry [96], and which must satisfy the boundary conditions:

$$\left(\frac{df_n}{dy} - b\sigma' f_n \right) \Big|_{0,L} = 0 \ . \tag{2.33}$$

For the zero-mode, this implies $c_1^0 = 0$ and $b = 2 \pm \sqrt{4+a}$. Imposing the normalization condition (2.30), the zero-mode profile is then given by:

$$f_0(y) = \sqrt{\frac{2Lk\,(b-1)}{e^{2kL(b-1)} - 1}} e^{bky} \ . \tag{2.34}$$

We will now focus on the particular case $a = b = 0$, for which the bulk scalar is scale invariant and the associated zero-mode function is flat:

$$f_0(y) \simeq \sqrt{2kL} \ , \tag{2.35}$$

where we used that $e^{-kL} \sim v/M_{Pl} \ll 1$. If we now replace this mode-function into the brane-localized terms in the action, we find the following effective interaction between the zero-mode and the Higgs fields:

$$\mathcal{L}_{\phi h} = \frac{1}{2} g_5^2 k e^{-2kL} \phi^2 h^2 \ , \tag{2.36}$$

where we have rescaled the Higgs field $h \to e^{kL} h$ in order for it to have a canonically normalized kinetic term in four dimensions, and denoted the zero-mode field $\phi_0(x) \equiv \phi(x)$. Thus, noting that $g_5^2 k$ is a dimensionless quantity and that the AdS curvature $k \simeq M_{Pl}$ is the fundamental scale in the RS scenario, we expect the effective four-dimensional coupling between ϕ and the Higgs field to be:

$$g = \sqrt{g_5^2 k} e^{-2kL} \simeq \mathcal{O}(1) \times \frac{\mathrm{v}}{M_{Pl}} \sim 10^{-16} \ . \tag{2.37}$$

Thus, assuming that the five-dimensional coupling has a natural value $g_5 \sim k^{-1/2}$, we conclude that, after the electroweak symmetry is broken, the zero-mode of our bulk scalar acquires a mass $m_\phi \sim \mathrm{v}^2/M_{Pl} \sim 10^{-5}$ eV, just like for the non-renormalizable interactions considered in the previous section. Of course the five-dimensional coupling

may somewhat differ from the natural scale without much fine-tuning of the extra-dimensional model, but this shows that the zero-mode of a scale invariant bulk scalar in the RS model acquires a mass in the correct range to account for the dark matter in the Universe as an oscillating scalar field. The effect of a Planck-suppressed non-renormalizable operator is thus analogous to a renormalizable interaction in a higher-dimensional warped geometry.

One of the assumptions of the generic analysis we performed in the previous sections is that the dark matter field acquires a Hubble-scale mass during inflation from a non-renormalizable coupling to the inflaton field. This can be implemented within the RS construction if, for example, the inflaton field χ also lives on the visible brane and we consider brane-localized interactions of the form:

$$S_{\Phi,\chi} = h_5 \int d^4x \int dy \sqrt{-G}\, \delta\left(y - L\right)\, \Phi^2\, V\left(\chi\right)\ . \tag{2.38}$$

Since, by dimensional analysis, $h_5 \sim k^{-3} \sim M_{Pl}^{-3}$, it is easy to conclude that the effective four-dimensional coupling between the inflaton and the dark matter zero-mode field is of the form $\phi^2 V(\chi)/k^2 \sim \phi^2 V(\chi)/M_{Pl}^2$, thus naturally yielding a Hubble-scale mass for the dark matter field during inflation which vanishes in the post-inflationary era.

Within the RS construction, the remaining KK modes of the bulk scalar field could, in principle, also contribute to the dark matter density if they oscillate with a sufficiently large amplitude after inflation. Although we will not analyze the properties of these modes in detail, referring the reader to existing discussions in the literature as e.g. Ref. [96], we must ensure that they will not *overcontribute* to the dark matter density. In particular, for $n > 1$, the mass spectrum for an even field with $a = b = 0$ is given by:

$$m_n \simeq \left(n + \frac{1}{4}\right) \pi k e^{-kL}\ , \tag{2.39}$$

such that the lowest KK masses lie at the TeV scale and are, hence, much heavier than the zero-mode. This could lead to an overabundance of dark matter, but we note that the KK mode functions are given approximately by:

$$f_n(y) \simeq \sqrt{2kL} e^{k(2y-L)} \frac{J_2\left(m_n e^{ky}/k\right)}{J_2\left(m_n e^{kL}/k\right)}\ , \tag{2.40}$$

where J_2 corresponds to the Bessel function of the first kind. This implies that their coupling to fields on the visible brane is exponentially larger than the coupling of the

zero-mode, with $f_n(L) = e^{kL} f_0(L)$, and consequently that their mass during inflation is necessarily much larger than the inflationary Hubble scale. Since these may actually be super-planckian, it is not possible to study their dynamics during inflation as for the case of the zero-mode, but this analysis nevertheless shows that we do not expect the KK modes of the bulk scalar to develop large expectation values during inflation and hence oscillate with a large amplitude in the post-inflationary eras. However, those heavy modes might decay rather quickly through gravitational interactions and then we expect that indeed only the zero-mode contributes significantly to the present abundance of non-relativistic matter.

Finally, in our previous dynamical analysis of the oscillating dark matter field, we have neglected the effects of any field self-interactions. Although the assumption of a bulk conformal symmetry for the five-dimensional scalar field implies that no bare self-interaction terms exist, we must take into account that this symmetry is broken on the visible brane by the interactions with the Higgs field (as well as the inflaton but this does not affect the post-inflationary dynamics). This generates, in particular, a quartic coupling for the dark matter zero-mode field through radiative corrections. At 1-loop, these corrections correspond to the diagram in Fig. 2.3, which up to numerical factors and the usual logarithms generates a quartic-self coupling $\lambda_\phi \sim g^4$.

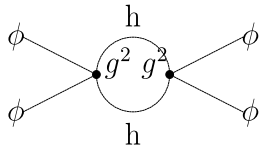

Figure 2.3: Feynman diagram inducing a dark matter self-coupling at 1-loop order.

Since after inflation the field has a large expectation value $\phi_{inf} \sim \alpha H_{inf}$, these self-interactions yield a contribution to the dark matter field mass $\Delta m_\phi^2 \sim \lambda_\phi \, \phi_{inf}^2 \sim g^4 H_{inf}^2$. It is easy to check that $\Delta m_\phi^2 / m_\phi^2 \sim H_{inf}^2 / M_{Pl}^2 \ll 1$, so that we may safely neglect the effect of these self-interactions on the dynamics of the dark matter field.

2.5 Summary

In this chapter, we have analyzed the possibility of an oscillating scalar field, ϕ, which acquires mass through the Higgs mechanism, accounting for the observed dark matter abundance in the Universe.

We have argued that the field acquires a large expectation value during inflation, just below the inflationary Hubble parameter, due to quasi-de Sitter quantum fluctuations, which sets the average initial amplitude of the field oscillations. Despite the large overall variance of the field, its fluctuations on the presently observable CMB scales are exponentially damped, since scalar fields generically acquire Hubble-scale masses through gravitationally-induced couplings to the inflaton. Thus, in contrast with e.g. axion fields, which remain massless during inflation and acquire large fluctuations on all super-horizon scales, inflationary fluctuations would not generate significant matter isocurvature perturbations in the present scenario.

After inflation the field becomes massless and its amplitude remains approximately frozen until the electroweak phase transition, after which the field acquires a small mass through its coupling to the Higgs field. Eventually the field becomes underdamped and begins to oscillate about the origin, behaving as cold dark matter. We have also imposed a $\mathbb{Z}_2$ symmetry on the Lagrangian that ensures the stability of the dark matter field. The observed dark matter abundance then allows us to determine the field mass as a function of the inflationary Hubble scale, and the current Planck bound on the tensor-to-scalar ratio [13] sets a lower bound on the field mass $m_\phi \gtrsim 10^{-6} - 10^{-5}$ eV.

If inflation occurs close to the GUT scale and the tensor-to-scalar ratio is within the range of planned CMB experiments, $r \gtrsim 10^{-3}$, we concluded that the mass of the scalar field must saturate the above bound, and we observed that this implies the approximate hierarchy between the dark matter mass and the Higgs expectation value:

$$\frac{m_\phi}{\mathrm{v}} \sim \frac{\mathrm{v}}{M_{Pl}} \ . \tag{2.41}$$

We have then explored different scenarios where this hierarchy may be attained. A first, more generic, possibility is that the dark matter and Higgs fields are only coupled through Planck-suppressed gravitational interactions. We have, in addition, presented a more concrete possibility that the dark matter field is the zero-mode of a five-dimensional scalar field living in a warped extra-dimension. In the context of the Randall-Sundrum model, this mode acquires a mass through its coupling to the Higgs field, which is confined to the visible brane at the bottom of the warped throat. We have also shown that, within this scenario, this field acquires a Hubble-scale mass during inflation, as initially assumed, when the inflaton is also localized on the visible brane.

A generic feature of these scenarios is that the dark matter field has no bare mass or self-interactions, which may be motivated by imposing a conformal/scale symmetry

that is broken only by the non-renormalizable or brane-localized interactions with the Higgs field after electroweak symmetry breaking. The resulting interactions between the dark matter and Higgs bosons are thus extremely suppressed, with an effective coupling $g \sim 10^{-16}$. On the one hand, this justifies neglecting any dissipative effects in the dynamics of the oscillating scalar field, which could e.g. lead to its evaporation and subsequent thermalization as considered in Ref. [31]. On the other hand, this will make its detection extremely difficult.

The dark matter field exhibits, however, some similarities with axions and other axion-like particles, namely in terms of its small mass and couplings to known particles. This suggests that it may be possible to probe the existence and properties of the proposed dark matter scalar field with experiments analogous to those employed in the search of axion-like particles, or even using similar indirect astrophysical signatures, as we will show in chapter 3. The nature and interaction structure of these fields are, nevertheless, sufficiently different that one may hope to distinguish them experimentally.

3 | General Higgs portal scalar field dark matter

In this chapter, we will consider a model of a complex scalar field acting as dark matter, Φ, interacting with the Higgs doublet, $\mathcal{H}$, only through scale-invariant interactions. We assume that scale invariance is spontaneously broken by some unspecified mechanism that generates both the Planck scale, M_{Pl}, and a negative squared mass for the Higgs field at the electroweak scale, thus working within an effective field theory where these mass scales are non-dynamical. The important assumption is that scale-invariance is preserved in the dark matter sector, such that the dark scalar only acquires mass after the EWPT. In addition, our scenario has also a U(1) symmetry (or $\mathbb{Z}_2$ symmetry for a real scalar, as we discuss later on) that, if unbroken, ensures the stability of the dark scalar. Its dynamics are thus fully determined by its interaction with the Higgs boson and gravity, as well as its self-interactions, all parametrized by dimensionless couplings. The relevant interaction Lagrangian density is thus given by:

$$-\mathcal{L}_{int} = \pm\, g^2 \left|\Phi\right|^2 \left|\mathcal{H}\right|^2 + \lambda_\phi \left|\Phi\right|^4 + V\left(\mathcal{H}\right) + \xi R \left|\Phi\right|^2 \ , \tag{3.1}$$

where the Higgs potential, $V\left(\mathcal{H}\right)$, has the usual "mexican hat" shape, g is the coupling between the Higgs and the dark scalar and λ_ϕ is the dark scalar's self-coupling. The last term in Eq. (3.1) corresponds to a non-minimal coupling of the dark matter field to curvature, where R is the Ricci scalar and ξ is a constant. Note that such a Lagrangian density is an extension of the model that we considered in chapter 2 where self-interactions played no role in the dynamics, giving origin to a very light dark scalar, $m_\phi \sim \mathcal{O}\left(10^{-5}\,\mathrm{eV}\right)$, and therefore a very small coupling to the Higgs boson, $g \sim 10^{-16}$. Such feeble interactions make such a dark matter candidate nearly impossible to detect in the near future, and in this present chapter we will show that the inclusion of self-interactions allows for heavier and hence more easily detectable dark scalars.

On the one hand, if the Higgs-dark scalar interaction has a positive sign, the U(1) symmetry remains unbroken in the vacuum and the dark scalar is stable. On the other hand, if the interaction has a negative sign, the U(1) symmetry may be spontaneously broken, which can lead to interesting astrophysical signatures. In this chapter we wish to provide a thourough discussion of the dynamics and phenomenology in both cases, highlighting their differences and similarities and exploring the potential to probe such a dark matter candidate both in the laboratory and through astrophysical observations. This chapter is based on Refs. [2, 3].

3.1 Dynamics before electroweak symmetry breaking

Before the EWPT, the dynamics of the field does not depend on the sign of the coupling to the Higgs, since it plays a sub-leading role. This allows us to describe the behavior of the field without making any distinction between the two cases. We will first explore the dynamics during the early period of inflation, where the non-minimal coupling to gravity plays the dominant role, and then the subsequent evolution in the radiation era, where the field dynamics is mainly driven by its quartic self-coupling.

3.1.1 Inflation

We consider a dark scalar field non-minimally coupled to gravity, with the full action being given by:

$$S = \int \sqrt{-g}\, d^4x \left[\frac{1}{2} M_{Pl}^2 f(\phi) R - \frac{1}{2} (\nabla\phi)^2 - V(\phi) \right] , \tag{3.2}$$

where $\Phi = \phi/\sqrt{2}$ and $f(\phi) = 1 - \xi\,\phi^2/M_{Pl}^2$ [6]. The equation of motion for the homogeneous field component in a flat FRW Universe is thus:

$$\ddot{\phi} + 3H\dot{\phi} + V'(\phi) + \xi R\phi = 0 , \tag{3.3}$$

such that the non-minimal coupling to gravity generates an effective mass for the field. We assume that inflation is driven by some other scalar field, which is consistent since,

[6] Since $\phi \ll M_{Pl}$ and $\xi \lesssim 1$, $f(\phi) \simeq 1$ and there is no significant difference between the Jordan and Einstein frames. In addition, ϕ is not the inflaton and, therefore, the gravitational dynamics during inflation is not altered by ϕ, regardless of its non-minimal coupling to curvature.

as we show below, the energy density of ϕ is sub-dominant during this phase. We will consider the case where $\xi \gg g$, λ_ϕ, such that the dynamics during inflation is mainly driven by the non-minimal coupling to gravity. Since during inflation $R \simeq 12\, H_{inf}^2$, where the nearly constant Hubble parameter can be written in terms of the tensor-to-scalar ratio r, as in Eq. (2.19), the effective field mass is:

$$m_\phi \simeq \sqrt{12\,\xi}\, H_{inf} \ , \tag{3.4}$$

with $m_\phi > H_{inf}$ for $\xi > 1/12$.

The mass of the dark scalar has to exceed the Hubble parameter during inflation, since otherwise it develops significant fluctuations on super-horizon scales that may give rise to observable cold dark matter isocurvature modes in the CMB anisotropy spectrum, which are severely constrained by data [94]. This implies that the classical field is driven towards the origin during inflation, but its average value can never vanish due to its de-Sitter quantum fluctuations on super-horizon scales. As stated in subsection 2.2, any massive scalar field exhibits quantum fluctuations that get stretched and amplified by the expansion of the Universe. For $m_\phi/H_{inf} > 3/2$ ($\xi > 3/16$), the amplitude of each super-horizon momentum mode is suppressed by the mass of the dark scalar field, yielding a spectrum [93]:

$$|\delta\phi_k|^2 \simeq \left(\frac{H_{inf}}{2\pi}\right)^2 \left(\frac{H_{inf}}{m_\phi}\right) \frac{2\pi^2}{(a\, H_{inf})^3} \ , \tag{3.5}$$

where $a(t)$ is the scale factor. Integrating over the super-horizon comoving momentum $0 < k < aH_{inf}$, at the end of inflation, the homogeneous field variance reads:

$$\left\langle \phi^2 \right\rangle \simeq \frac{1}{3} \left(\frac{H_{inf}}{2\pi}\right)^2 \frac{1}{\sqrt{12\xi}} \ , \tag{3.6}$$

setting the average amplitude of the field at the onset of the post-inflationary era, ϕ_{inf}:

$$\phi_{inf} = \sqrt{\langle \phi^2 \rangle} \simeq \alpha\, H_{inf} \qquad \alpha \simeq 0.05\, \xi^{-1/4} \ . \tag{3.7}$$

On the other hand, if $\xi < 3/16$, $m_\phi/H_{inf} < 3/2$, the spectrum is given by Eq. (2.13). Following the same steps as in subsection 2.2, using Eqs. (2.13)-(2.17) and recalling that $\nu_\phi = \left(\frac{9}{4} - \frac{m_\phi^2}{H_{inf}^2}\right)^{1/2}$, for 55 e-folds of inflation, this yields $\nu_\phi \lesssim 1.3$, implying that $m_\phi \gtrsim 0.75\, H_{inf}$ and setting a lower bound:

$$\xi \gtrsim 0.05 \ , \tag{3.8}$$

which thus gives for the average homogeneous field amplitude at the end of inflation:

$$\phi_{inf} = \sqrt{\langle \phi^2 \rangle} \simeq \alpha \, H_{inf} \qquad \alpha \lesssim 0.25 \ , \tag{3.9}$$

as found in subsection 2.2.

Note that the energy-momentum tensor for the dark scalar is given by:

$$\begin{aligned} T_{\mu\nu} = & \left(1 - 4\xi\right) \nabla_\mu \phi \nabla_\nu \phi + 4\xi \phi \left(g_{\mu\nu} \nabla_\alpha \nabla^\alpha - \nabla_\mu \nabla_\nu\right) \phi \\ & + g_{\mu\nu} \left[- \left(\frac{1}{2} - 4\xi \right) \nabla_\alpha \phi \nabla^\alpha \phi - V\left(\phi\right) - \xi R \phi^2 \right] + 2\xi \phi^2 R_{\mu\nu} \ , \end{aligned} \tag{3.10}$$

where $R_{\mu\nu}$ is the Ricci tensor. The energy density and pressure of the field are thus, respectively,

$$\rho_\phi = \frac{\dot{\phi}^2}{2} + V\left(\phi\right) + 12\xi H \phi \dot{\phi} + 6\xi \phi^2 H^2 \ , \tag{3.11}$$

$$p_\phi = \frac{1}{2} \left(1 - 8\xi\right) \dot{\phi}^2 - V\left(\phi\right) + 4\xi \phi V'\left(\phi\right) + 4\xi \phi \dot{\phi} H + \xi \phi^2 \left[\left(8\xi - 1\right) R + 2 \, \frac{\ddot{a}}{a} + 4 \, H^2 \right] \ ,$$

where a is the scale factor. Using $\dot{\phi} \sim m_\phi \phi$ for an underdamped field, we can easily see that $\rho_\phi \lesssim H_{inf}^4$ for $\xi \lesssim 10$, so that the dark scalar will not affect the inflationary dynamics even for large values of its non-minimal coupling to gravity. Note that this assumes also that the Higgs field does not acquire a large expectation value during inflation, which is natural since de Sitter fluctuations also generate an average Higgs value $\lesssim H_{inf}$ [24].

After inflation, the field will oscillate about the minimum of its potential and its effective mass $m_\phi \gg H$, and we show in Appendix B that, for $\xi \lesssim 1$, all modifications to the dark field's energy density and pressure due to its non-minimal coupling to gravity become sub-dominant or average out to zero, thus recovering the conventional form for $\xi = 0$. In addition, since $R = 0$ in a radiation-dominated era and $R \sim \mathcal{O}(H^2)$ in subsequent eras, the non-minimal coupling's contribution to the field's mass also becomes negligible. Thus, we may safely neglect the effects of the non-minimal coupling to gravity in its post-inflationary evolution, hence its only role is to make the field sufficiently heavy during inflation so to prevent the generation of significant isocurvature modes in the CMB anisotropy spectrum.

We should also briefly mention that, during the (p)reheating period, the Ricci scalar oscillates with the inflaton field, χ, since $R = (3p_\chi - \rho_\chi)/M_{Pl}^2 \sim m_\chi^2 \chi^2 / M_{Pl}^2$, inducing an effective biquadratic coupling between the dark scalar and the inflaton, $g_{\phi\chi}^2 \sim \xi m_\chi^2 / M_{Pl}^2 \ll 1$. This interaction will lead to ϕ-particle production during

reheating but, since $q_\phi = g_{\phi\chi}^2 \chi^2/4m_\chi^2 \sim \xi\chi^2/M_{Pl}^2 \lesssim 1$ with $\chi \lesssim M_{Pl}$ during reheating, this should not be very efficient. In particular, it is natural to assume that the inflaton couples more strongly to other fields, which will thus be produced more efficiently and consequently reduce the amplitude of the inflaton's oscillations before any significant ϕ-particle production occurs. In addition, such particles remain relativistic until $T < m_\phi \ll T_{EW}$, and as we will see this implies that their density is much more diluted than the density of the homogeneous dark scalar condensate. We therefore expect ϕ-particle production during reheating to yield a negligible contribution to the present dark matter abundance.

3.1.2 Radiation era

After inflation and the reheating period, which we assume for simplicity to be "instantaneous", i.e. sufficiently fast, the Universe undergoes a radiation-dominated era for which $R = 0$. Above the electroweak scale, the potential is then dominated by the quartic term,

$$V(\phi) \simeq \lambda_\phi \frac{\phi^4}{4} \ . \tag{3.12}$$

The field is in an overdamped regime until the effective field mass, $m_\phi = \sqrt{3\,\lambda_\phi}\,\phi$, exceeds the Hubble parameter in this era. At this point, the field begins oscillating about the origin with an amplitude that decays as $a^{-1} \propto T$ and $\rho_\phi \sim a^{-4}$, thus behaving like dark radiation.

The temperature at the onset of the post-inflationary field oscillations can be found by equating the effective field mass with the Hubble parameter (Eq. (1.34)):

$$T_{rad} = \lambda_\phi^{1/4} \sqrt{\phi_{inf}\, M_{Pl}} \left(\frac{270}{\pi^2\, g_*}\right)^{1/4} \ , \tag{3.13}$$

where g_* is the number of relativistic degrees of freedom. The temperature T_{rad} is thus below the reheating temperature, $T_{rh} \sim \sqrt{M_{Pl}\, H_{inf}}$. Since the field behaves like radiation, its amplitude decreases with T:

$$\phi_{rad}(T) = \frac{\phi_{inf}}{T_{rad}}\, T = \left(\frac{\pi^2\, g_*}{270}\right)^{1/4} \left(\frac{\phi_{inf}}{M_{Pl}}\right)^{1/2} \frac{T}{\lambda_\phi^{1/4}} \ . \tag{3.14}$$

Notice that, above the electroweak scale, thermal effects maintain the Higgs field localized in the vicinity of the origin, with average thermal fluctuations $\langle h^2 \rangle \ll T^2$, as shown e.g. in Ref. [98]. We can use this to show that the Higgs-dark scalar field

interactions play a subdominant role before the EWPT. In particular, in the parametric regime that we are interested in (see Eqs. (3.40) and (3.49)), $g \sim 10^{-3}\lambda_\phi^{1/4}$, $\xi \lesssim 1$ and $r < 0.1$:

$$\frac{g^2\phi_{rad}^2 \langle h^2\rangle /4}{\lambda_\phi \phi_{rad}^4/4} \sim \frac{\langle h^2\rangle}{T^2} \ll 1, \tag{3.15}$$

since $\langle h^2\rangle \sim \frac{T^5}{M_{Pl}^3}$ according to Ref. [98].

The dark scalar continues to behave like radiation until the EWPT, at which point the Higgs field acquires its vacuum expectation value, $\mathcal{H} = h/\sqrt{2} = \mathrm{v}/\sqrt{2}$, generating a mass for the dark scalar. The EWPT transition will be completed once the leading thermal contributions to the Higgs potential become Boltzmann-suppressed, which occurs approximately at $T_{EW} \sim m_W$, where m_W is the W boson's mass. Comparing the quadratic and quartic terms in the dark scalar potential at T_{EW}, we find:

$$\frac{g^2\,\mathrm{v}^2\,\phi_{EW}^2/4}{\lambda_\phi \phi_{EW}^4/4} \simeq 10^7\,\xi^{1/4}\left(\frac{r}{0.01}\right)^{-1/2}\frac{g^2}{\lambda_\phi^{1/2}}\,, \tag{3.16}$$

where we used that $g_{*S} \simeq 86.25$ for the number of relativistic degrees of freedom contributing to entropy at T_{EW}, and defined $\phi_{EW} \equiv \phi_{rad}(T_{EW})$. Since $r \lesssim 0.1$ [94], in the parametric regime $g \gtrsim 10^{-4}\lambda_\phi^{1/4}$, $\xi \lesssim 1$, we conclude that the quadratic term is dominant at T_{EW}, implying that the field starts behaving as non-relativistic matter already at the EWPT. We will verify explicitly below that this is, in fact, the parametric regime of interest for the field to account for all the present dark matter abundance.

For $T < T_{EW}$ the dynamics of the field is different depending on whether the Higgs portal coupling is positive or negative, so that we will study these cases separately. We need, however, to ensure that the coherent behaviour of the homogeneous scalar field is preserved until the EWPT, as we explore in detail below.

3.1.3 Condensate evaporation

If its interactions are sufficiently suppressed, the dark scalar field behaves as a long-lived oscillating condensate, i.e, a set of particles with zero (or actually sub-Hubble) momentum that exhibit a collective behavior, and is never in thermal equilibrium with the SM particles. Thereby, we must analyze the constraints on g and λ_ϕ to prevent its evaporation and thermalization into a WIMP-like candidate, the phenomenology of which was studied in Ref. [24]. There are two main processes that may lead to condensate evaporation, as we describe in detail below - Higgs annihilation into higher-

momentum ϕ particles and the perturbative production of ϕ particles by the oscillating background field.

3.1.3.1 Higgs annihilation into higher-momentum ϕ particles

Higgs bosons in the cosmic plasma may annihilate into ϕ pairs, with a rate given by, for $T \gtrsim T_{EW}$:

$$\Gamma_{hh\to\phi\phi} = n_h \langle \sigma v \rangle \,, \tag{3.17}$$

where $v \sim c \equiv 1$ and n_h is the number density of Higgs bosons in the termal bath,

$$n_h = \frac{\zeta(3)}{\pi^2} T^3 \ . \tag{3.18}$$

Before the EWPT, the momentum of the Higgs particles is of the order of the thermal bath temperature, $|\mathbf{p}| \sim T$, and the cross-section for the process is

$$\sigma \sim \frac{g^4}{64\pi} \frac{1}{\left(1+\frac{m_h^2}{T^2}\right)} \frac{1}{T^2} \sqrt{1+\frac{m_h^2-m_\phi^2}{T^2}}. \tag{3.19}$$

For $T < T_{EW}$, the Higgs bosons decay into Standard Model degrees of freedom and the production of ϕ stops, so that we must require $\Gamma_{hh\to\phi\phi} \lesssim H$ to prevent the thermalization of the dark scalar condensate for $T > T_{EW}$. Since $\Gamma_{hh\to\phi\phi} \propto T$ and $H \propto T^2$, the strongest constraint is at T_{EW}, which leads to an upper bound on g, using Eqs. (1.34), (3.17), (3.18) and (3.19):

$$g \lesssim 8 \times 10^{-4} \left(\frac{g_*}{100}\right)^{1/8} \ , \tag{3.20}$$

corresponding to an upper bound on the dark scalar's mass $m_\phi \lesssim 100$ MeV.

3.1.3.2 Perturbative production of ϕ particles by the oscillating background field

Another possibility for the condensate's evaporation is the production of ϕ particles from the coherent oscillations of the background condensate. Particle production from an oscillating background field in a quartic potential has been studied in detail in Refs. [32, 99, 100]. For $T > T_{EW}$, ϕ particles are massless and interact with the background field. The coupling between the background field and particle fluctuations, $\delta\phi$, is:

$$\mathcal{L}_{int} = -\frac{3}{2} \lambda_\phi \, \phi^2 \, \delta\phi^2 \ . \tag{3.21}$$

For a quartic potential, the oscillating condensate evolves as [100]:

$$\phi\left(t\right)=\frac{\sqrt{\pi}\,\Gamma\left(\frac{3}{4}\right)}{\Gamma\left(\frac{5}{4}\right)}\,\phi_{rad}\sum_{n=1}^{\infty}\left(e^{i(2n-1)\omega t}+e^{-i(2n-1)\omega t}\right)\,\frac{e^{-\frac{\pi}{2}(2n-1)}}{1+e^{-\pi(2n-1)}}\;, \tag{3.22}$$

with $\omega=\frac{1}{2}\sqrt{\frac{\pi}{6}}\,\frac{\Gamma(\frac{3}{4})}{\Gamma(\frac{5}{4})}\,m_{\phi}$ and $m_{\phi}=\sqrt{3\lambda_{\phi}}\,\phi_{rad}$ before the EWPT. The corresponding particle production rate is then given by [100]:

$$\Gamma_{\phi\to\delta\phi\delta\phi}\simeq 8.86\,\frac{9\,\lambda_{\phi}^{2}}{32\pi\,m_{\phi}^{3}}\,\rho_{\phi}\;, \tag{3.23}$$

The energy density, ρ_{ϕ}, can be averaged over field oscillations:

$$\rho_{\phi}=\frac{1}{2}\langle\dot{\phi}\left(t\right)^{2}\rangle+\frac{\lambda_{\phi}}{4}\,\langle\phi\left(t\right)^{4}\rangle\;. \tag{3.24}$$

We have computed this numerically, using Eq. (3.22), and obtained:

$$\rho_{\phi}\simeq\frac{1}{4}\,\lambda_{\phi}\,\phi_{rad}^{4}\;, \tag{3.25}$$

implying a particle production rate:

$$\Gamma_{\phi\to\delta\phi\delta\phi}\simeq 4\times10^{-2}\,\lambda_{\phi}^{3/2}\,\phi_{rad}\;. \tag{3.26}$$

This is valid for $T>T_{EW}$, whilst after the EWPT the ϕ particles acquire mass and the production channel is blocked. Once again, since $\Gamma_{\phi\to\delta\phi\delta\phi}\propto T$ in a quartic potential, and we must require $\Gamma_{\phi\to\delta\phi\delta\phi}\lesssim H$ to prevent the thermalization, the most stringent constraint is at T_{EW}, where $\phi_{rad}=\phi_{EW}$, which places an upper bound on the dark scalar's self-coupling:

$$\lambda_{\phi}<6\times10^{-10}\left(\frac{g_{*}}{100}\right)^{1/5}\left(\frac{r}{0.01}\right)^{-1/5}\xi^{1/10}\;. \tag{3.27}$$

If the constraints (3.20) and (3.27) are satisfied, the dark scalar is never in thermal equilibrium with the cosmic plasma, behaving like an oscillating condensate of zero-momentum particles throughout its cosmic history. We will see below that Eq. (3.27) yields the most stringent constraint on the model.

3.2 Dynamics after the electroweak symmetry breaking

At the EWPT, the field starts behaving differently depending on the sign of the Higgs portal coupling. If this coupling is negative, the field may acquire a vacuum

expectation value and thus become unstable, although sufficiently long-lived to account for dark matter. On the other hand, if the coupling is positive, the U(1) symmetry remains unbroken after the EWPT and the field never decays. In this section, we explore the field dynamics in each case.

3.2.1 Negative Higgs portal coupling

In this case, the relevant interaction potential is:

$$V(\phi, h) = -\frac{g^2}{4}\,\phi^2\,h^2 + \frac{\lambda_\phi}{4}\,\phi^4 + \frac{\lambda_h}{4}\,\left(h^2 - \tilde{v}^2\right)^2 \ . \tag{3.28}$$

As soon as the temperature drops below the electroweak scale, both the Higgs field and the dark scalar acquire non-vanishing vacuum expectation values for $g^4 < 4\lambda_\phi\lambda_h$, which we take to be the relevant parametric regime:

$$h_0 = \left(1 - \frac{g^4}{4\,\lambda_\phi\,\lambda_h}\right)^{-1/2} \tilde{v} \equiv \mathrm{v}, \qquad \phi_0 = \frac{g\,\mathrm{v}}{\sqrt{2\lambda_\phi}} \ , \tag{3.29}$$

where $\mathrm{v} = 246\,\mathrm{GeV}$. This induces a mass-mixing between the "flavour" basis ϕ and h fields, described by the squared mass matrix

$$M^2 = \mathrm{v}^2 \begin{pmatrix} g^2 & -\frac{g^3}{\sqrt{2\lambda_\phi}} \\ -\frac{g^3}{\sqrt{2\lambda_\phi}} & 2\lambda_h \end{pmatrix} . \tag{3.30}$$

For small mixing, the mass eigenvalues are approximately given by:

$$m^2_{\tilde{\phi}} \simeq g^2\mathrm{v}^2\left(1 - \frac{g^4}{4\,\lambda_h\,\lambda_\phi}\right) \ , \qquad m^2_{\tilde{h}} \simeq 2\lambda_h\,\mathrm{v}^2\left(1 + \frac{g^6}{8\,\lambda_h^2\,\lambda_\phi}\right) \ . \tag{3.31}$$

The corresponding eigenvectors are:

$$\tilde{\phi} = \begin{pmatrix} 1 \\ \epsilon_- \end{pmatrix}, \qquad \tilde{h} = \begin{pmatrix} -\epsilon_- \\ 1 \end{pmatrix} \ , \tag{3.32}$$

where the mixing parameter, $\epsilon_- \ll 1$, corresponds to

$$\epsilon_- = \frac{g^3}{2\sqrt{2\,\lambda_\phi}\,\lambda_h} = \frac{g^2\,\phi_0\,\mathrm{v}}{m_h^2} \ . \tag{3.33}$$

The mass eigenstates can then be written in terms of the flavour-basis fields as:

$$\tilde{\phi} = \phi - \epsilon_-\,h \ , \qquad \tilde{h} = h + \epsilon_-\,\phi \ . \tag{3.34}$$

This mixing is extremely relevant for the direct and indirect detection of the dark scalar as we discuss in subsection 3.3.2. In this scenario, differentiating the Lagrangian twice with respect to ϕ, yields the mass of the field:

$$m_\phi = g\,\mathrm{v}\ . \tag{3.35}$$

As we have seen in subsection 3.1.2, the field starts behaving as cold dark matter at $T_{EW} \sim m_W$. The amplitude of the oscillations at this stage is given by Eq. (3.14), which can be rewritten as:

$$\begin{aligned}\phi_{EW} &\simeq \left(\frac{4\,\pi^2\,g_*}{270}\right)^{1/4}\,\left(\frac{\phi_{inf}}{M_{Pl}}\right)^{1/2}\,\frac{T_{EW}}{\mathrm{v}}\,\frac{\lambda_\phi^{1/4}}{g}\,\phi_0 \\ &\simeq 10^{-4}\,g_*^{1/4}\,\xi^{-1/8}\left(\frac{T_{EW}}{m_W}\right)\left(\frac{r}{0.01}\right)^{1/4}\,\frac{\lambda_\phi^{1/4}}{g}\,\phi_0.\end{aligned} \tag{3.36}$$

From Eq. (3.36), in the parametric regime $g \gtrsim 10^{-4}\,\lambda_\phi^{1/4}$, $\phi_{EW} \lesssim \phi_0$, for $\xi \gtrsim 1$. This implies that the potential minimum will move smoothly from the origin to ϕ_0, where the field starts to oscillate with an amplitude $\phi_{DM} = x_{DM}\,\phi_0$, with $x_{DM} \lesssim 1$. In fact, a rigorous study of the dynamics of the field for $T_{EW} < T < T_{CO}$, where T_{CO} corresponds to the electroweak crossover temperature, would necessarily involve numerical simulations that are beyond the scope of this work. We may nevertheless estimate the uncertainty associated to the field's amplitude. Since $T_{EW} \lesssim T_{CO}$ by an $\mathcal{O}\,(1)$ factor, and given that $\phi \sim T$ while behaving as radiation and $\phi \sim T^{3/2}$ while behaving as non-relativistic matter, the field's amplitude might decrease by at most an $\mathcal{O}\,(1)$ factor as well. Therefore, we expect the field's amplitude to be smaller than ϕ_0 at T_{EW} by $x_{DM} \lesssim 1$. Notice that x_{DM} is thus not an additional parameter of the model, but only a theoretical uncertainty in our analysis that does not affect the order of magnitude of the dark matter abundance and lifetime, as we shall see below.

As soon as the field reaches ϕ_0, it stops behaving like dark radiation and starts to oscillate as cold dark matter. The field's amplitude of oscillations about ϕ_0 evolves according to

$$\phi\,(T) = \phi_{DM}\left(\frac{T}{T_{EW}}\right)^{3/2}\ . \tag{3.37}$$

At this point, the number of particles in a comoving volume becomes constant:

$$\frac{n_\phi}{s} = \frac{45}{4\pi^2 g_{*S}}\frac{m_\phi\,\phi_{DM}^2}{T_{EW}^3}\ , \tag{3.38}$$

where $s = \frac{2\pi^2}{45}\,g_{*S}\,T^3$ is the entropy density of radiation, $n_\phi \equiv \frac{\rho_\phi}{m_\phi}$ is the dark matter number density and $g_{*S} \simeq 86.25$ at T_{EW}. Using this, we can compute the present dark

matter abundance, similarly to what we have done in Eq. (2.9). Thus, we obtain the following relation between the present dark matter abundance and m_ϕ:

$$m_\phi = (6\,\Omega_{\phi,0})^{1/2} \left(\frac{g_{*S}}{g_{*S0}}\right)^{1/2} \left(\frac{T_{EW}}{T_0}\right)^{3/2} \frac{H_0 M_{Pl}}{\phi_{DM}}, \tag{3.39}$$

where g_{*S0}, T_0 and H_0 are the present values of the number of relativistic degrees of freedom, CMB temperature and Hubble parameter, respectively. We thus obtain the following relation between the couplings g and λ_ϕ, fixing $\Omega_{\phi,0} \simeq 0.26$:

$$g \simeq 2 \times 10^{-3} \left(\frac{x_{DM}}{0.5}\right)^{-1/2} \lambda_\phi^{1/4} \ . \tag{3.40}$$

This expression satisfies the constraint $g^4 < 4\lambda_\phi\lambda_h$ and $\phi_{EW} \lesssim \phi_0$. Given this relation between couplings, Eq. (3.27) yields, as anticipated, the strongest constraint, limiting the viable dark matter mass to be $\lesssim 1\,\mathrm{MeV}$.

It should be emphasized that the properties of our model depend strongly on whether the U(1) symmetry is global or local. In particular, if the symmetry is global, it leads to tight constraints on the dark scalar mass. We study the cosmological implications of the spontaneous symmetry breaking (both local and global) in section 3.4.

3.2.2 Positive Higgs portal coupling

As we have seen before, for $T > T_{EW}$, the field is oscillating as radiation. If the coupling between the Higgs and the dark scalar has a positive sign, as soon as the EWPT occurs, the only field that undergoes spontaneous symmetry breaking is the Higgs field. The corresponding interaction Lagrangian is:

$$\mathcal{L}_{int} = +\frac{g^2}{4}\,\phi^2\,\mathrm{v}^2 + \frac{\lambda_\phi}{4}\,\phi^4 + \frac{\lambda_h}{4}\left(h^2 - \mathrm{v}^2\right)^2 \ . \tag{3.41}$$

The interactions with the Higgs are responsible for providing the dark scalar mass, which is given in this case by

$$m_\phi = \frac{1}{\sqrt{2}}\,g\,\mathrm{v} \ , \tag{3.42}$$

differing from the mass of the negative coupling case, Eq. (3.35), by a factor of $\sqrt{2}$. Although there is no spontaneous U(1) symmetry breaking, there is in practice an effective mass-mixing between the Higgs and dark scalar fields, given that the latter's

value is oscillating about the origin but does not vanish exactly, yielding an effective mixing parameter:

$$\epsilon_+ = \frac{g^2\,\phi\,\mathrm{v}}{m_h^2}\ , \tag{3.43}$$

where ϕ denotes the time-dependent field amplitude. Since the dark matter energy density depends on the amplitude of the field,

$$\rho_\phi = \frac{1}{2}\,m_\phi^2\,\phi^2\ , \tag{3.44}$$

Eq. (3.43) can be rewritten as

$$\epsilon_+ = \frac{2\,\sqrt{2\,\rho_\phi}}{\mathrm{v}\,m_h^2}\,m_\phi\ . \tag{3.45}$$

At T_{EW}, the field starts to behave as cold dark matter, and its amplitude varies as:

$$\phi\,(T) = \frac{\phi_{inf}}{T_{rad}}\,\left(\frac{T^3}{T_{EW}}\right)^{1/2}\ , \tag{3.46}$$

so that the number of particles per comoving volume reads:

$$\frac{n_\phi}{s} = \frac{45}{4\pi^2}\,\frac{1}{g_{*S}}\,m_\phi\,\frac{\phi_{inf}^2}{T_{rad}^2}\,\frac{1}{T_{EW}}\ . \tag{3.47}$$

Analogously to the negative coupling case, we may compute the field's mass, taking into account the present dark matter abundance, $\Omega_{\phi,0}$:

$$m_\phi = \sqrt{6\,\Omega_{\phi,0}}\,\frac{H_0\,M_{Pl}}{\phi_{inf}}\,\left(\frac{g_{*S}}{g_{*S0}}\right)^{1/2}\,\frac{T_{rad}\,T_{EW}^{1/2}}{T_0^{3/2}}\ , \tag{3.48}$$

leading to the following relation between g and λ_ϕ:

$$g \simeq 9\times 10^{-3}\,\xi^{1/8}\,\left(\frac{r}{0.01}\right)^{1/4}\,\lambda_\phi^{1/4}\ . \tag{3.49}$$

Once again, Eq. (3.27) yields the strongest constraint and, as in the case of the negative coupling, the dark scalar's mass must be smaller than 1 MeV to account for the present dark matter abundance.

It must be highlighted that, in this scenario, once the dark matter abundance is fixed, the value of g depends on all other parameters of the model, λ_ϕ, r and ξ, contrary to the negative coupling case, where the Higgs portal coupling is only related to λ_ϕ as given in Eq. (3.40). In other words, in the positive coupling case the field's mass depends on the initial conditions set by inflationary dynamics, whilst in the case with spontaneous symmetry breaking the final dark matter abundance is effectively independent of the initial conditions, and all dynamics depends essentially on the vacuum expectation value, ϕ_0, which sets the amplitude of field oscillations.

3.3 Phenomenology

Having discussed the dynamics of the dark scalar throughout the cosmic history and determined the parametric ranges for which it may account for the present dark matter abundance, in this section we discuss different physical phenomena that may be used to probe the model. This includes searching for direct signatures in the laboratory, as well as for indirect signals in astrophysical observations.

3.3.1 Astrophysical Signatures

Given the smallness of the Higgs portal coupling required for preventing the scalar condensate's evaporation before the EWPT, it is likely that any signatures of such a dark matter candidate require large fluxes of ϕ particles or the particles it interacts with, which may be difficult to produce in the laboratory. Astrophysical signatures may, however, be enhanced by the large dark matter density within our galaxy and other astrophysical systems, and thus we shall explore in this section the possibility of indirectly detecting the dark scalar through its annihilation or decay.

3.3.1.1 Dark matter annihilation

Over the past decades, the emission of a 511 keV γ-ray line has been observed, by several experiments, in a region around the galactic center (see e.g. Ref. [101] for a review). The 511 keV line is characteristic of electron-positron annihilation, as has been shown by the INTEGRAL/SPI observations [102–104] and has a flux of $\Phi_{GC} = 9.9 \times 10^{-4}\,\mathrm{cm}^{-2}\,s^{-1}$ [105]. This photon excess in the galactic bulge is intriguing because, although it is common to find positron sources in the galaxy (namely, from core collapse of supernovae and low-mass X-ray binaries), most of these astrophysical objects are localized in the galactic disk rather than in the galactic center [101].

An alternative possibility to explain this line is considering dark matter annihilation into an e^-e^+ pair. Although light WIMPs are practically excluded as a possible explanation [106], other plausible dark matter candidates could predict this photon excess. In this context, we study the annihilation of ϕ particles into e^-e^+ and into photons, presenting the predictions for the photon flux associated with our dark matter candidate in the galactic center.

In general, the flux of photons from an angular region $\Delta\Omega$ from dark matter

annihilation is given by:

$$\Phi_{ann} = \frac{1}{2m_\phi^2} N_\gamma \frac{\langle \sigma v \rangle}{4\pi} \int_{l.o.s} dl\,(s,\Psi)\ \rho^2\left(r\,(s,\Psi)\right) \int_{\Delta\Omega} d\Omega\ , \tag{3.50}$$

where ρ is the dark matter density for a given profile, r is the radial distance from the galactic center, Ψ is the angle between the direction of observation in the sky and the galactic center, the integral is evaluated along the line-of-sight (l.o.s) and N_γ is the number of photons produced by the annihilation [107]. We can split Eq. (3.50) into two parts: one that only depends on the particle physics,

$$\frac{1}{2m_\phi^2} N_\gamma \frac{\langle \sigma v \rangle}{4\pi}\ , \tag{3.51}$$

and another one depending only on the astrophysical properties:

$$J\,(\Omega) = \int_{l.o.s} dl\,(s,\Psi)\ \rho^2\left(r\,(s,\Psi)\right) \int_{\Delta\Omega} d\Omega\ , \tag{3.52}$$

and analyze each one separately.

Let us first focus on the particle physics component. Consider the case in which the ϕ particles annihilate via virtual Higgs exchange, H^*, and the latter decays into Standard Model particles. Since $m_\phi \lesssim 1$ MeV (by the constraint imposed on λ_ϕ, Eq. (3.27)), the possible final decay products are only electron-positron pairs and photons for non-relativistic dark scalars. Following Eq. (3.51), it is necessary to compute the cross section of the process. In the center-of-mass frame, using $E_\phi \simeq m_\phi$, the 4-momentum of H^* is $p_h = (2\,m_\phi, \mathbf{0})$, implying that the invariant mass of the virtual Higgs is $m_{H^*} = 2\,m_\phi$. By energy conservation, if the final state is a fermion-antifermion pair, the momentum of each particle reads $|\mathbf{p}_f| = m_\phi\sqrt{1 - m_f^2/m_\phi^2}$, where m_f is the fermion's mass. Using this, the cross section for dark matter annihilation into a virtual Higgs and its subsequent decay into fermions reads:

$$\langle \sigma v_{rel} \rangle_{fermions} \simeq \frac{N_c}{8\pi}\frac{D}{\mathrm{v}^2} \frac{m_\phi^4}{\left(4m_\phi^2 - m_h^2\right)^2 + m_h^2\Gamma_h^2} \left(\frac{m_f}{\mathrm{v}}\right)^2 \left(1 - \frac{m_f^2}{m_\phi^2}\right)^{3/2}\ , \tag{3.53}$$

where N_c is the number of colors ($N_c = 1$ for leptons and $N_c = 3$ for quarks), $\Gamma_h = 4.07 \times 10^{-3}\,\mathrm{GeV}$ [108] is the total Higgs decay rate, and $D = 1$ for the case where the U(1) symmetry is spontaneously broken and $D = 4$ otherwise.

In the case where we have a pair of photons in the final state, the momentum of each photon is $|\mathbf{p}_\gamma| = m_\phi$. The cross-section for this process is:

$$\langle \sigma v_{rel} \rangle_\gamma \simeq \frac{D}{32\sqrt{2}\,\pi^3} \frac{m_\phi^4}{\mathrm{v}^2} \frac{G_F\,\alpha_{QED}^2\,m_\phi^2}{\left(4m_\phi^2 - m_h^2\right)^2 + m_h^2\Gamma_h^2} F^2\ , \tag{3.54}$$

where $G_F = 1.17 \times 10^{-5}\,\mathrm{GeV}^{-2}$ is Fermi's constant, $\alpha_{QED} \simeq 1/137$ is the fine structure constant and

$$F = \left| \sum_f N_c\, Q_f^2\, A_{1/2}^H\left(\tau_f\right) + A_1^H\left(\tau_{\mathbf{w}}\right) \right| \simeq \frac{11}{3} \tag{3.55}$$

is a factor that takes into account the loop contributions of all charged fermions and the W boson to $H^* \to \gamma\gamma$, with $\tau_i = 4m_i^2/m_\phi^2 \gg 1$ for all particle species involved, for $m_\phi \ll$ MeV [109]. We point out that for the decay of a virtual Higgs all charged fermions give essentially the same loop contribution, whilst for an on-shell Higgs boson only the top quark contributes significantly.

Concerning the astrophysical part, one needs to consider the profile that best describes the dark matter distribution in a particular region of the Universe to compute the so-called J-factor in Eq. (3.52). In the case of the galactic center, the most appropriate models are the cuspy profile ones. Following Ref. [108], using a generalized Navarro-Frenk-White profile (NFW) to describe the dark matter distribution in the galactic center,

$$\rho\left(r\right) = \rho_s \left(\frac{r}{r_s}\right)^{-\gamma} \left(1 + \frac{r}{r_s}\right)^{-3+\gamma} , \tag{3.56}$$

where r is the spherical distance from the galactic center, $\gamma = 1.2$, $\rho_s = 0.74\,\mathrm{GeV/cm}^3$ and $r_s = 19.5$ kpc, hence, the corresponding J-factor is:

$$J \simeq 1.79 \times 10^{23}\,\mathrm{GeV}^2\,\mathrm{cm}^{-5}. \tag{3.57}$$

Using the last expressions, the predicted flux of photons originated by the annihilation of ϕ particles into a virtual Higgs and the decay of the latter into an electron-positron pair, for the galactic center, is given by:

$$\Phi_{\phi\phi\to e^-e^+} \simeq \frac{D}{32\,\pi^2} \frac{J}{\left(4m_\phi^2 - m_h^2\right)^2 + m_h^2\Gamma_h^2} \left(\frac{m_\phi}{\mathrm{v}}\right)^2 \left(\frac{m_e}{\mathrm{v}}\right)^2 \left(1 - \frac{m_e^2}{m_\phi^2}\right)^{3/2} . \tag{3.58}$$

Since $m_\phi \lesssim 1$ MeV and $m_\phi \gtrsim 0.511$ MeV so that it can annihilate into an electron-positron pair, we can simplify this to give:

$$\Phi_{\phi\phi\to e^-e^+} \simeq 1 \times 10^{-27}\, D \left(\frac{m_\phi}{\mathrm{MeV}}\right)^2 \mathrm{cm}^{-2}\, s^{-1} , \tag{3.59}$$

which is clearly insufficient to explain the galactic center excess but shows how the electron-positron flux varies with the mass of the dark scalar and hence the Higgs portal coupling.

The flux coming from the annihilation of ϕ into a virtual Higgs and its decay into photons reads:

$$\Phi_{\phi\phi\to\gamma\gamma} \simeq 10^{-31}\, D \left(\frac{m_\phi}{\text{MeV}}\right)^4 \text{cm}^{-2}\, s^{-1} \ . \tag{3.60}$$

The fluxes we have found for the annihilation of ϕ particles into a virtual Higgs and its decay into an electron-positron pair or photons are thus extremely suppressed, which makes its indirect detection through annihilation a very difficult challenge.

3.3.1.2 Dark matter decay

Our dark matter candidate exhibits a small mixing $\epsilon_\pm$ with the Higgs boson, as we have seen in section 3.2 and may, therefore, decay into the same channels as the Higgs boson, provided that they are kinematically accessible, and the decay width is suppressed by a factor $\epsilon_\pm^2$ relative to the corresponding Higgs partial width, $\Gamma_{\phi\to pp} = \epsilon_\pm^2\, \Gamma_{H^*\to XX}$, where X corresponds to a generic particle. With the dark matter mass bound obtained above, the only kinematically accessible decay channel is into photon pairs [7], with partial decay width:

$$\Gamma_{H^*\to\gamma\gamma} = \frac{G_F\, \alpha_{QED}^2\, m_\phi^3}{128\sqrt{2}\,\pi^3} F^2 \ , \tag{3.61}$$

where F is defined in Eq. (3.55). This yields for the dark scalar's lifetime:

$$\tau_\phi^{(-)} \simeq 7 \times 10^{27} \left(\frac{7\,\text{keV}}{m_\phi}\right)^5 \left(\frac{x_{DM}}{0.5}\right)^2 \text{sec} \ , \tag{3.62}$$

in the case with spontaneous symmetry breaking and

$$\tau_\phi^{(+)} \simeq 4 \times 10^{71} \left(\frac{7\,\text{keV}}{m_\phi}\right)^5 \text{sec} \ , \tag{3.63}$$

for the positive coupling. As expected, the case with no spontaneous symmetry breaking yields an effectively stable dark matter candidate, with the probability of decay into photons being tremendously suppressed. In the negative coupling case, the dark scalar's lifetime is larger than the age of the Universe, but there is a realistic possibility of producing an observable monochromatic line in the galactic spectrum.

In fact, the XMM-Newton X-ray observatory has recently detected a line at 3.5 keV in the Galactic Center (GC), Andromeda and Perseus cluster [110–113]. The origin

[7] The decay $\phi \to e^+e^-$ may be possible for dark matter masses saturating the obtained bound, but in this case condensate evaporation may not be negligible and, hence, we do not consider this possibility in detail

of the line is not well-established, although dark matter decay and/or annihilation are valid possibilities [113–118]. There are other astrophysical processes that might explain the 3.5 keV line [119]. However, some independent studies suggest that those processes cannot provide a satisfactory explanation [120–122]. In addition, some groups state that such a photon excess is not present in dwarf galaxies, such as Draco [123], while others assert that the line is only too faint to be detected with the technology that we have at our current disposal, not ruling out a possible dark matter decay interpretation [14]. The authors of [14], in particular, conclude that observations of dwarf spheroidal galaxies cannot exclude the dark matter decay explanation of the line.

The analysis in Refs. [14, 112] has shown that the intensity of the line observed in the GC, Andromeda and the Perseus cluster could be explained by the decay of a dark matter particle with a mass of $\simeq 7$ keV and a lifetime in the range $\tau_\phi \sim (6-9)\times 10^{27}$ sec. This would also explain the absence of such a line in the blank-sky data set. Concerning the positive coupling scenario, the dark scalar's lifetime (Eq. (3.63)) is not compatible with the required range. However, the scenario where ϕ undergoes spontaneous symmetry breaking *predicts* a dark matter lifetime (Eq. (3.62)) exactly in the above-mentioned range, up to an uncertainty on the value of the field amplitude after the EWPT parametrized by $x_{DM} \lesssim 1$, for $m_\phi = 7\,\text{keV}$. This is illustrated in Fig. 3.1.

For this mass value, we have $g \simeq 3\times 10^{-8}$ and, from Eq. (3.40), $\lambda_\phi \simeq 4\times 10^{-20}$, which satisfy the constraints in Eqs. (3.20) and (3.27). Note that such a small quartic self-coupling for the scalar field is technically natural, since quantum corrections to this coupling from interactions with the Higgs field are $\lesssim g^4 \sim 10^{-30}$.

We do not aim to explain here the smallness of these couplings, which would require going beyond the effective theory approach that we have followed in this work. We nevertheless note that small couplings can be naturally obtained in the context of extra-dimensional geometries, as in the warped dark scalar field scenario developed in chapter 2. This issue is also essentially on the same footing as explaining the smallness of fermion masses, namely the electron.

We should emphasize the uniqueness of the result for the spontaneous symmetry breaking scenario. In this case, our model predicts that the decay of ϕ into photons produces a 3.5 keV line compatible with the observational data, with effectively only a single free parameter, either g or λ_ϕ. Recall that the initial conditions of the field depend on the parameters r and ξ, the first one determining the initial oscillation amplitude in the radiation era, whilst the latter is responsible for suppressing cold

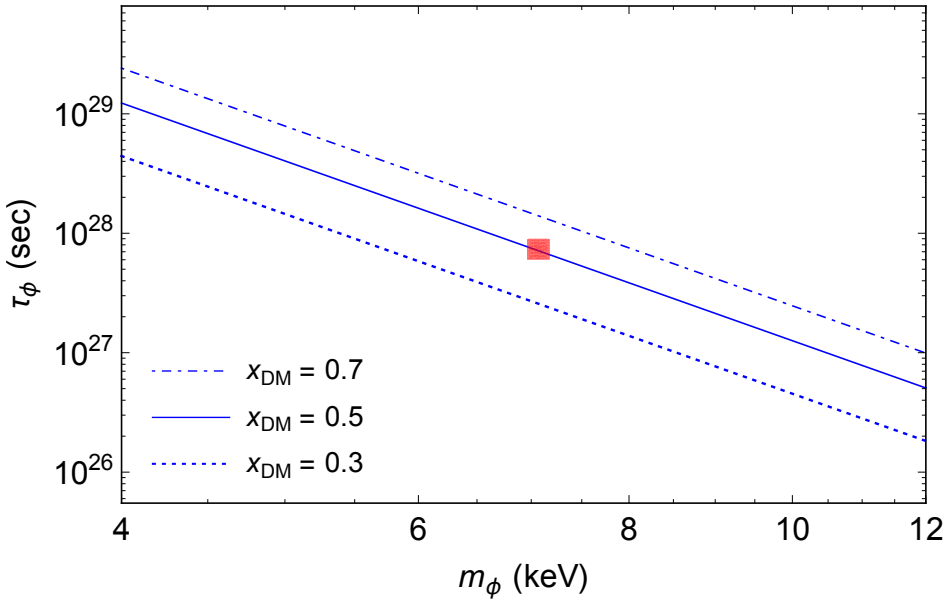

Figure 3.1: Lifetime of the scalar field dark matter as a function of its mass, for different values of $x_{DM} \lesssim 1$ parametrizing the uncertainty in the value of the field oscillation amplitude after the EWPT. The shaded horizontal band corresponds to the values of τ_ϕ that can account for the intensity of the 3.5 keV X-ray line observed by XMM-Newton for a mass around 7 keV including the uncertainty in the photon energy combining different observations [14].

dark matter isocurvature perturbations. However, after the EWPT, the field oscillates around ϕ_0, which only depends on g and λ_ϕ. Its amplitude is of the order of ϕ_0, meaning that r and ξ do not play a significant role below T_{EW}. In other words, the field loses the memory of its initial conditions at the EWPT, and ξ and r do not affect its dynamics afterwards. Therefore, we have three observables that rely on just two parameters (g and λ_ϕ) - the present dark matter abundance, the dark scalar's mass and its lifetime. However, assuming that the dark scalar field accounts for all the dark matter in the Universe imposes a relation between g and λ_ϕ (Eq. (3.40)), implying that m_ϕ and τ_ϕ depend exclusively on the Higgs portal coupling. Hence, the prediction for the magnitude of the 3.5 keV line in different astrophysical objects is quite remarkable and, as far as we are aware, it has not been achieved by other scenarios, where the dark matter's mass and lifetime can be tuned by different free parameters.

3.3.2 Laboratory Signatures

Since $m_\phi \lesssim$ MeV, the coupling between the dark scalar and the Higgs boson, g, is extremely small, which hampers the detection of dark matter candidates of this kind. However, the small $h-\phi$ mass mixing may nevertheless lead to interesting experimental signals that one could hope to probe in the laboratory with improvements in current technology. In this section, we explore examples of such signatures, namely invisible Higgs decays, photon-dark scalar oscillations in an external electromagnetic field and dark matter-induced oscillations of fundamental constants, such as the electron mass and α_{QED}.

3.3.2.1 Invisible Higgs decays into dark scalars

The simplest and cleanest way to test the Higgs portal scalar field dark matter scenario in collider experiments is to look for invisible Higgs decays into dark scalar pairs, with a decay width:

$$\Gamma_{h\to\phi\phi} = \frac{1}{8\pi}\,\frac{g^4 \mathrm{v}^2}{4\,m_h}\sqrt{1-\frac{4m_\phi^2}{m_h^2}}\ , \tag{3.64}$$

where m_h is the Higgs mass. The current experimental limit on the branching ratio for Higgs decay into invisible particles is [124]:

$$Br\left(\Gamma_{h\to inv}\right) = \frac{\Gamma_{h\to inv}}{\Gamma_h + \Gamma_{h\to inv}} \lesssim 0.23\ . \tag{3.65}$$

Assuming that $\Gamma_{h\to inv} = \Gamma_{h\to\phi\phi}$ and using $\Gamma_h = 4.07\times10^{-3}$ GeV [108], this yields the following bound on the Higgs portal coupling g:

$$g \lesssim 0.13\ , \tag{3.66}$$

which is much less restrictive than the cosmological bound in Eq. (3.20). Conversely, for $m_\phi <$ MeV to ensure the survival of the dark scalar condensate up to the present day, we obtain the following upper bound on the branching ratio:

$$Br\left(\Gamma_{h\to inv}\right) < 10^{-19}\ . \tag{3.67}$$

This is, unfortunately, too small to be measured with current technology, but may serve as motivation for extremely precise measurements of the Higgs boson's width in future collider experiments, given any other experimental or observational hints for light Higgs portal scalar field dark matter, such as, for instance, the 3.5 keV line discussed above.

3.3.2.2 Light Shining Through Walls

The dark scalar exhibits a small coupling to photons through its mass mixing with the Higgs boson, which couples indirectly to the electromagnetic field via W-boson and charged fermion loops [109]. This will allow us to explore experiments that make use of the coupling to the electromagnetic field to probe dark matter candidates, as the case of "light shining through a wall" experiments (LSTW). These experiments are primarily designed to detect WISPs - Weakly Interacting Sub-eV Particles, such as axions and axion-like particles (ALPs), taking advantage of their small coupling to photons. Therefore, we intend to apply the same detection principles to our dark scalar field, given its similarities with ALPs, in terms of small masses and couplings.

In LSTW experiments, photons are shone into an opaque absorber, and some of them may be converted into WISPs, which traverse the absorber wall. Behind the wall, some WISPs reconvert back into photons that may be detected. This can be achieved using an external magnetic (or electric) field, which works as a mixing agent, making the photon-WISP oscillations possible and allowing for the conversion of photons into WISPs and vice-versa. Using the paradigmatic case of a pseudo-scalar axion/ALP, the interaction term between the latter and photons is of the form:

$$\mathcal{L}_{a\gamma\gamma} = \frac{g_{a\gamma\gamma}}{4}\, a\, F_{\mu\nu}\tilde{F}^{\mu\nu} = -g_{a\gamma\gamma}\, a\, \mathbf{E}.\mathbf{B}\ , \tag{3.68}$$

where $F_{\mu\nu}$ is the electromagnetic field tensor, $\tilde{F}^{\mu\nu}$ its dual and a the axion/ALP field. For the QCD axion, the coupling $g_{a\gamma\gamma}$ reads

$$g_{a\gamma\gamma} = \frac{\alpha_{QED}\, K}{2\pi\, F_a} \simeq 2\times 10^{-15} K \left(\frac{m_a}{10^{-5}\,\mathrm{eV}}\right)\ \mathrm{GeV}^{-1}\ , \tag{3.69}$$

with $F_a \simeq 6\times 10^{11}\ \left(\frac{m_a}{10^{-5}\,\mathrm{eV}}\right)^{-1}$ GeV denoting the axion decay constant, m_a the axion mass and $K \sim \mathcal{O}\,(1-10)$ is a model-dependent factor [125–127]. For scalar WISPs the interaction with the electromagnetic field is given by [128, 129]:

$$\mathcal{L}_{a\gamma\gamma} = \frac{g_{a\gamma\gamma}}{4}\, a\, F_{\mu\nu}F^{\mu\nu} = g_{a\gamma\gamma}\, a\, \left(\mathbf{B}^2 - \mathbf{E}^2\right)\ . \tag{3.70}$$

In both cases, the presence of an external magnetic field, $\mathbf{B}_{ext}$, gives rise to a mass mixing term between a and photons, thus inducing photon-ALPs oscillations. In the relativistic limit, the WISP wavenumber is $k_a \approx \omega - \frac{m_a^2}{2\omega}$, where ω is the photon angular frequency [128]. Using this, considering the conversion of a photon into a WISP in a constant magnetic field of length L, in a symmetric LSTW setup, the conversion

probability of a photon into a WISP, $P_{\gamma\to a}$, is the same as for the inverse process, $P_{a\to\gamma}$, being given by [128, 130]:

$$P_{\gamma\to a} = 4\,\frac{g_{a\gamma\gamma}^2\,B_{ext}^2\,\omega^2}{m_a^4}\,\sin^2\left(\frac{m_a^2\,L}{4\,\omega}\right)\,. \tag{3.71}$$

Therefore, the total conversion probability along the path is simply the square of Eq. (3.71) [130]:

$$P_{\gamma\to a\to\gamma} = 16\,\frac{g_{a\gamma\gamma}^4\,B_{ext}^4\,\omega^4}{m_a^8}\,\sin^4\left(\frac{m_a^2\,L}{4\,\omega}\right)\,. \tag{3.72}$$

In the specific case of the QCD axion, for $L \ll 4\omega/m_a^2$, the LSTW probability is approximately given by:

$$P_{\gamma\to a\to\gamma} = 6\times10^{-59}\,\left(\frac{B_{ext}}{1\text{ T}}\right)^4\left(\frac{m_a}{10^{-5}\text{ eV}}\right)^4\left(\frac{L}{1\text{ m}}\right)^4\,, \tag{3.73}$$

and, using the parameters of the LSTW experiment ALPS ("Any Light Particle Search experiment) at DESY [128] ($\omega = 2.33$ eV, $B_{ext} = 5$ T and $L = 4.21$ m), the probability of shining a photon through a wall via an intermediate axion with $m_a \sim 10^{-5}$ eV is about $P_{\gamma\to a\to\gamma} \simeq 10^{-53}$ and the coupling to photons is $g_{a\gamma\gamma} \sim 10^{-15}\,\text{GeV}^{-1}$. The upgrade of LSTW experiments intends to achieve a sensitivity in the photon-WISP coupling of $g_{a\gamma\gamma} < 10^{-11}\,\text{GeV}^{-1}$, corresponding to an improvement of 3 orders of magnitude comparing with ALPS 2010 results [129, 130].

In our case, the Higgs coupling to two photons is expressed by the following term in the Lagrangian [131]:

$$\mathcal{L}_{h\gamma\gamma} = \frac{g_{h\gamma\gamma}}{4}\,h\,F_{\mu\nu}F^{\mu\nu}\,, \tag{3.74}$$

where the coupling $g_{h\gamma\gamma}$ has the form

$$g_{h\gamma\gamma} = \frac{\alpha_{QED}\,F}{\pi\,\text{v}}\,, \tag{3.75}$$

with F given by Eq. (3.55). Using the mixing $\phi - h$ in Eq. (3.34) we can write

$$\mathcal{L}_{\phi\gamma\gamma} = -\frac{g_{h\gamma\gamma}}{4}\,\epsilon\,\tilde{\phi}\,F_{\mu\nu}F^{\mu\nu}\,, \tag{3.76}$$

and we may define the effective coupling of the dark scalar field to photons, $g_{\phi\gamma\gamma}$, as:

$$g_{\phi\gamma\gamma} = g_{h\gamma\gamma}\,\epsilon\,, \tag{3.77}$$

where $\epsilon = \epsilon_-$ for the negative coupling between ϕ and h, and $\epsilon = \epsilon_+$ otherwise. For the former, we find

$$g_{\phi\gamma\gamma}^{(-)} \simeq 2\times10^{-26}\,\left(\frac{m_\phi}{10^{-5}\,\text{eV}}\right)\left(\frac{x_{DM}}{0.5}\right)^{-1}\,\text{GeV}^{-1}\,, \tag{3.78}$$

while for the case without spontaneous symmetry breaking we obtain:

$$g^{(+)}_{\phi\gamma\gamma} \simeq 8 \times 10^{-49} \left(\frac{m_\phi}{10^{-5}\,\mathrm{eV}}\right) \mathrm{GeV}^{-1} \ , \tag{3.79}$$

where we have used the cosmological value of the dark matter energy density. Hence, even for the most promising case with spontaneous symmetry breaking the effective coupling to photons of our dark scalar is 11 orders of magnitude below the corresponding axion-photon coupling for the same mass, with the probability for LSTW thus being suppressed by $\sim 10^{-44}$ with respect to the axion. This makes our dark scalar much harder to detect in LSTW experiments, and hence requiring a very substantial improvement in technology.

3.3.2.3 Oscillation of fundamental constants

The scenario proposed in this chapter may also be of interest for different values of m_ϕ if the dark matter interpretation of the 3.5 keV line is refuted. In particular, for $10^{-22}\,\mathrm{eV} < m_\phi < 0.1\,\mathrm{eV}$, the light dark scalar will exhibit a coherent behavior on galactic scales, and its mixing with photons and other SM particles through the Higgs portal may lead to small oscillations of fundamental constants, namely α_{QED} and the electron mass.

The Standard Model Yukawa interactions can be generically written as:

$$\mathcal{L}_{hff} = \frac{g_f}{\sqrt{2}}\, \bar{f}\, f\, h \ , \tag{3.80}$$

where g_f is the Yukawa coupling. Using the $\phi - h$ mass mixing in Eq. (3.34), the electron's mass after the EWPT is thus given by:

$$m_e \simeq \frac{g_f\, \mathrm{v}}{\sqrt{2}} \left(1 - \frac{d_{m_e}}{\sqrt{2}\, M_{Pl}}\, \phi_{CDM}\right) \ , \tag{3.81}$$

where ϕ_{CDM} corresponds to the present amplitude of the scalar field and d_{m_e} is a dimensionless quantity that works as an effective "dilatonic" coupling and is normalized by the Planck mass, such that [132, 133]:

$$\frac{d_{m_e}}{\sqrt{2}\, M_{Pl}} = \frac{\epsilon_\pm}{\mathrm{v}}, \tag{3.82}$$

where ϵ_- was computed in Eq. (3.33) and ϵ_+ in Eq. (3.43).

In the case where ϕ undergoes spontaneous symmetry breaking, the dilatonic coupling $d^{(-)}_{m_e}$ is

$$d^{(-)}_{m_e} \simeq 6 \times 10^{-16} \left(\frac{m_\phi}{10^{-15}\,\mathrm{eV}}\right) \left(\frac{x_{DM}}{0.5}\right)^{-1} \ , \tag{3.83}$$

while, for a positive Higgs portal coupling,

$$d_{m_e}^{(+)} \simeq 2 \times 10^{-38} \left(\frac{m_\phi}{10^{-15}\,\mathrm{eV}} \right) \ . \tag{3.84}$$

Similarly, we may compute the variation of the fine structure constant due to the oscillating dark scalar field. We have seen that the interaction with the Higgs boson introduces a small coupling to the electromagnetic field (Eq.(3.76)), which will induce a variation on the fine structure constant of the form [134]:

$$\alpha'_{QED} \simeq \alpha_{QED} \left(1 + \frac{d_\alpha}{\sqrt{2}\, M_{Pl}}\, \phi_{CDM} \right) \ , \tag{3.85}$$

where, after the EWPT,

$$d_\alpha^{(-)} \simeq 7 \times 10^{-16} \left(\frac{m_\phi}{10^{-15}\,\mathrm{eV}} \right) \left(\frac{x_{DM}}{0.5} \right)^{-1} \ , \tag{3.86}$$

and

$$d_\alpha^{(+)} \simeq 3 \times 10^{-38} \left(\frac{m_\phi}{10^{-15}\,\mathrm{eV}} \right) \ . \tag{3.87}$$

The dilatonic couplings d_{m_e} and d_α have thus comparable values, both with or without spontaneous symmetry breaking, which is a distinctive prediction of our model.

Despite the smallness of these dilatonic couplings, there are a few ongoing experiments designed to detect oscillations of fundamental couplings, using, for instance, atomic clock spectroscopy measurements and resonant-mass detectors [133–141]. For instance, atomic spectroscopy using dysprosium can probe the d_{m_e} coupling in the mass range $10^{-24}\,\mathrm{eV} \lesssim m_\phi \lesssim 10^{-15}\,\mathrm{eV}$, for $10^{-7} \lesssim d_{m_e} \lesssim 10^{-1}$. In turn, the current AURIGA experiment may reach $10^{-5} \lesssim d_{m_e}$, $d_\alpha \lesssim 10^{-3}$ in the narrow interval $10^{-12}\,\mathrm{eV} \lesssim m_\phi \lesssim 10^{-11}\,\mathrm{eV}$, whereas the planned DUAL detector intends to achieve, for $10^{-12}\,\mathrm{eV} \lesssim m_\phi \lesssim 10^{-11}\,\mathrm{eV}$, sensitivity to detect $10^{-6} \lesssim d_{m_e}$, $d_\alpha \lesssim 10^{-2}$. From Eqs. (3.83)-(3.87), we conclude that current technology is not enough to probe our model, which may nevertheless serve as a motivation to significantly improve the sensitivity of such experiments.

We should also point out that ultra-light scalars with mass below 10^{-10} eV can lead to superradiant instabilities in astrophysical black holes that may lead to distinctive observational signatures, such as gaps in the mass-spin Regge plot as first noted in [142]. However, these instabilities should only be able to distinguish our Higgs portal dark matter candidate from other ultra-light scalars, such as axions and axion-like particles, if non-gravitational interactions also play a significant dynamical role (see e.g. Ref. [127]).

3.4 Cosmological implications of the spontaneous symmetry breaking

Throughout our analysis, we have assumed that the model exhibits a U(1) symmetry which, in the case of a negative sign for the coupling between the Higgs and the dark scalar, is spontaneously broken at the EWPT. The implications of such symmetry breaking depend on whether it is a global or a local symmetry. The Lagrangian density is of the form:

$$\mathcal{L} = \partial_\mu \Phi \partial^\mu \Phi^\dagger + \mathcal{L}_{int} \ , \tag{3.88}$$

where $\mathcal{L}_{int}$ is given by Eq. (3.1).

First, let us suppose that the Lagrangian density is invariant under a global U(1) symmetry, i.e. that the complex dark scalar is invariant under the following transformation:

$$\Phi \to e^{i\alpha} \Phi \ , \tag{3.89}$$

where α is a constant parameter. Expanding the kinetic term for $\Phi = \phi e^{i\theta}/\sqrt{2}$ and introducing the rescaled field $\sigma = \phi_0 \, \theta$, we find the following kinetic and interaction terms between the dark scalar, ϕ, and the associated Goldstone boson, σ:

$$\partial_\mu \Phi \partial^\mu \Phi^\dagger = \frac{1}{2} \left[\partial_\mu \phi \partial^\mu \phi + \frac{\phi^2}{\phi_0^2} \partial_\mu \sigma \partial^\mu \sigma + 2 \, \frac{\phi}{\phi_0} \, \partial_\mu \sigma \partial^\mu \sigma + \partial_\mu \sigma \partial^\mu \sigma \right] \ . \tag{3.90}$$

The third term on the right-hand-side of Eq. (3.90) allows for the decay of ϕ into two massless σ particles, which could imply the complete evaporation of the dark scalar condensate. The corresponding decay width is then:

$$\Gamma_{\phi \to \sigma\sigma} = \frac{1}{64 \, \pi} \, \frac{m_\phi^3}{\phi_0^2} \ , \tag{3.91}$$

such that, using the relation between g and λ_ϕ in Eq. (3.40),

$$\Gamma_{\phi \to \sigma\sigma} \simeq 7 \times 10^{21} \left(\frac{x_{DM}}{0.5} \right)^{-1/2} \lambda_\phi^{5/4} \, \mathrm{sec}^{-1} \ , \tag{3.92}$$

corresponding to

$$\tau_{\phi \to \sigma\sigma} \simeq 10^{-22} \left(\frac{x_{DM}}{0.5} \right)^{1/2} \lambda_\phi^{-5/4} \, \mathrm{sec} \ . \tag{3.93}$$

The field is sufficiently long-lived to account for dark matter if $\tau_{\phi \to \sigma\sigma} > t_{\mathrm{univ}} \sim 4 \times 10^{17} \, \mathrm{sec}$, placing an upper bound on λ_ϕ:

$$\lambda_\phi < 2 \times 10^{-32} \left(\frac{x_{DM}}{0.5} \right)^{2/5} \ , \tag{3.94}$$

and thus restricting the viable range for the dark matter mass to:

$$m_\phi \lesssim 5\,\mathrm{eV}. \tag{3.95}$$

Therefore, if the U(1) symmetry were global, there would be a stricter constraint on the value of λ_ϕ, and our dark matter model could not, in particular, explain the 3.5 keV line.

However, we may consider a local U(1) gauge symmetry, where the Lagrangian is invariant under

$$\Phi \to e^{i\alpha(x)}\Phi \ , \tag{3.96}$$

which can be achieved by introducing a gauge field and covariant derivative such that:

$$D_\mu\Phi = \partial_\mu\Phi - i\,e'\,A_\mu\Phi, \tag{3.97}$$

$$A_\mu \to A_\mu + \frac{\partial_\mu\alpha\,(x)}{e'} \ , \tag{3.98}$$

where e' denotes the associated gauge coupling. In this case, expanding the scalar kinetic term in the unitary gauge, where the Goldstone boson is manifestly absorbed into the longitudinal component of the "dark photon" gauge field, we get:

$$D_\mu\Phi D^\mu\Phi^\dagger = \frac{1}{2}\partial_\mu\phi\partial^\mu\phi + \frac{1}{2}\,e'^2\,A_\mu A^\mu\,\phi^2 + \frac{1}{2}\,e'^2\,\phi_0\,\phi\,A_\mu A^\mu + \frac{1}{2}\,e'^2\,\phi_0^2\,A_\mu A^\mu, \tag{3.99}$$

where the second and the third terms correspond to dark scalar-dark photon interactions and the last term gives the mass of the dark photon, γ':

$$m_{\gamma'} = e'\,\phi_0 \ . \tag{3.100}$$

For $m_{\gamma'} < m_\phi/2$, the dark scalar may decay into two dark photons with a decay width

$$\Gamma_{\phi\to\gamma'\gamma'} \simeq \frac{1}{16\pi}\sqrt{1-\frac{4\,m_{\gamma'}^2}{m_\phi^2}}\,\frac{m_{\gamma'}^4}{m_\phi\,\phi_0^2}\left(3+\frac{1}{4}\,\frac{m_\phi^4}{m_{\gamma'}^4}-\frac{m_\phi^2}{m_{\gamma'}^2}\right) \ . \tag{3.101}$$

This remains finite even in the limit $e' \to 0$ and, in fact, it tends to the value in Eq. (3.91), since in this limit the symmetry is global and the decay into massless Goldstone bosons is allowed.

On the other hand, for $m_{\gamma'} > m_\phi/2$, the dark scalar's decay into dark photon pairs becomes kinematically forbidden. This requires:

$$e' > \sqrt{2\,\lambda_\phi} \ , \tag{3.102}$$

which does not pose a significant constraint, given the magnitude of the scalar self-couplings considered in our analysis. Note that even if this condition is satisfied the scalar self-coupling is stable against gauge radiative corrections, since $\delta\lambda_\phi/\lambda_\phi \sim e'^4/\lambda_\phi \gtrsim \lambda_\phi$ and the self-coupling is typically very small in the scenarios under consideration.

It is important to mention that, similarly to the case studied in subsection 3.1.3.2, before the EWPT, the dark scalar's oscillations may also lead to the production of dark photons, through the second term in Eq. (3.99). This leads to an upper bound on the squared gauge coupling comparable to that obtained for the scalar self-interactions in Eq. (3.27), and thus nevertheless compatible with the stability condition Eq. (3.102). The dark photons could, in addition, be thermally produced in the early Universe in the presence of kinetic mixing with ordinary photons, but since there are no particles charged under both U(1) gauge groups, such mixing is absent in our model. In fact, $2 \leftrightarrow 2$ scattering processes involving dark and visible photons are only generated through the Higgs portal scalar mixing, which yields a dimension-6 operator that is suppressed with respect to the dark scalar's effective (visible) photon coupling by the smallness of the dark U(1) gauge coupling. Hence, within the parametric regime described above, the dark photons are not significantly produced in the early Universe and can neither make a significant contribution to the dark matter abundance nor lead to the condensate's decay or evaporation.

Notice that the spontaneous breaking of a U(1) symmetry can lead to the generation of cosmic strings at the EWPT. The ratio between the energy density of such cosmic strings, ρ_s, and the background density, ρ_c, reads [65]

$$\frac{\rho_s}{\rho_c} \sim G\mu \simeq 10^{-6}\left(\frac{\phi_0}{10^{16}\,\mathrm{GeV}}\right)^2, \tag{3.103}$$

where G is Newton's gravitational constant and μ is the string's energy per unit length. Nevertheless, as we reported in Ref. [2], $\phi_0 \ll 10^{16}\,\mathrm{GeV}$ even for very suppressed λ_ϕ (for instance, ϕ_0 is always smaller than $10^{16}\,\mathrm{GeV}$ for $\lambda_\phi > 10^{-66}$), implying that the ratio Eq. (3.103) is negligible and that, therefore, this does not pose additional constraints on the model.

Finally, we note that all the dynamics and predictions of our model could be achieved, however, by considering only a real scalar field with a $\mathbb{Z}_2$ symmetry. Spontaneous breaking of such a symmetry then leads to the generation of domain walls at the EWPT, which could have disastrous consequences for the cosmological dynamics.

However, it has been argued that a statistical bias in the initial configuration of the scalar field could effectively yield a preferred minimum and thus make the domain wall network decay [143]. In particular, according to Ref. [143], inflation itself may produce such a bias through the quantum fluctuations of the scalar field that become frozen on super-horizon scales. Since our dark scalar never thermalizes with the ambient cosmic plasma, such a bias could survive until the EWPT and therefore lead to the destruction of any domain wall network generated during the phase transition. A detailed study of the evolution of domain wall networks in the context of the proposed scenario is beyond the scope of this work, but this nevertheless suggests that a real scalar field, with no additional undesired degrees of freedom, may yield a consistent cosmological scenario for dark matter with spontaneous symmetry breaking.

In summary, we conclude that the cosmological consistency of the scenarios with spontaneous symmetry breaking requires either a complex scalar field transforming under a gauged U(1) symmetry with sufficiently large gauge coupling or possibly a real scalar field transforming under a $\mathbb{Z}_2$ symmetry.

3.5 Summary

In this chapter we have analyzed the dynamics and the phenomenology of a non-thermal dark matter candidate corresponding to an oscillating scalar field that, as all other known elementary particles, acquires mass solely through the Higgs mechanism. The model assumes an underlying scale invariance of the interactions that is broken by an unspecified mechanism to yield the electroweak and Planck scales.

The dynamics of the scalar field may be summarized in the following way. During inflation, the field acquires a Hubble-scale mass through a non-minimal coupling to gravity that drives the classical field towards the origin, while de Sitter quantum fluctuations generate a sub-Hubble field value on average. The Hubble scale mass also suppresses potentially significant cold dark matter isocurvature modes in the CMB anisotropies spectrum. After inflation, this non-minimal coupling plays no significant role in the dynamics, which is driven essentially by the scalar potential. After inflation, the field oscillates in a quartic potential, behaving as dark radiation, until the EWPT. At this point the field acquires mass through the Higgs mechanism, and starts behaving as non-relativistic matter.

If the Higgs portal coupling is positive, the dark scalar oscillates about the origin in

a quadratic potential until the present day, while for a negative coupling it undergoes spontaneous symmetry breaking and oscillates about a non-vanishing vacuum expectation value. Whereas in the former case the present dark matter abundance depends on all model parameters, including the non-minimal coupling to gravity and the scale of inflation, in the latter scenario it is determined uniquely the the Higgs portal coupling and the dark scalar's self-interactions. The suppression of particle production processes that could lead to the oscillating condensate's evaporation places strong constraints on the value of these couplings, and we generically find that the dark scalar's mass must lie below the MeV scale. It should be pointed out that the aim of this work is not to explain the smallness of the dark matter couplings. In fact, in the parametric regime that we are interested in ($g/\lambda^{1/4} \sim 10^{-3} - 10^{-2}$), both g and λ_ϕ are technically natural, since their relation is not significantly affected by radiative corrections, which makes them as natural as the electron Yukawa coupling. Nevertheless, small couplings can be naturally achieved in theories with extra dimensions, as we have shown in chapter 2.

While there are several phenomenological consequences of the Higgs portal interactions of the dark scalar that could allow for its detection, the required suppression of the latter makes this rather challenging in practice. Possible laboratory signatures include invisible Higgs decays, dark scalar-photon oscillations and induced oscillations of the fine structure constant and the electron mass. Indirect astrophysical signatures are also possible, namely dark matter annihilation or decay into photons. All these processes could lead to a robust identification of our proposed dark matter candidate, but unfortunately they lie generically below the reach of current technology, even for the case with spontaneous breaking that is generically easier to detect experimentally. An interesting exception is the decay of a 7 keV dark scalar in the case with spontaneous symmetry breaking, whose decay into photons may naturally explain 3.5 keV emission line observed in the GC, the Andromeda galaxy and the Perseus cluster.

In summary, the proposed oscillating scalar field is a viable dark matter candidate with distinctive observational and experimental signatures, constituting a promising alternative to WIMPs, which have so far evaded detection. While it is certainly amongst the "darkest" dark matter candidates available in the literature, there may already be astrophysical hints for its existence, and we hope that this work may motivate future technological developments that may allow for testing its implications in the laboratory.

4 | Can dark matter drive electroweak symmetry breaking?

4.1 Motivation

In this chapter we intend to study a scenario where an oscillating scalar field accounting for dark matter, Φ, drives a non-thermal electroweak symmetry breaking (EWSB). This possibililty can be accomplished if the reheating temperature, T_R, is below ~ 100 GeV such that the electroweak symmetry is never thermally restored. This requires a late decay of the inflaton field and, consequently, an early-matter era. Hence, we consider the case where Φ is coupled to the Higgs field, $\mathcal{H}$, and the effects of self-interactions and a non-minimal coupling (NMC) to curvature, similar to what we have done in the previous chapters (see Refs. [2, 3]). This chapter is based on Ref. [4].

The relevant Lagrangian density is the following:

$$-\mathcal{L}_{int} = g^2 |\Phi|^2 |\mathcal{H}|^2 + \lambda_\phi |\Phi|^4 + V(\mathcal{H}) - \xi R |\Phi|^2 , \tag{4.1}$$

where $V(\mathcal{H})$ is the Higgs potential, with the usual "mexican hat" shape, g is the coupling between the Higgs and the dark scalar, λ_ϕ is the dark scalar's self-coupling, ξ is a non-minimal coupling of the dark matter field to curvature and R the Ricci scalar.

In this scenario, the NMC term between Φ and R is negative, allowing the dark scalar to develop a large vev during inflation, which contributes to the Higgs mass during the same period. Given the interaction between the dark scalar and the Higgs fields, the minimum of the Higgs potential depends on the amplitude of the dark scalar field and, when the latter reaches a threshold value, EWSB occurs, as we will discuss in detail in the following sections.

4.2 Inflation

During inflation, the relevant Lagrangian for the dynamics of the Higgs and dark scalar field, assuming they have no significant interactions with the inflaton field, is:

$$-\mathcal{L}_{inf} = \frac{g^2}{4}\,\phi^2 h^2 + \frac{\lambda_\phi}{4}\phi^4 - \frac{\xi}{2}R\phi^2, \tag{4.2}$$

where $\Phi = \frac{\phi}{\sqrt{2}}$, $\mathcal{H} = \frac{h}{\sqrt{2}}$ and the Ricci scalar can be written in terms of the Hubble parameter,

$$R_{inf} \simeq 12\, H_{inf}^2\ , \tag{4.3}$$

where H_{inf} is defined in Eq. (2.19). Since the interaction term between ϕ and R has a negative sign, the dark scalar acquires a vev during inflation, ϕ_{inf}. This can be computed in the usual way, $\frac{dV}{d\phi} = \frac{dV}{dh} = 0$, yielding

$$\phi_{inf} = \sqrt{\frac{12\,\xi\, H_{inf}^2}{\lambda_\phi}}, \qquad h_{inf} = 0. \tag{4.4}$$

The dark scalar then provides a large mass to the Higgs field during inflation:

$$m_h = \frac{1}{\sqrt{2}}\, g\, \phi_{inf} \simeq \frac{g}{\lambda_\phi^{1/2}}\, \sqrt{6\,\xi}\, H_{inf}. \tag{4.5}$$

We will see later that $g/\sqrt{\lambda_\phi} \sim 10^2$ if the dark scalar accounts for all dark matter. The introduction of a scalar singlet with a vev coupled to the Higgs field may stabilize the potential of the latter during this period. As we have pointed out in subsection 1.2.4, the Higgs self-coupling, λ_h, becomes negative for energy scales above $10^{10} - 10^{12}$ GeV [54]. However, the induced Higgs mass during inflation shifts the field value at which the potential becomes negative towards values $\gtrsim 10^{10}$ GeV. In addition, the presence of the coupling decreases the amplitude of the quantum fluctuations of the Higgs field. Notice that, as we have seen in subsection 2.2, light fields during inflation exhibit quantum fluctuations of the order of $H_{inf} \sim 10^{12}$ GeV, (for values of the tensor-to-scalar ratio not too suppressed). However, if the Higgs is massive during inflation, its quantum fluctuations are given by [93]:

$$\left\langle h^2 \right\rangle \simeq \left(\frac{H_{inf}}{2\pi}\right)^2 \frac{H_{inf}}{m_h}, \tag{4.6}$$

which, using Eq. (4.5), simplifies to

$$\left\langle h^2 \right\rangle \simeq \left(\frac{H_{inf}}{2\pi}\right)^2 \frac{\lambda_\phi^{1/2}}{g\,\sqrt{6\,\xi}}, \tag{4.7}$$

corresponding to an amplitude of the quantum fluctuations $\sqrt{\langle h^2 \rangle} \sim 10^{11}$ GeV for $r \sim 10^{-2}$. Thus, the coupling between the Higgs and the dark scalar prevents the former from falling into the putative large field true minimum during inflation.

At the onset of the post-inflationary era, the dark scalar field will start to oscillate with an amplitude given by Eq. (4.4). We note that the dark scalar is also heavy during inflation, such that its de Sitter quantum fluctuations, with an amplitude $\sqrt{\langle \delta\phi^2 \rangle} \simeq 0.05\,\xi^{-1/4}\,H_{inf}$ [2, 3], have a negligible effect on its expectation value $\phi_{inf} \gtrsim H_{inf}$, the latter setting the initial amplitude for field oscillations in the post-inflationary epoch.

4.3 Post-inflationary period

In this model we assume that, after inflation, the inflaton field, χ, does not decay immediately. Instead, this component evolves like matter, while oscillating about the minimum of its potential, and an early matter-era dominates the Universe until reheating occurs. Therefore, there are some significant changes in the dynamics of the Universe with respect to the usual radiation dominated epoch. The scale factor, a, evolves in time as $a_{matt} \sim t^{2/3}$ and the Ricci scalar has a non-vanishing value, $R_{matt} = 3\,H^2$, unlike its value during the radiation era ($R_{rad} = 0$). The evolution of the inflaton energy density can be summarized in the following expression:

$$\rho_\chi\,(a) = 3\,H_{end}^2\,(r)\;M_{Pl}^2\,\left(\frac{a}{a_{end}}\right)^{-3}, \tag{4.8}$$

where the subscript “end" corresponds to the end of inflation. Note that H_{end} depends on the inflationary model that we are assuming. Let us consider, for instance, the case where inflation is driven by a field with a quadratic potential, $V\,(\chi) = \frac{1}{2}\,m_\chi^2\,\chi^2$, where m_χ is the inflaton's mass. The number of e-folds of inflation, after the observable CMB scales become super-horizon, is given by:

$$N_e = -\frac{1}{M_{Pl}^2}\int_{\chi_*}^{\chi_{end}} \frac{V\,(\chi)}{V'\,(\chi)}\,d\chi, \tag{4.9}$$

where χ_{end} corresponds to the value of the inflaton field at the end of inflation and χ_* is the value of the inflaton field during inflation, with $\chi_* \gg \chi_{end}$. Solving this integral, in the particular case where the inflaton has a quadratic potential, the number of e-folds reads:

$$N_e \simeq \frac{1}{4\,M_{Pl}^2}\,\chi_*^2. \tag{4.10}$$

The slow-roll parameter ϵ_χ is defined as

$$\epsilon_\chi = \frac{1}{2} M_{Pl}^2 \left(\frac{V'(\chi)}{V(\chi)} \right)^2 , \tag{4.11}$$

and, at the end of inflation, $\epsilon_{\chi_{end}} \sim 1$. In the case of the quadratic potential,

$$\epsilon_{\chi_{end}} = \frac{2\, M_{Pl}^2}{\chi_{end}^2} \Rightarrow \chi_{end}^2 = 2\, M_{Pl}^2. \tag{4.12}$$

Therefore, the energy density of the inflaton at the end of inflation can be written at the expense of the energy density of the inflaton $50 - 60$ e-folds before the end of inflation, when the relevant CMB scales become super-horizon:

$$\rho_\chi(\chi_{end}) = \frac{V(\chi_{end})}{V(\chi_*)} \rho_\chi(\chi_*) , \tag{4.13}$$

where $\rho_\chi(\chi_{end}) = \frac{3\, H_{end}^2}{M_{pl}^2}$ and $\rho_\chi(\chi_*) = \frac{3\, H_{inf}^2}{M_{pl}^2}$. From Eqs. (4.10) and (4.12),

$$\frac{V(\chi_{end})}{V(\chi_*)} \simeq \frac{1}{2\, N_e}. \tag{4.14}$$

Inserting the last expression into Eq. (4.13), the Hubble parameter at the end of inflation, H_{end}, is:

$$H_{end} = \frac{1}{\sqrt{2\, N_e}} H_{inf.} \tag{4.15}$$

Although the quadratic potential is already in some tension with Planck bounds on the tensor-to-scalar ratio [94], we will consider the above relation with $N_e = 60$ henceforth in our discussion, bearing in mind that a different relation between H_{end} and H_{inf} may lead to somewhat different results. Note that this model dependence is nevertheless degenerate with the unknown value of the tensor-to-scalar ratio, which we take as a free parameter.

At some point, the inflaton decays and reheats the Universe, establishing the beginning of the radiation-dominated epoch. This scenario resembles the so-called Polonyi problem found in many supergravity models (see, for e.g., Refs. [144–146]). We assume that the inflaton transfers all its energy density into Standard Model degrees of freedom at a reheating temperature T_R:

$$\rho_\chi(a_R) = \frac{\pi^2}{30} g_{*R}\, T_R^4, \tag{4.16}$$

where g_{*R} is the number of relativistic degrees of freedom at reheating. The reheating temperature must be above ~ 10 MeV, as the Universe must be radiation-dominated

during Big Bang nucleosynthesis (BBN). We will consider the case where reheating does not restore the electroweak symmetry, such that electroweak symmetry breaking is controlled by the dynamics of the dark matter scalar field, i.e, $T_R \lesssim 80$ GeV. It is important to note that before reheating there is no notion of temperature, since the inflaton has not yet decayed. Using Eqs. (4.8) and (4.16), the number of e-folds from inflation until reheating, N_R, reads:

$$\begin{aligned} N_R &= -\frac{1}{3}\ln\left(2\,N_e\,\frac{\pi^2}{90}\right) - \frac{1}{3}\ln\left(g_{*R}\right) - \frac{4}{3}\ln\left(T_R\right) + \frac{2}{3}\ln\left(H_{inf}\left(r\right)\right) + \frac{2}{3}\ln\left(M_{Pl}\right) \\ &\simeq 46 + \frac{1}{3}\ln\left(g_{*R}^{-1}\left(\frac{T_R}{\mathrm{GeV}}\right)^{-4}\left(\frac{r}{0.01}\right)\right), \end{aligned} \tag{4.17}$$

where we used $N_e = 60$.

The interesting feature of this model is that the dark scalar will control a non-thermal EWSB. From Eq. (4.1), it is easy to see that the minimum of the Higgs potential occurs at

$$|h| = \sqrt{\mathrm{v}^2 - \frac{g^2\,\phi^2}{2\,\lambda_h}}. \tag{4.18}$$

EWSB then takes place when the amplitude of the field becomes smaller then the value:

$$\phi_c = \sqrt{2\,\lambda_h}\,\frac{\mathrm{v}}{g}, \tag{4.19}$$

and that, in a few e-folds, the Higgs field should attain its final vev $|h| = \mathrm{v}$. In the following subsections, we will study the dynamics of the dark scalar when reheating occurs after or before EWSB. Note, however, that N_R (Eq. (4.17)) is determined solely by r and T_R, being independent of when EWSB takes place. Hence, our model exhibits five free parameters: r, ξ, g, λ_ϕ and T_R.

4.3.1 Reheating after electroweak symmetry breaking

The first scenario we study is the one where reheating occurs after EWSB, as illustrated in Fig. 4.1. Before EWSB, the quartic term dominates the energy density of the dark scalar, since $\phi \propto a^{-1}$, while $R \propto H \propto a^{-3/2}$, i.e, the NMC term decays more rapidly. Hence, the dark scalar behaves like radiation until EWSB and, at this point, we assume that the quadratic term of the dark scalar's potential takes over, which imposes constraints on our model, as we will consider in detail in subsection 4.4.

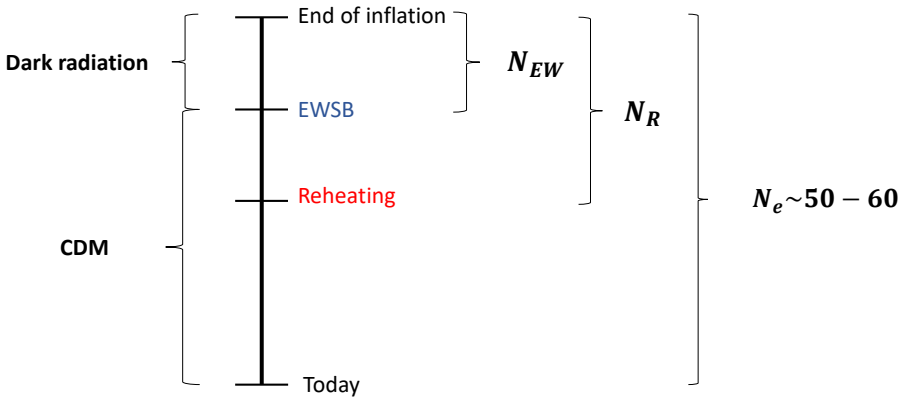

Figure 4.1: Time scale of the events: in this scenario, reheating occurs after EWSB. The dark scalar behaves like dark radiation until EWSB and like CDM afterwards. N_R corresponds to the number of e-folds from inflation until reheating and N_{EW} is the number of e-folds from inflation until EWSB.

Therefore, the dark scalar exhibits two behaviors:

$$\begin{cases} \phi_{rad}(a) = \phi_{inf}\left(\frac{a}{a_{end}}\right)^{-1}, & a_{end} < a < a_c \\ \phi_{DM}(a) = \phi_c\left(\frac{a}{a_c}\right)^{-3/2}, & a > a_c \end{cases}, \tag{4.20}$$

where a_c is the scale factor at which the EWSB takes place. At EWSB, we have:

$$\phi_c = \phi_{inf}\left(\frac{a_c}{a_{end}}\right)^{-1} \tag{4.21}$$

and, therefore, the number of e-folds from inflation until EWSB, N_{EW}, is given by

$$\begin{aligned} N_{EW} &= \ln(\phi_{inf}) - \ln(\phi_c) \\ &\simeq 27 + \ln\left(\sqrt{\xi}\,\frac{g}{\sqrt{\lambda_\phi}}\left(\frac{r}{0.01}\right)^{1/2}\right). \end{aligned} \tag{4.22}$$

Once reheating occurs, the Universe enters the usual radiation-dominated epoch. Thus, we can now consider a temperature and the number of dark matter particles in a comoving volume, n_ϕ/s, becomes constant. The dark scalar amplitude is, then:

$$\begin{aligned} \phi(a_R) &= \phi_c\left(\frac{a_R}{a_c}\right)^{-3/2} \\ &= \phi_c\, e^{-\frac{3}{2}(N_R - N_{EW})}. \end{aligned} \tag{4.23}$$

where

$$N_R - N_{EW} = 20.7 - \frac{1}{3}\ln(g_{*R}) - \frac{4}{3}\ln\left(\frac{T_R}{\text{GeV}}\right) - \frac{1}{6}\ln\left(\frac{r}{0.01}\right) - \ln\left(\sqrt{\xi}\,\frac{g}{\sqrt{\lambda_\phi}}\right). \tag{4.24}$$

Introducing the last equation into Eq. (4.23), the amplitude of the field at reheating becomes:

$$\phi_R \equiv \phi\left(a_R\right) = 3.2\times10^{-14}\,\phi_c\,\sqrt{g_{*R}}\,\left(\frac{r}{0.01}\right)^{1/4}\,\left(\frac{T_R}{\mathrm{GeV}}\right)^2\,\left(\sqrt{\xi}\,\frac{g}{\sqrt{\lambda_\phi}}\right)^{3/2}$$
$$= 4\times10^{-12}\,\sqrt{g_{*R}}\,\left(\frac{r}{0.01}\right)^{1/4}\,\left(\frac{T_R}{\mathrm{GeV}}\right)^2\,\left(\sqrt{\xi}\,\frac{g^{1/3}}{\sqrt{\lambda_\phi}}\right)^{3/2}\,\mathrm{GeV}. \qquad (4.25)$$

The number of particles in a comoving volume at T_R is, then:

$$\left(\frac{n_\phi}{s}\right)_R = \frac{1}{2}\,m_\phi\,\phi_R^2\,\frac{45}{2\pi^2}\,\frac{1}{g_{*R}}\,\frac{1}{T_R^3}, \qquad (4.26)$$

where m_ϕ stands for the dark scalar mass once the electroweak symmetry is broken and is given by:

$$m_\phi = \frac{1}{\sqrt{2}}\,g\,\mathrm{v}. \qquad (4.27)$$

The present dark matter abundance then reads:

$$\Omega_{\phi,0} = \frac{m_\phi}{3\,H_0^2\,M_{Pl}^2}\left(\frac{n_\phi}{s}\right)_R\,s_0$$
$$= \frac{m_\phi^2}{6\,H_0^2\,M_{Pl}^2}\,\phi_R^2\,\frac{g_{*0}}{g_{*R}}\,\left(\frac{T_0}{T_R}\right)^3, \qquad (4.28)$$

where g_{*0}, T_0 and H_0 are the present values of the number of relativistic degrees of freedom, CMB temperature and Hubble parameter, respectively.

Replacing Eq. (4.25) into the last expression, using Eq. (4.27) and fixing $\Omega_{\phi,0} = 0.26$, we get a relation between g and λ_ϕ:

$$g \simeq 4\times10^2\,\left(\frac{T_R}{10\,\mathrm{GeV}}\right)^{-1/3}\,\left(\frac{r}{0.01}\right)^{-1/6}\,\xi^{-1/2}\,\lambda_\phi^{1/2}, \qquad (4.29)$$

which depends only on ξ, r and T_R.

4.3.2 Reheating before electroweak symmetry breaking

The second putative scenario is the case where reheating occurs before EWSB, as illustrated in Fig. 4.2. Since the number of e-folds from inflation until reheating does not depend on when EWSB takes place (only depends on the inflaton and its decay into Standard Model particles), N_R is given by Eq. (4.17). In turn, N_{EW} only depends on ϕ_{inf} and ϕ_c and, therefore, it was computed already in Eq. (4.22). The difference between this and the previous scenario is that N_{EW} should be larger than

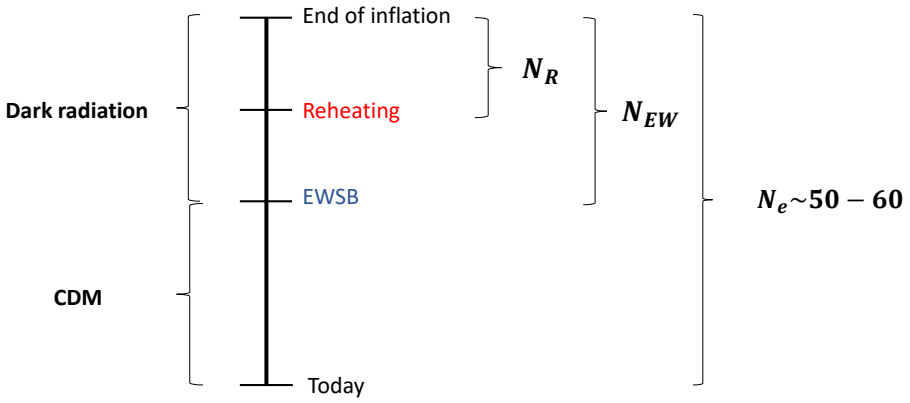

Figure 4.2: Time scale of the events: in this putative scenario, reheating occurs before EWSB. The dark scalar behaves like dark radiation until EWSB and like CDM afterwards. N_R corresponds to the number of e-folds from inflation until reheating and N_{EW} is the number of e-folds from inflation until EWSB.

N_R. The dark scalar behaves like dark radiation from reheating until EWSB, and after which n_ϕ/s becomes constant. From reheating onwards, the Universe enters the usual radiation-dominated epoch and $R = 0$.

The amplitude of the field at reheating is different from the previous scenario:

$$\phi_R = \phi_{inf} \left(\frac{a_R}{a_{end}}\right)^{-1} = \phi_{inf}\, e^{-N_R}, \tag{4.30}$$

and now we have a defined temperature and can write the amplitude of the field as a function of the temperature:

$$\phi_{rad}\,(T) = \phi_R \frac{T}{T_R} \left(\frac{g_{*T}}{g_{*R}}\right)^{1/3}. \tag{4.31}$$

This can be used to compute the temperature at which EWSB occurs, T_c:

$$T_c = \frac{\phi_c}{\phi_R}\, T_R \left(\frac{g_{*c}}{g_{*R}}\right)^{-1/3}. \tag{4.32}$$

At T_c the dark scalar stops holding the Higgs at the origin. Notice, however, that T_c must be smaller than the usual $T_{EW} \sim 80$ GeV, so that the dark scalar can control the EWSB and the latter is not restored by thermal effects. By doing the same procedure as in the previous subsection, since n_ϕ/s is constant as soon the field starts to behave like CDM, the present dark matter abundance is:

$$\Omega_{\phi,0} = \frac{m_\phi^2}{6\, H_0^2\, M_{Pl}^2}\, \phi_c^2\, \frac{g_{*0}}{g_{*c}} \left(\frac{T_0}{T_c}\right)^3. \tag{4.33}$$

Once the electroweak symmetry is broken, the dark scalar mass is $m_\phi = \left(1/\sqrt{2}\right) g\,\mathrm{v}$, as we have seen in Eq. (4.27). In turn, $\phi_c = \sqrt{2\,\lambda_h}\,\mathrm{v/g}$, as stated in Eq. (4.19). Introducing these two quantities in Eq. (4.33), and solving for T_c, we get:

$$T_c = \left(\frac{2\,\lambda_h\,\mathrm{v}^4}{12\,H_0^2\,M_{Pl}^2}\right)^{1/3} \left(\frac{g_{*0}}{g_{*c}}\right)^{1/3} \frac{T_0}{\Omega_{\phi,0}^{1/3}} \sim 7\times 10^5 \left(\frac{g_{*0}}{g_{*c}}\right)^{1/3} \mathrm{GeV}, \tag{4.34}$$

where we have fixed $\Omega_{\phi,0} = 0.26$.

Hence, from Eq. (4.34), we may conclude that, for reheating to occur before EWSB, T_c must be well above $T_{EW} \sim 80$ GeV. This is not consistent with our reasoning given that, at that temperature, the Higgs thermal mass is still sufficiently large to hold the latter at the origin, such that EWSB does not occur at T_c as assumed and, consequently, the dark scalar remains massless and behaves as dark radiation, as opposed to our starting assumption. In the remainder of this chapter, we will thus focus only on the case where reheating occurs after EWSB, given that in this scenario the dark scalar, in addition to being a viable dark matter candidate, can also control a non-thermal EWSB.

4.4 Model constraints

As stated, this model assumes that inflation is driven by some field, χ. Therefore, we have to ensure that the dark scalar is sub-dominant during inflation:

$$V\left(\phi_{inf}\right) < 3\,H_{inf}^2 M_{Pl}^2. \tag{4.35}$$

During inflation, the amplitude of the field is given by Eq. (4.4), and its energy density is dominated by the quartic and NMC terms:

$$\begin{aligned} V\left(\phi_{inf}\right) &\simeq \frac{\lambda_\phi}{4}\phi_{inf}^4 - \frac{\xi}{2}\,R\,\phi_{inf}^2 \\ &\simeq -\frac{12^2}{4}\xi^2\,\frac{H^4}{\lambda_\phi}. \end{aligned} \tag{4.36}$$

Using Eqs. (4.35) and (4.36),

$$\left|-\frac{12^2}{4}\xi^2\,\frac{H^4}{\lambda_\phi}\right| < 3\,H_{inf}^2 M_{Pl}^2 \Rightarrow \phi_{inf} < \frac{M_{Pl}}{\sqrt{\xi}}, \tag{4.37}$$

preventing the dark scalar from affecting the dynamics of inflation.

Moreover, we assume that the field starts to behave like CDM at EWSB. This means that the quadratic term has to dominate over the quartic term at EWSB, that is, $g^2\,\mathrm{v}^2\,\phi_c^2/\left(\lambda_\phi\,\phi_c^4\right) > 1$, which translates into the following condition:

$$g^4 > 2\,\lambda_h\lambda_\phi. \tag{4.38}$$

Furthermore, radiative corrections to the quartic coupling from the Higgs-portal coupling sould be small, unless we accept some degree of fine-tuning:

$$\delta\lambda_\phi \sim \frac{g^4}{16\pi^2} < \lambda_\phi. \tag{4.39}$$

From the experimental point of view, the Higgs may decay into dark scalar pairs with a decay width

$$\Gamma_{h\to\phi\phi} \simeq \frac{1}{8\pi}\,\frac{g^4\mathrm{v}^2}{4\,m_h}, \tag{4.40}$$

leading to a Higgs branching ratio to invisible particles, $Br\left(\Gamma_{h\to inv}\right)$ (we assume $\Gamma_{h\to inv} = \Gamma_{h\to\phi\phi}$) :

$$Br\left(\Gamma_{h\to inv}\right) = \frac{\Gamma_{h\to inv}}{\Gamma_h + \Gamma_{h\to inv}}. \tag{4.41}$$

Current limits from the LHC establish an upper bound for the branching ratio [124]:

$$Br\left(\Gamma_{h\to inv}\right) < 0.23. \tag{4.42}$$

Using $\Gamma_h = 4.07\times10^{-3}$ GeV [108], the branching ratio as function of the dark scalar mass is

$$Br\left(\Gamma_{h\to inv}\right) \simeq \frac{m_\phi^4}{8\times10^5 + m_\phi^4}, \tag{4.43}$$

corresponding to an upper bound on g:

$$g < 0.13, \tag{4.44}$$

which translates into an upper bound $m_\phi \lesssim 22.6$ GeV. In addition, we should impose constraints on the model to avoid the evaporation of the condensate and its consequent thermalization into a WIMP-like candidate.

4.4.1 Condensate evaporation

The dark scalar provides mass to the Higgs field for the period before EWSB. Since ϕ is oscillating, this could induce oscillations of the Higgs mass, given that the latter depends on the dark scalar field, which could constitute a problem: if $m_h < \sqrt{3\,\lambda_\phi}\,\phi_{rad}$,

Higgs production by the oscillating condensate is possible and this may destroy the condensate. However, there are ways of evading this scenario.

One of them is to provide initial conditions to the field so that its absolute value, and hence the Higgs mass, does not oscillate. To do so, we can introduce a mechanism similar to the Affleck-Dine mechanism [147], making the field oscillate in the complex plane such that its modulus does not (significantly) oscillate. In this way, the condition

$$m_h > \sqrt{3\,\lambda_\phi}\,\phi_{rad} \tag{4.45}$$

is always satisfied. For this we need to introduce angular momentum in field space, which can be accomplished by introducing terms in the potential that depend also on the phase of the dark scalar field. One possibility is that the interaction term between the field and the curvature depends on the value of the field, and not on its absolute value. Other possibilities are non-renormalizable terms in the dark scalar's potential. This violates explicitly the global $U(1)$ symmetry but the $\mathbb{Z}_2$ symmetry remains intact, avoiding the dark scalar decay. Notice that these are natural possibilities, since gravitational interactions do not, in principle, respect global symmetries, so that $U(1)$ violating terms arising from gravitational interactions should in general be present. Therefore, we may consider the following potential:

$$V(\phi) = -\xi\,R\left(\phi^2 + h.c.\right) + \frac{1}{M_{Pl}^4}\left(c\,\phi^{n+4} + h.c.\right) + \lambda_\phi\,|\Phi|^4 + g^2\,|\Phi|^2\,|\mathcal{H}|^2\,, \quad n > 4, \tag{4.46}$$

where c is an $\mathcal{O}(1)$ constant and n is an integer. Note that the non-minimal coupling term disappears when reheating occurs and the non-renormalizable term becomes suppressed with time faster than ϕ^4. Since the value of Ricci scalar during inflation differs from its value at the end of inflation, the phase of ϕ at the minimum is different during and after inflation, thus making the dark scalar oscillate in the complex plane. This prevents $|\phi|$ from oscillating significantly, such that the Higgs never becomes light enough to be produced.

Another way of solving the problem is to couple the Higgs field to the inflaton, χ, with an interaction term of the form

$$g_h^2\,\chi^2\,|\mathcal{H}|^2, \tag{4.47}$$

where g_h is the Higgs coupling to the inflaton. Notice that when reheating occurs and the Universe enters a radiation-dominated epoch, χ vanishes. In addition, the dark

matter field continues to control the EWSB, since the inflaton, behaving like matter, decays with $a^{-3/2}$, more rapidly than the dark scalar, which decays with a^{-1}.

The contribution of the inflaton term to the Higgs mass is

$$m_h = \frac{1}{\sqrt{2}}\, g_h\, \chi. \tag{4.48}$$

We have to ensure that (see Eq. (4.45))

$$\frac{1}{\sqrt{2}}\, g_h\, \chi_c > \sqrt{3\,\lambda_\phi}\, \phi_c, \tag{4.49}$$

which imposes an upper bound on g_h. The inflaton's amplitude at EWSB, χ_c, is

$$\chi_c = \chi_{end} \left(\frac{\phi_c}{\phi_{inf}}\right)^{3/2}, \tag{4.50}$$

where χ_{end} is the inflaton's amplitude at the end of inflation. Introducing the last expression into Eq. (4.49) and using the relation between g and λ_ϕ, the lower limit on g_h is:

$$g_h \gtrsim 2 \left(\frac{r}{10^{-4}}\right)^{2/3} \left(\frac{T_R}{10\,\mathrm{GeV}}\right)^{-1/6} \left(\frac{\chi_{end}}{M_{Pl}}\right)^{-1} \xi^{5/4} \left(\frac{H_{end}}{H_{inf}}\sqrt{N_e}\right)^{3/2}. \tag{4.51}$$

Notice that smaller values of r, corresponding to lower inflationary scales, allow for lower couplings g_h. Also, note that the Higgs mass receives two oscillating contributions to its mass, from ϕ and χ. However, since they will not, in general, be in phase, the Higgs mass should not oscillate significantly thus preventing its production.

The Universe is still in a matter-dominated era at EWSB if the reheating period occurs after that. The Hubble parameter can be computed using the expression for the inflaton's energy density given in Eq. (4.8):

$$\begin{aligned} H_c^2 &= \frac{\rho_\chi\,(a_c)}{3\,M_{Pl}^2} \\ &= \frac{H_{inf}^2}{2\,N_e}\, e^{-3N_{EW}}. \end{aligned} \tag{4.52}$$

Provided that there is no thermal bath at EWSB, the only possible channel for the condensate evaporation is the perturbative production of ϕ-particles by the oscillating background condensate. The dark scalar behaves like radiation until EWSB and the condensate decay width is given by [2, 3]:

$$\Gamma_{\phi\to\delta\phi\delta\phi} \simeq 4\times 10^{-2}\,\lambda_\phi^{3/2}\,\phi_{rad}, \tag{4.53}$$

where, at EWSB, $\phi_{rad} = \phi_c$. Condensate evaporation is avoided if the following condition holds

$$\left.\frac{\Gamma_{\phi\to\delta\phi\delta\phi}}{H}\right|_c < 1. \tag{4.54}$$

Note that, after EWSB, this production channel is blocked (see Refs. [2,3]). Therefore, from Eq. (4.54) we find that

$$g < 6\times 10^{-13}\left(\frac{r}{0.01}\right)^{-1/2}\xi^{-3/2}\,\lambda_\phi^{-3/2}, \tag{4.55}$$

and using the relation between g and λ_ϕ (Eq. (4.29)), the upper bound on g reads (for $N_e = 60$):

$$g < 0.06\left(\frac{T_R}{10\,\mathrm{GeV}}\right)^{-1/4}\left(\frac{r}{0.01}\right)^{-1/4}\xi^{-3/4}. \tag{4.56}$$

4.5 Results

In this subsection we summarize our results, taking into account all the different constraints analyzed earlier. We present the results for the regions in the (λ_ϕ, g) plane where all model constraints are satisfied, namely Eqs. (4.37) - (4.39) and (4.55). We choose to represent the results for values of the tensor-to-scalar ratio $r = 10^{-2}$ and non-minimal coupling $\xi = 0.1, 1$, as illustrated in Fig. 4.3.

In Fig. 4.3, we can see that there is a window where our model can explain dark matter, for masses larger than the ones we found in the scenarios of the previous chapters. For instance, we can see that $g \sim 10^{-2}$ is allowed, which corresponds to $m_\phi \sim 1$ GeV. We may conclude that an early matter-era blocks light masses, mainly because we do not want our dark matter candidate to affect the dynamics of inflation.

In fact, it is possible to get an analytic expression for the window of possible values for g and λ_ϕ, taking into account the intersections with the "forbidden" regions. Hence, since we do not want that the dark scalar affects inflation (Eq. (4.37)) and using the relation between the Higgs portal and the dark scalar self-interactions couplings (Eq. (4.29)), the constraint on g becomes

$$g > 10^3\left(\frac{T_R}{10\,\mathrm{GeV}}\right)^{-1/3}\left(\frac{r}{0.01}\right)^{-1/6}\xi^{1/2}\,\frac{H_{inf}}{M_{Pl}}, \tag{4.57}$$

which translates into

$$m_\phi > 3\left(\frac{T_R}{10\,\mathrm{GeV}}\right)^{-1/3}\left(\frac{r}{0.01}\right)^{1/3}\xi^{1/2}\,\mathrm{GeV}. \tag{4.58}$$

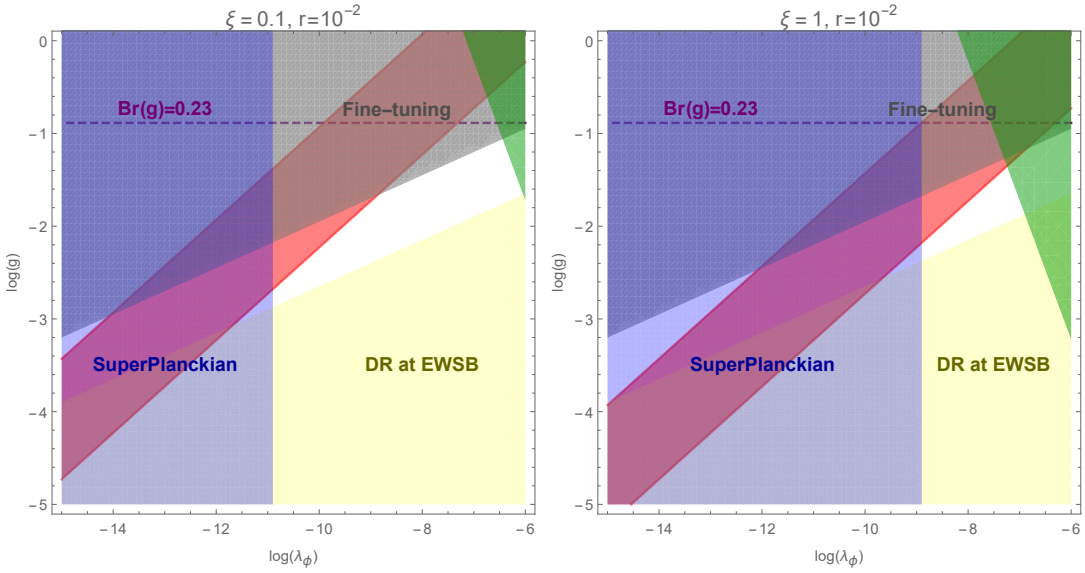

Figure 4.3: Regions in the (λ_ϕ, g) plane where the constraints in Eqs. (4.37) - (4.39) and Eq. (4.55) are satisfied, for $r = 10^{-2}$ and $\xi = 0.1, 1$. The red band encompasses the values of g and corresponding λ_ϕ that can account for the present dark matter abundance, if ϕ makes up all the dark matter, for $10\,\text{MeV} < T_R < 80\,\text{GeV}$ (the upper line in the red band corresponds to $T_R = 10\,\text{MeV}$ and the lower line corresponds to $T_R = 80\,\text{GeV}$). The excluded regions correspond to fine-tuned models (dark gray), super-Planckian dark scalar vevs during inflation, i.e, $\phi_{inf} > M_{Pl}/\sqrt{\xi}$, (blue) and scenarios where the dark scalar behaves as dark radiation and not as dark matter at or after EWSB (yellow). The dashed purple line yields the current experimental limit on the branching ratio of the Higgs invisible decays, $\text{Br}_{inv} \lesssim 0.23$, and the green region in the upper right corner corresponds to scenarios for which the condensate evaporates.

In turn, requiring that the field behaves like CDM at EWSB (Eq. (4.38)), and using the relation between couplings (Eq. (4.29)), we find a lower bound on g:

$$g > \frac{\sqrt{2\,\lambda_h}}{4\times 10^2}\left(\frac{T_R}{10\,\mathrm{GeV}}\right)^{1/3}\left(\frac{r}{0.01}\right)^{1/6}\xi^{1/2}, \tag{4.59}$$

and, consequently, a lower bound on the mass

$$m_\phi \gtrsim 0.2\left(\frac{T_R}{10\,\mathrm{GeV}}\right)^{1/3}\left(\frac{r}{0.01}\right)^{1/6}\xi^{1/2}\,\mathrm{GeV}. \tag{4.60}$$

The fine-tuning constraint allows only Higgs portal couplings below the following threshold

$$g < \frac{(16\,\pi^2)^{1/2}}{4\times 10^2}\left(\frac{T_R}{10\,\mathrm{GeV}}\right)^{1/3}\left(\frac{r}{0.01}\right)^{1/6}\xi^{1/2}, \tag{4.61}$$

imposing an upper bound on the mass:

$$m_\phi \lesssim 6\left(\frac{T_R}{10\,\mathrm{GeV}}\right)^{1/3}\left(\frac{r}{0.01}\right)^{1/6}\xi^{1/2}\,\mathrm{GeV}. \tag{4.62}$$

Taking into account all these restrictions, together with the bound coming from the condensate evaporation, Eq. (4.56), and knowing beforehand the region that the LHC is already able to probe, Eq. (4.44), we can build a plot and check the possible values for masses, predicted by our model, for $r = 10^{-2}$ and $r = 10^{-4}$, and non-minimal coupling $\xi = 0.1, 1, 10$. This is illustrated in Fig. 4.4.

From Fig. 4.4 we may conclude that our model predicts masses for the dark scalar in the range of $1 - 8$ GeV, depending on the values of the tensor-to-scalar ratio and non-minimal coupling chosen.

For instance, for $m_\phi \simeq 6$ GeV, this provides $Br\left(\Gamma_{h\to inv}\right) \simeq 2\times 10^{-3}$, which might be probed in the LHC in the near future, given that this is not too far from the current experimental limit (Eq. (4.42)). However, notice that large values of the NMC are only allowed for lower values of r.

4.6 Summary

In this chapter, we have analyzed the possibility of an oscillating scalar field, accounting for all the dark matter in the Universe, driving a non-thermal spontaneous breaking of the electroweak symmetry. The dark scalar is coupled to the Higgs field through a standard “Higgs-portal" biquadratic term, has no bare mass terms due to an underlying scale invariance of the theory, and has a negative non-minimal coupling

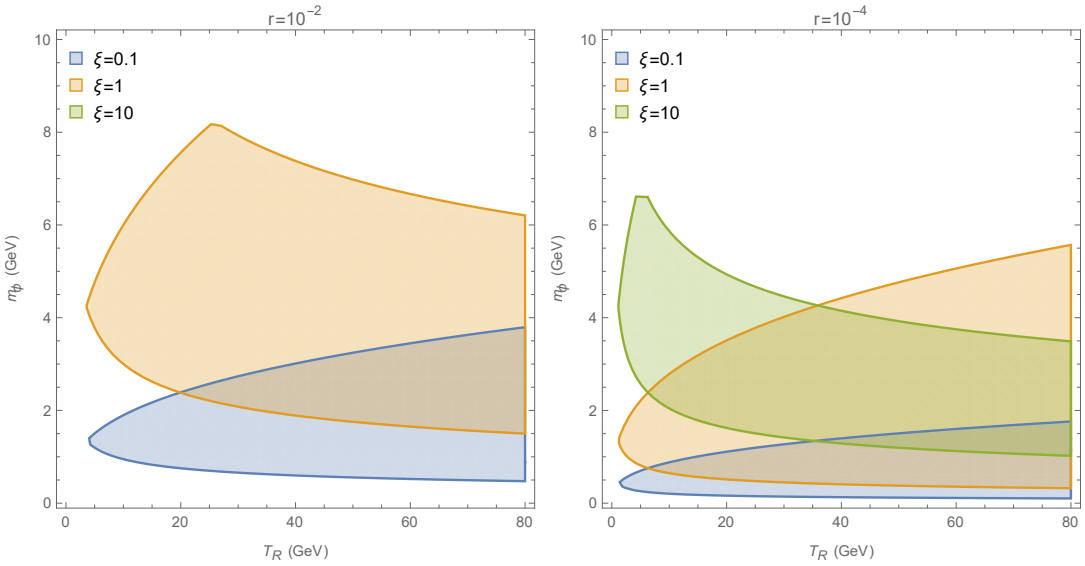

Figure 4.4: Allowed values for the dar scalar mass as a function of the reheating tempeature, for $10\,\text{MeV} < T_R < 80\,\text{GeV}$ and considering different values for the non-minimal coupling to curvature ξ and tensor-to-scalar ratio r.

to curvature. The latter, in particular, allows the dark scalar to develop a large expectation value during inflation. This holds the Higgs field at the origin both during and after inflation, until the dark scalar's oscillation amplitude drops below a critical value at which EWSB takes place. This prevents, in particular, the Higgs field from falling into the putative global minimum at large field values during inflation, ensuring at least the metastability of the electroweak vacuum.

The proposed scenario assumes a late decay of the inflaton field, such that reheating does not restore the electroweak symmetry, while the reheating temperature is still large enough to ensure a successful primordial nucleosynthesis[8]. Therefore, the Universe is still dominated by the inflaton field for a parametrically long period after inflation, while it oscillates about the minimum of its potential and behaves as a pressureless fluid. In fact, we have shown that consistent scenarios require reheating to occur only after EWSB, such that the latter occurs in the inflaton matter-dominated epoch essentially in vacuum.

Compared to other scenarios of scalar field dark matter where the Higgs is the only source of mass for the dark scalar field [1–3], we have shown that this allows for larger Higgs-portal couplings and hence dark scalar masses, since there are no

[8]We note that such low reheating temperatures require non-thermal baryogenesis scenarios such as e.g. the Affleck-Dine mechanism [147, 148].

thermalized particles in the Universe that could lead to an efficient evaporation of the scalar condensate until EWSB takes place. The dark scalar's oscillations, while it behaves as dark radiation, could themselves lead to particle production, but this can either be kinematically blocked in the case of Higgs production or made less efficient by the faster expansion of the Universe in a matter-dominated regime, as compared to the standard radiation epoch.

Overall, we have concluded that consistent scenarios where the dark scalar (1) does not affect the inflationary dynamics, (2) has technically natural values for its self-coupling (i.e. requiring no fine tuning), and (3) starts behaving as cold dark matter after it breaks the electroweak symmetry, require dark scalar masses in the few GeV range, unless inflation occurs much below the grand unification scale. This looks promising from the experimental perspective, since it allows for Higgs invisible branching ratios $\lesssim 10^{-3}$, which may be within the reach of colliders in a hopefully not too distant future.

We thus reply "Yes, it can" to the fundamental question posed in this work and hope that testing this idea may shed a new light on the nature of dark matter and on its role in the cosmic history.

5 | Conclusions

Dark matter constitutes almost 27% of the matter-energy content of the Universe, with evidence arising from different analysis, such as the galaxy rotation curves, the CMB anisotropies and the case of the Bullet Cluster, as depicted in subsection 1.4.1. Although its origin and nature remain unknown, there is a plethora of models that try to explain what dark matter is made of. Most of these dark matter candidates are WIMPs, a set of particles produced thermally in the early Universe and, despite the vast number of ongoing experiments that try to catch them, WIMPs have evaded observations so far. Maybe it is time to search for another type of dark matter candidate and present an alternative to the WIMP paradigm.

With this idea in mind, in this thesis, we propose an alternative dark matter candidate: an oscillating scalar field that acquires its mass through the Higgs mechanism. Although the connection between dark matter and the Higgs is not novel, since in the literature we can find several models that explore this link, our idea has a different feature: due to very feeble interactions with the Higgs, the oscillating scalar field behaves like a scalar condensate that is never in thermal equilibrium during all of its cosmic history, making it different from a WIMP. The present work elaborates on the dynamics and phenomenology of such dark matter candidate.

Hence, in chapter 2, we have considered a simple model, where the oscillating scalar field has negligible self-interactions. The field remains massless until the electroweak phase transition, where the Higgs field acquires its vev and provides mass to our dark matter candidate. We were able to find a relation between its mass and initial amplitude of oscillations that can account for the observed dark matter abundance. We have then described the dynamics of the dark scalar during inflation, which sets the initial conditions for the post-inflationary evolution and we have presented particular realizations of a weak coupling between the dark scalar and Higgs fields leading to the required field mass to account for dark matter, considering firstly the case of non-

renormalizable operators and then a bulk scalar field in the Randall-Sundrum scenario for a warped extra-dimension. Since the coupling to the Higgs is so small, $g \sim 10^{-16}$, this dark matter candidate may be very difficult to find in a near future.

In chapter 3, we have extended the model introduced previously by including a quartic term in the field's potential accounting for its self-interactions. We have studied the dark scalar field dynamics from the inflationary period to the electroweak phase transition. We have analyzed separately the cases where the Higgs portal coupling is positive and negative, and computed the present dark matter abundance in both scenarios. Assuming that this candidate accounts for all dark matter, we have obtained a relation between the Higgs portal coupling, g, and the self-interactions coupling, λ_ϕ. In addition, we have explored the phenomenology of these scenarios, discussing possible astrophysical signatures and experiments that could test them in the laboratory. In particular, we have shown that there is a promising case for detecting this dark scalar: a 7 keV dark scalar may decay into photons, which naturally explains the observed galactic and extra-galactic 3.5 keV X-ray line.

Finally, in chapter 4, we have analyzed the possibility that an oscillating scalar field, accounting for dark matter and coupled to the Higgs boson, controls a non-thermal electroweak symmetry breaking. We have assumed a late decay of the inflaton field, which leads to an early-matter era. In addition, the dark scalar acquires a vev during inflation, which contributes to the Higgs mass during the same period. The minimum of the Higgs is then controlled by the dark scalar field and the electroweak symmetry breaking takes place when the amplitude of the latter falls below a critical value. We have studied the cases where reheating occurs after or before the electroweak symmetry breaking and found that this model provides a dark matter candidate heavier than the ones considered in the previous chapters, making it more likely to be detected in laboratory experiments.

As a final note, this work has shown that dark matter, as the known particles in the Standard Model, may acquire mass through the Higgs mechanism, despite its hidden/sequestered nature. It has demonstrated, in addition, that the Higgs portal can offer alternative dark matter candidates to the thermal WIMPs typically considered in the literature, and that the properties of dark matter can also be used to probe the mechanism behind inflation in the early Universe. We thus hope that our work motivates further exploration of the different possibilities presented and other potentially related scenarios.

A | Effects of the reheating period in the ultra-light Higgs Portal scalar field dark matter scenario

Despite the mass of the dark matter field vanishing in the radiation-era before electroweak symmetry breaking, one must check whether the reheating period can affect the results presented in subsection 2.2. During this period,

$$\frac{m_\phi^2}{H^2} = 3c\frac{V(\chi)}{V(\chi) + \frac{1}{2}\dot{\chi}^2 + \rho_R} \ , \tag{A.1}$$

where ρ_R corresponds to the radiation energy density. Since during inflation we have $m_\phi^2/H^2 \simeq 3c \sim 1$, the dark matter field will be overdamped (or at most critically damped), $m_\phi \lesssim H$, in the post-inflationary eras, as we mentioned above, and we do not expect the dark matter field to oscillate during reheating. Nevertheless, before the radiation era, where $m_\phi^2/H^2 \sim V(\chi)/\rho_R \ll 1$, there may be a period of inflaton matter-domination, where the latter oscillates about the minimum of its potential but has not yet decayed significantly. Neglecting ρ_R in the equation above, we have $m_\phi^2/H^2 = 3c/2$, and it is easy to check that during this period the field amplitude decays as t^α, where

$$\alpha = \frac{1}{2}\left(-1 + \sqrt{1 - \frac{8}{3}c}\right) \ . \tag{A.2}$$

Thus, the field does not oscillate in this period for $c < 3/8$, which corresponds to $m_\phi \lesssim 1.1 H_{inf}$ during inflation, which is compatible with the Planck bounds on CMB isocurvature modes. For example, for $c = 1/3$, we have $\alpha = -1/3$, such that the field amplitude will decay as $a^{-1/2}$, implying that the inflaton-dominated matter era may

last for a few e-folds without significantly decreasing the dark matter field amplitude. The duration of this era is, of course, model-dependent, and we note that there are scenarios where this era is, in fact, absent and the slow-roll regime is immediately followed by radiation-domination, such as when the inflaton has a quartic potential or in warm inflation scenarios (see e.g. Ref. [149]).

The interactions between the inflaton and the ϕ field may also lead to the production of ϕ-particles during reheating. We expect this to be a negligible process in general due to the non-renormalizable nature of the interactions, since close to the minimum of the inflaton potential at χ_0, we have:

$$\mathcal{L} = c\frac{V(\chi)\phi^2}{M_P^2} = \frac{c}{2}\frac{m_\chi^2}{M_P^2}\chi^2\phi^2 + \ldots \equiv g^2\chi^2\phi^2 + \ldots \tag{A.3}$$

where $m_\chi^2 = V''(\chi_0)$ is the inflaton mass at the minimum and we assumed a vanishing vacuum energy. If this mass coincides with the inflaton mass during inflation, $m_\chi^2 = 3\eta H_{inf}^2$, taking into account the amplitude and tilt of the primordial curvature spectrum, this yields an effective coupling:

$$g^2 \sim 10^{-12}\left(\frac{\eta}{0.01}\right)\left(\frac{r}{0.01}\right) \ . \tag{A.4}$$

This coupling may be even more suppressed if the inflaton mass at the minimum is considerably smaller than its value during inflation. It is thus not hard to envisage scenarios where the inflaton couples more strongly to Standard Model particles such that only a negligible fraction of the inflaton's energy is converted into ϕ-particles during reheating, ensuring a sufficiently long radiation-dominated era.

One may nevertheless ask whether such particles could contribute to the present dark matter abundance. Due to their extremely small coupling to Standard Model particles (as we described in the previous sections) and to the inflaton, ϕ-particles never thermalize in the cosmic history, so that their final abundance is set entirely by their initial abundance, i.e. by the inflaton decay $\chi \to \phi\phi$. Their initial number density is thus (following Ref. [150]):

$$n_{\phi i} = B_\phi n_\chi = 2B_\phi \frac{\pi^2}{30}\frac{g_*}{m_\chi}\frac{T_R^4}{} \ , \tag{A.5}$$

where T_R is the reheating temperature, assuming instantaneous reheating in the worst-case scenario, and B_ϕ is the branching ratio of inflaton decays into dark matter particles. The latter may be relativistic when produced if the ϕ mass is already considerably smaller than the inflaton mass, such that they have initial momentum

$p_{\phi i} \sim m_\chi/2$. As they are always decoupled from the cosmic plasma, their momentum simply redshifts with expansion by a factor e^{-N_e}, where N_e denotes the number of e-folds of expansion after inflation. Taking $m_\phi \sim \sqrt{\eta} H_{inf} \sim 10^{12}$ GeV and $N_e \simeq 60$, we obtain a present momentum $p_{\phi 0} \sim 10^{-5}$ eV, which is comparable to the present mass of the dark matter particles in the range of interest to our scenario. This means that the dark matter particles should only be mildly relativistic today, $E_{\phi 0} \sim m_\phi$. Then:

$$\Omega_{\phi 0} \simeq \frac{m_\phi n_{\phi 0}}{3H_0^2 M_P^2} = \frac{m_\phi s_0}{3H_0 M_P^2}\left(\frac{n_{\phi i}}{s_i}\right) \simeq 0.01 B_\phi \left(\frac{m_\phi}{10^{-5}\text{ eV}}\right)\left(\frac{T_R}{10^{15}\text{ GeV}}\right)\left(\frac{m_\chi}{10^{12}\text{ GeV}}\right)^{-1}, \tag{A.6}$$

where we have used that n_ϕ/s remains constant for a decoupled species. We thus see that, due to the smallness of their mass, ϕ-particles from the inflaton decay generically give a negligible contribution to the present dark matter abundance, even if the branching ratio is not too suppressed.

In summary, we do not expect the reheating period to considerably modify our analysis in general in chapter 2, so that we may neglect its effects in computing the present dark matter abundance.

B | Effects of the non-minimal coupling to gravity on an oscillating scalar field

Consider a homogeneous scalar field ϕ that is oscillating about the minimum of a potential $V(\phi)$ much faster than Hubble expansion, i.e. in the regime where the effective field mass $m_\phi \gg H$. In this regime we then have that:

$$\frac{d}{dt}\langle\phi\dot{\phi}\rangle = \langle\dot{\phi}^2\rangle + \langle\phi\ddot{\phi}\rangle = \langle\dot{\phi}^2\rangle - \langle V'(\phi)\phi\rangle = 0 \ , \tag{B.1}$$

in a stationary configuration for quantities averaged over the oscillating period, where we have used the equation of motion $\ddot{\phi} = -V'(\phi)$ discarding the sub-leading effects of expansion. We thus obtain the virial theorem:

$$\begin{aligned} \langle\dot{\phi}^2\rangle &= \langle\phi V'(\phi)\rangle \\ &= n\langle V(\phi)\rangle, \end{aligned} \tag{B.2}$$

where the second line is valid for a potential of the form $V(\phi) \sim \phi^n$. Since $R \sim H^2 \ll m_\phi^2$ and $\dot{\phi} \sim m_\phi\phi$, we may discard the terms that include R or H explicitly in the expressions for the field's energy density and pressure given in Eq. (3.11), assuming $\xi \lesssim 1$. We may then write these quantities approximately as:

$$\begin{aligned} \rho_\phi &\simeq \frac{\dot{\phi}^2}{2} + V(\phi) \ , \\ p_\phi &\simeq \frac{1}{2}\dot{\phi}^2 - V(\phi) - 4\xi\left(\dot{\phi}^2 - \phi V'(\phi)\right) \ . \end{aligned} \tag{B.3}$$

It is easy to check, using the virial relation (B.2), that the term proportional to ξ vanishes on average, thus yielding the usual expressions for the energy density and

pressure of a homogeneous scalar field in minimally-coupled general relativity. This leads to the following equation of state parameter w:

$$\begin{aligned} w &\equiv \frac{p}{\rho} \\ &\simeq \frac{n-2}{n+2}. \end{aligned} \tag{B.4}$$

Also, for $m_\phi \gg H$, the field's equation of motion reads

$$\ddot{\phi} + 3H\dot{\phi} + V'(\phi) = 0 \ , \tag{B.5}$$

and, multiplying both sides by $\dot{\phi}$, we obtain the standard continuity equation:

$$\frac{d}{dt}\left(\frac{1}{2}\dot{\phi}^2 + V(\phi)\right) + 3H\dot{\phi}^2 = \dot{\rho_\phi} + 3H(\rho_\phi + p_\phi) = 0 \ . \tag{B.6}$$

Hence, the non-minimal coupling to gravity ξ does not affect the field's dynamics and properties in an underdamped regime.

References

[1] Orfeu Bertolami, Catarina Cosme, and João G. Rosa. Scalar field dark matter and the Higgs field. *Phys. Lett.*, B759:1–8, 2016.

[2] Catarina Cosme, João G. Rosa, and O. Bertolami. Scalar field dark matter with spontaneous symmetry breaking and the 3.5 keV line. *Phys. Lett.*, B781:639–644, 2018.

[3] Catarina Cosme, João G. Rosa, and O. Bertolami. Scale-invariant scalar field dark matter through the Higgs portal. *JHEP*, 05:129, 2018.

[4] Catarina Cosme, João G. Rosa, and Orfeu Bertolami. Can dark matter drive electroweak symmetry breaking? 2018.

[5] Nicolás Bernal, Catarina Cosme, and Tommi Tenkanen. Phenomenology of Self-Interacting Dark Matter in a Matter-Dominated Universe. 2018.

[6] Nicolás Bernal, Catarina Cosme, Tommi Tenkanen, and Ville Vaskonen. Scalar singlet dark matter in non-standard cosmologies. 2018.

[7] Giuseppe Degrassi, Stefano Di Vita, Joan Elias-Miro, Jose R. Espinosa, Gian F. Giudice, Gino Isidori, and Alessandro Strumia. Higgs mass and vacuum stability in the Standard Model at NNLO. *JHEP*, 08:098, 2012.

[8] Yoshiaki Sofue and Vera Rubin. Rotation curves of spiral galaxies. *Ann. Rev. Astron. Astrophys.*, 39:137–174, 2001.

[9] NASA. Bullet cluster. *Credit: X-ray: NASA/CXC/CfA/M.Markevitch et al.; Optical: NASA/STScI; Magellan/U.Arizona/D.Clowe et al.; Lensing Map: NASA/STScI; ESO WFI; Magellan/U.Arizona/D.Clowe et al.*

[10] N. Aghanim et al. Planck 2018 results. VI. Cosmological parameters. 2018.

[11] Daniel Baumann. Cosmology part iii mathematical tripos. *Cambridge University.*

[12] Nicolás Bernal, Matti Heikinheimo, Tommi Tenkanen, Kimmo Tuominen, and Ville Vaskonen. The Dawn of FIMP Dark Matter: A Review of Models and Constraints. *Int. J. Mod. Phys.*, A32(27):1730023, 2017.

[13] P. A. R. Ade et al. Planck 2015 results. XX. Constraints on inflation. 2015.

[14] Oleg Ruchayskiy, Alexey Boyarsky, Dmytro Iakubovskyi, Esra Bulbul, Dominique Eckert, Jeroen Franse, Denys Malyshev, Maxim Markevitch, and Andrii Neronov. Searching for decaying dark matter in deep XMM-Newton observation of the Draco dwarf spheroidal. *Mon. Not. Roy. Astron. Soc.*, 460(2):1390–1398, 2016.

[15] Gianfranco Bertone, Dan Hooper, and Joseph Silk. Particle dark matter: Evidence, candidates and constraints. *Phys. Rept.*, 405:279–390, 2005.

[16] Brian Patt and Frank Wilczek. Higgs-field portal into hidden sectors. 2006.

[17] M.C. Bento, O. Bertolami, R. Rosenfeld, and L. Teodoro. Selfinteracting dark matter and invisibly decaying Higgs. *Phys.Rev.*, D62:041302, 2000.

[18] M.C. Bento, O. Bertolami, and R. Rosenfeld. Cosmological constraints on an invisibly decaying Higgs boson. *Phys.Lett.*, B518:276–281, 2001.

[19] John March-Russell, Stephen M. West, Daniel Cumberbatch, and Dan Hooper. Heavy Dark Matter Through the Higgs Portal. *JHEP*, 07:058, 2008.

[20] Anirban Biswas and Debasish Majumdar. The Real Gauge Singlet Scalar Extension of Standard Model: A Possible Candidate of Cold Dark Matter. *Pramana*, 80:539–557, 2013.

[21] Maxim Pospelov and Adam Ritz. Higgs decays to dark matter: beyond the minimal model. *Phys. Rev.*, D84:113001, 2011.

[22] Namit Mahajan. Anomalous gauge boson couplings, 125 GeV Higgs and singlet scalar dark matter. 2012.

[23] James M. Cline, Kimmo Kainulainen, Pat Scott, and Christoph Weniger. Update on scalar singlet dark matter. *Phys. Rev.*, D88:055025, 2013. [Erratum: Phys. Rev.D92,no.3,039906(2015)].

[24] Kari Enqvist, Sami Nurmi, Tommi Tenkanen, and Kimmo Tuominen. Standard Model with a real singlet scalar and inflation. *JCAP*, 1408:035, 2014.

[25] Chris Kouvaris, Ian M. Shoemaker, and Kimmo Tuominen. Self-Interacting Dark Matter through the Higgs Portal. *Phys. Rev.*, D91(4):043519, 2015.

[26] Raul Costa, António P. Morais, Marco O. P. Sampaio, and Rui Santos. Two-loop stability of a complex singlet extended Standard Model. *Phys. Rev.*, D92:025024, 2015.

[27] Michael Duerr, Pavel Fileviez Pérez, and Juri Smirnov. Scalar Dark Matter: Direct vs. Indirect Detection. *JHEP*, 06:152, 2016.

[28] Huayong Han and Sibo Zheng. Higgs-portal Scalar Dark Matter: Scattering Cross Section and Observable Limits. 2015.

[29] Huayong Han and Sibo Zheng. New Constraints on Higgs-portal Scalar Dark Matter. *JHEP*, 12:044, 2015.

[30] Sami Nurmi, Tommi Tenkanen, and Kimmo Tuominen. Inflationary Imprints on Dark Matter. *JCAP*, 1511(11):001, 2015.

[31] Tommi Tenkanen. Cosmic inflation constrains scalar dark matter. *Cogent Phys.*, 2(1):1029845, 2015.

[32] Kimmo Kainulainen, Sami Nurmi, Tommi Tenkanen, Kimmo Tuominen, and Ville Vaskonen. Isocurvature Constraints on Portal Couplings. *JCAP*, 1606(06):022, 2016.

[33] Juan Garcia-Bellido, Javier Rubio, Mikhail Shaposhnikov, and Daniel Zenhausern. Higgs-Dilaton Cosmology: From the Early to the Late Universe. *Phys. Rev.*, D84:123504, 2011.

[34] Fedor Bezrukov, Georgios K. Karananas, Javier Rubio, and Mikhail Shaposhnikov. Higgs-Dilaton Cosmology: an effective field theory approach. *Phys. Rev.*, D87(9):096001, 2013.

[35] Pedro G. Ferreira, Christopher T. Hill, and Graham G. Ross. Scale-Independent Inflation and Hierarchy Generation. *Phys. Lett.*, B763:174–178, 2016.

[36] Pedro G. Ferreira, Christopher T. Hill, and Graham G. Ross. Weyl Current, Scale-Invariant Inflation and Planck Scale Generation. *Phys. Rev.*, D95(4):043507, 2017.

[37] Matti Heikinheimo, Antonio Racioppi, Martti Raidal, Christian Spethmann, and Kimmo Tuominen. Physical Naturalness and Dynamical Breaking of Classical Scale Invariance. *Mod. Phys. Lett.*, A29:1450077, 2014.

[38] Emidio Gabrielli, Matti Heikinheimo, Kristjan Kannike, Antonio Racioppi, Martti Raidal, and Christian Spethmann. Towards Completing the Standard Model: Vacuum Stability, EWSB and Dark Matter. *Phys. Rev.*, D89(1):015017, 2014.

[39] Alberto Salvio and Alessandro Strumia. Agravity. *JHEP*, 06:080, 2014.

[40] Matti Heikinheimo, Tommi Tenkanen, and Kimmo Tuominen. WIMP miracle of the second kind. *Phys. Rev.*, D96(2):023001, 2017.

[41] Astrid Eichhorn, Yuta Hamada, Johannes Lumma, and Masatoshi Yamada. Quantum gravity fluctuations flatten the Planck-scale Higgs potential. *Phys. Rev.*, D97(8):086004, 2018.

[42] Alberto Salvio. Inflationary Perturbations in No-Scale Theories. *Eur. Phys. J.*, C77(4):267, 2017.

[43] S. L. Glashow. Partial Symmetries of Weak Interactions. *Nucl. Phys.*, 22:579–588, 1961.

[44] Abdus Salam and John Clive Ward. Electromagnetic and weak interactions. *Phys. Lett.*, 13:168–171, 1964.

[45] Steven Weinberg. A model of leptons. *Phys. Rev. Lett.*, 19:1264–1266, Nov 1967.

[46] G. 'tHooft. Renormalization of massless yang-mills fields. *Nuclear Physics B*, 33(1):173 – 199, 1971.

[47] Murray Gell-Mann. A Schematic Model of Baryons and Mesons. *Phys. Lett.*, 8:214–215, 1964.

[48] G. Zweig. An SU(3) model for strong interaction symmetry and its breaking. Version 1. 1964.

[49] Morad Aaboud et al. Measurement of the Higgs boson mass in the $H \to ZZ^* \to 4\ell$ and $H \to \gamma\gamma$ channels with $\sqrt{s} = 13$ TeV pp collisions using the ATLAS detector. *Phys. Lett.*, B784:345–366, 2018.

[50] P. W. Anderson. Plasmons, gauge invariance, and mass. *Phys. Rev.*, 130:439–442, Apr 1963.

[51] F. Englert and R. Brout. Broken symmetry and the mass of gauge vector mesons. *Phys. Rev. Lett.*, 13:321–323, Aug 1964.

[52] Peter W. Higgs. Broken symmetries and the masses of gauge bosons. *Phys. Rev. Lett.*, 13:508–509, Oct 1964.

[53] G. S. Guralnik, C. R. Hagen, and T. W. B. Kibble. Global conservation laws and massless particles. *Phys. Rev. Lett.*, 13:585–587, Nov 1964.

[54] Dario Buttazzo, Giuseppe Degrassi, Pier Paolo Giardino, Gian F. Giudice, Filippo Sala, Alberto Salvio, and Alessandro Strumia. Investigating the near-criticality of the Higgs boson. *JHEP*, 12:089, 2013.

[55] Joan Elias-Miro, Jose R. Espinosa, Gian F. Giudice, Gino Isidori, Antonio Riotto, and Alessandro Strumia. Higgs mass implications on the stability of the electroweak vacuum. *Phys. Lett.*, B709:222–228, 2012.

[56] José Ramón Espinosa. Vacuum Stability and the Higgs Boson. *PoS*, LATTICE2013:010, 2014.

[57] Matthew Gonderinger, Yingchuan Li, Hiren Patel, and Michael J. Ramsey-Musolf. Vacuum Stability, Perturbativity, and Scalar Singlet Dark Matter. *JHEP*, 01:053, 2010.

[58] Oleg Lebedev. On Stability of the Electroweak Vacuum and the Higgs Portal. *Eur. Phys. J.*, C72:2058, 2012.

[59] Andrew Liddle. *An introduction to modern cosmology; 2nd ed.* Wiley, Chichester, 2003.

[60] Edmund J. Copeland, M. Sami, and Shinji Tsujikawa. Dynamics of dark energy. *Int.J.Mod.Phys.*, D15:1753–1936, 2006.

[61] Daniel Baumann. Inflation. In *Physics of the large and the small, TASI 09, proceedings of the Theoretical Advanced Study Institute in Elementary Particle Physics, Boulder, Colorado, USA, 1-26 June 2009*, pages 523–686, 2011.

[62] David H. Lyth and Andrew R. Liddle. *The primordial density perturbation: Cosmology, inflation and the origin of structure*. 2009.

[63] Alan H. Guth. Inflationary universe: A possible solution to the horizon and flatness problems. *Phys. Rev. D*, 23:347–356, Jan 1981.

[64] Andrei D. Linde. A New Inflationary Universe Scenario: A Possible Solution of the Horizon, Flatness, Homogeneity, Isotropy and Primordial Monopole Problems. *Phys. Lett.*, 108B:389–393, 1982. [Adv. Ser. Astrophys. Cosmol.3,149(1987)].

[65] Edward W. Kolb and Michael S. Turner. The Early Universe. *Front. Phys.*, 69:1–547, 1990.

[66] F. Zwicky. Die Rotverschiebung von extragalaktischen Nebeln. *Helvetica Physica Acta*, 6:110–127, 1933.

[67] G. Bertone. *Particle Dark Matter: Observations, Models and Searches*. Cambridge University Press, 2010.

[68] Douglas Clowe, Marusa Bradac, Anthony H. Gonzalez, Maxim Markevitch, Scott W. Randall, Christine Jones, and Dennis Zaritsky. A direct empirical proof of the existence of dark matter. *Astrophys. J.*, 648:L109–L113, 2006.

[69] Bing-Lin Young. A survey of dark matter and related topics in cosmology. *Frontiers of Physics*, 12(2):121201, Oct 2016.

[70] Leszek Roszkowski, Enrico Maria Sessolo, and Sebastian Trojanowski. WIMP dark matter candidates and searches - current status and future prospects. *Rept. Prog. Phys.*, 81(6):066201, 2018.

[71] D. S. Akerib et al. Results from a search for dark matter in the complete LUX exposure. *Phys. Rev. Lett.*, 118(2):021303, 2017.

[72] E. Aprile et al. Dark Matter Search Results from a One Ton-Year Exposure of XENON1T. *Phys. Rev. Lett.*, 121(11):111302, 2018.

[73] R. Bernabei et al. First model independent results from DAMA/LIBRA-phase2. 2018.

[74] Lawrence J. Hall, Karsten Jedamzik, John March-Russell, and Stephen M. West. Freeze-In Production of FIMP Dark Matter. *JHEP*, 03:080, 2010.

[75] David J. E. Marsh. Axion Cosmology. *Phys. Rept.*, 643:1–79, 2016.

[76] R. J. Crewther, P. Di Vecchia, G. Veneziano, and Edward Witten. Chiral Estimate of the Electric Dipole Moment of the Neutron in Quantum Chromodynamics. *Phys. Lett.*, 88B:123, 1979. [Erratum: Phys. Lett.91B,487(1980)].

[77] J. M. Pendlebury et al. Revised experimental upper limit on the electric dipole moment of the neutron. *Phys. Rev.*, D92(9):092003, 2015.

[78] R. D. Peccei and H. R. Quinn. CP conservation in the presence of pseudoparticles. *Physical Review Letters*, 38:1440–1443, June 1977.

[79] Andreas Ringwald. Alternative dark matter candidates: Axions. *PoS*, NOW2016:081, 2016.

[80] M. Milgrom. A Modification of the Newtonian dynamics as a possible alternative to the hidden mass hypothesis. *Astrophys. J.*, 270:365–370, 1983.

[81] Antonio De Felice and Shinji Tsujikawa. f(R) theories. *Living Rev. Rel.*, 13:3, 2010.

[82] Orfeu Bertolami, Christian G. Boehmer, Tiberiu Harko, and Francisco S. N. Lobo. Extra force in f(R) modified theories of gravity. *Phys. Rev.*, D75:104016, 2007.

[83] M. Lubini, C. Tortora, J. Naf, Ph. Jetzer, and S. Capozziello. Probing the dark matter issue in f(R)-gravity via gravitational lensing. *Eur. Phys. J.*, C71:1834, 2011.

[84] Georges Aad et al. Observation of a new particle in the search for the Standard Model Higgs boson with the ATLAS detector at the LHC. *Phys. Lett.*, B716:1–29, 2012.

[85] Serguei Chatrchyan et al. Observation of a new boson at a mass of 125 GeV with the CMS experiment at the LHC. *Phys. Lett.*, B716:30–61, 2012.

[86] Vanda Silveira and A Zee. Scalar phantoms. *Physics Letters B*, 161(1):136–140, 1985.

[87] C.P. Burgess, Maxim Pospelov, and Tonnis ter Veldhuis. The Minimal model of nonbaryonic dark matter: A Singlet scalar. *Nucl.Phys.*, B619:709–728, 2001.

[88] Osamu Seto, Kazunori Kohri, and Takashi Nakamura. Oscillating scalar field dark matter in supergravity. *JHEP*, 09:032, 2001.

[89] O. Bertolami and R. Rosenfeld. The Higgs portal and an unified model for dark energy and dark matter. *Int.J.Mod.Phys.*, A23:4817–4827, 2008.

[90] Orfeu Bertolami, Pedro Carrilho, and Jorge Parámos. Two-scalar-field model for the interaction of dark energy and dark matter. *Phys.Rev.*, D86:103522, 2012.

[91] David J. E. Marsh, Daniel Grin, Renee Hlozek, and Pedro G. Ferreira. Tensor Interpretation of BICEP2 Results Severely Constrains Axion Dark Matter. *Phys. Rev. Lett.*, 113(1):011801, 2014.

[92] Daniel Baumann and Liam McAllister. *Inflation and String Theory*. Cambridge Monographs on Mathematical Physics. Cambridge University Press, 2015.

[93] Antonio Riotto. Inflation and the theory of cosmological perturbations. In *Astroparticle physics and cosmology. Proceedings: Summer School, Trieste, Italy, Jun 17-Jul 5 2002*, pages 317–413, 2002.

[94] Y. Akrami et al. Planck 2018 results. X. Constraints on inflation. 2018.

[95] Lisa Randall and Raman Sundrum. A Large mass hierarchy from a small extra dimension. *Phys. Rev. Lett.*, 83:3370–3373, 1999.

[96] Tony Gherghetta and Alex Pomarol. Bulk fields and supersymmetry in a slice of AdS. *Nucl. Phys.*, B586:141–162, 2000.

[97] Orfeu Bertolami and Carla Carvalho. Spontaneous symmetry breaking in the bulk as a localization mechanism of fields on the brane. *Phys. Rev.*, D76:104048, 2007.

[98] Mar Bastero-Gil, Arjun Berera, Robert Brandenberger, Ian G. Moss, Rudnei O. Ramos, and João G. Rosa. The role of fluctuation-dissipation dynamics in setting initial conditions for inflation. *JCAP*, 1801(01):002, 2018.

[99] Patrick B. Greene, Lev Kofman, Andrei D. Linde, and Alexei A. Starobinsky. Structure of resonance in preheating after inflation. *Phys. Rev.*, D56:6175–6192, 1997.

[100] Kazuhide Ichikawa, Teruaki Suyama, Tomo Takahashi, and Masahide Yamaguchi. Primordial Curvature Fluctuation and Its Non-Gaussianity in Models with Modulated Reheating. *Phys. Rev.*, D78:063545, 2008.

[101] N. Prantzos et al. The 511 keV emission from positron annihilation in the Galaxy. *Rev. Mod. Phys.*, 83:1001–1056, 2011.

[102] Pierre Jean, J. Knodlseder, W. Gillard, N. Guessoum, K. Ferriere, A. Marcowith, V. Lonjou, and J. P. Roques. Spectral analysis of the galactic e+ e- annihilation emission. *Astron. Astrophys.*, 445:579–589, 2006.

[103] J. Knodlseder et al. The All-sky distribution of 511 keV electron-positron annihilation emission. *Astron. Astrophys.*, 441:513–532, 2005.

[104] Eugene Churazov, R. Sunyaev, S. Sazonov, M. Revnivtsev, and D. Varshalovich. Positron annihilation spectrum from the Galactic Center region observed by SPI/INTEGRAL. *Mon. Not. Roy. Astron. Soc.*, 357:1377–1386, 2005.

[105] Pierre Jean et al. Early SPI / INTEGRAL measurements of 511 keV line emission from the 4th quadrant of the Galaxy. *Astron. Astrophys.*, 407:L55, 2003.

[106] Ryan J. Wilkinson, Aaron C. Vincent, Céline Boehm, and Christopher McCabe. Ruling out the light weakly interacting massive particle explanation of the Galactic 511 keV line. *Phys. Rev.*, D94(10):103525, 2016.

[107] Lars Bergstrom, Piero Ullio, and James H. Buckley. Observability of gamma-rays from dark matter neutralino annihilations in the Milky Way halo. *Astropart. Phys.*, 9:137–162, 1998.

[108] Alessandro Cuoco, Benedikt Eiteneuer, Jan Heisig, and Michael Krämer. A global fit of the γ-ray galactic center excess within the scalar singlet Higgs portal model. *JCAP*, 1606(06):050, 2016.

[109] Abdelhak Djouadi. The Anatomy of electro-weak symmetry breaking. I: The Higgs boson in the standard model. *Phys. Rept.*, 457:1–216, 2008.

[110] Esra Bulbul, Maxim Markevitch, Adam Foster, Randall K. Smith, Michael Loewenstein, and Scott W. Randall. Detection of An Unidentified Emission Line in the Stacked X-ray spectrum of Galaxy Clusters. *Astrophys. J.*, 789:13, 2014.

[111] Alexey Boyarsky, Oleg Ruchayskiy, Dmytro Iakubovskyi, and Jeroen Franse. Unidentified Line in X-Ray Spectra of the Andromeda Galaxy and Perseus Galaxy Cluster. *Phys. Rev. Lett.*, 113:251301, 2014.

[112] Alexey Boyarsky, Jeroen Franse, Dmytro Iakubovskyi, and Oleg Ruchayskiy. Checking the Dark Matter Origin of a 3.53 keV Line with the Milky Way Center. *Phys. Rev. Lett.*, 115:161301, 2015.

[113] Nico Cappelluti, Esra Bulbul, Adam Foster, Priyamvada Natarajan, Megan C. Urry, Mark W. Bautz, Francesca Civano, Eric Miller, and Randall K. Smith. Searching for the 3.5 keV Line in the Deep Fields with Chandra: the 10 Ms observations. 2017.

[114] Tetsutaro Higaki, Kwang Sik Jeong, and Fuminobu Takahashi. The 7 keV axion dark matter and the X-ray line signal. *Phys. Lett.*, B733:25–31, 2014.

[115] Joerg Jaeckel, Javier Redondo, and Andreas Ringwald. 3.55 keV hint for decaying axionlike particle dark matter. *Phys. Rev.*, D89:103511, 2014.

[116] Emilian Dudas, Lucien Heurtier, and Yann Mambrini. Generating X-ray lines from annihilating dark matter. *Phys. Rev.*, D90:035002, 2014.

[117] Farinaldo S. Queiroz and Kuver Sinha. The Poker Face of the Majoron Dark Matter Model: LUX to keV Line. *Phys. Lett.*, B735:69–74, 2014.

[118] Julian Heeck and Daniele Teresi. Cold keV dark matter from decays and scatterings. 2017.

[119] Tesla E. Jeltema and Stefano Profumo. Discovery of a 3.5 keV line in the Galactic Centre and a critical look at the origin of the line across astronomical targets. *Mon. Not. Roy. Astron. Soc.*, 450(2):2143–2152, 2015.

[120] A. Boyarsky, J. Franse, D. Iakubovskyi, and O. Ruchayskiy. Comment on the paper "Dark matter searches going bananas: the contribution of Potassium (and Chlorine) to the 3.5 keV line" by T. Jeltema and S. Profumo. 2014.

[121] Esra Bulbul, Maxim Markevitch, Adam R. Foster, Randall K. Smith, Michael Loewenstein, and Scott W. Randall. Comment on "Dark matter searches going bananas: the contribution of Potassium (and Chlorine) to the 3.5 keV line". 2014.

[122] Dmytro Iakubovskyi. Checking the potassium origin of the new emission line at 3.5 keV using the K XIX line complex at 3.7 keV. *Mon. Not. Roy. Astron. Soc.*, 453(4):4097–4101, 2015.

[123] Tesla E. Jeltema and Stefano Profumo. Deep XMM Observations of Draco rule out at the 99% Confidence Level a Dark Matter Decay Origin for the 3.5 keV Line. *Mon. Not. Roy. Astron. Soc.*, 458(4):3592–3596, 2016.

[124] Georges Aad et al. Constraints on new phenomena via Higgs boson couplings and invisible decays with the ATLAS detector. *JHEP*, 11:206, 2015.

[125] Stephen L. Adler. Axial vector vertex in spinor electrodynamics. *Phys. Rev.*, 177:2426–2438, 1969. [,241(1969)].

[126] S. L. Cheng, C. Q. Geng, and W. T. Ni. Axion - photon couplings in invisible axion models. *Phys. Rev.*, D52:3132–3135, 1995.

[127] João G. Rosa and Thomas W. Kephart. Stimulated Axion Decay in Superradiant Clouds around Primordial Black Holes. *Phys. Rev. Lett.*, 120(23):231102, 2018.

[128] Javier Redondo and Andreas Ringwald. Light shining through walls. *Contemp. Phys.*, 52:211–236, 2011.

[129] Klaus Ehret et al. New ALPS Results on Hidden-Sector Lightweights. *Phys. Lett.*, B689:149–155, 2010.

[130] Klaus Ehret. The ALPS Light Shining Through a Wall Experiment - WISP Search in the Laboratory. In *Proceedings, 45th Rencontres de Moriond on Electroweak Interactions and Unified Theories: La Thuile, Italy, March 6-13, 2010*, pages 455–466, 2010.

[131] K. Melnikov and Oleg I. Yakovlev. Higgs —> two photon decay: QCD radiative correction. *Phys. Lett.*, B312:179–183, 1993.

[132] Thibault Damour and John F. Donoghue. Equivalence Principle Violations and Couplings of a Light Dilaton. *Phys. Rev.*, D82:084033, 2010.

[133] Ken Van Tilburg, Nathan Leefer, Lykourgos Bougas, and Dmitry Budker. Search for ultralight scalar dark matter with atomic spectroscopy. *Phys. Rev. Lett.*, 115(1):011802, 2015.

[134] Y. V. Stadnik and V. V. Flambaum. Improved limits on interactions of low-mass spin-0 dark matter from atomic clock spectroscopy. *Phys. Rev.*, A94(2):022111, 2016.

[135] Y. V. Stadnik and V. V. Flambaum. Searching for dark matter and variation of fundamental constants with laser and maser interferometry. *Phys. Rev. Lett.*, 114:161301, 2015.

[136] Asimina Arvanitaki, Junwu Huang, and Ken Van Tilburg. Searching for dilaton dark matter with atomic clocks. *Phys. Rev.*, D91(1):015015, 2015.

[137] Y. V. Stadnik and V. V. Flambaum. Can dark matter induce cosmological evolution of the fundamental constants of Nature? *Phys. Rev. Lett.*, 115(20):201301, 2015.

[138] Y. V. Stadnik and V. V. Flambaum. Enhanced effects of variation of the fundamental constants in laser interferometers and application to dark matter detection. *Phys. Rev.*, A93(6):063630, 2016.

[139] A. Hees, J. Guéna, M. Abgrall, S. Bize, and P. Wolf. Searching for an oscillating massive scalar field as a dark matter candidate using atomic hyperfine frequency comparisons. *Phys. Rev. Lett.*, 117(6):061301, 2016.

[140] Asimina Arvanitaki, Savas Dimopoulos, and Ken Van Tilburg. Sound of Dark Matter: Searching for Light Scalars with Resonant-Mass Detectors. *Phys. Rev. Lett.*, 116(3):031102, 2016.

[141] Asimina Arvanitaki, Peter W. Graham, Jason M. Hogan, Surjeet Rajendran, and Ken Van Tilburg. Search for light scalar dark matter with atomic gravitational wave detectors. 2016.

[142] Asimina Arvanitaki, Savas Dimopoulos, Sergei Dubovsky, Nemanja Kaloper, and John March-Russell. String Axiverse. *Phys. Rev.*, D81:123530, 2010.

[143] Sebastian E. Larsson, Subir Sarkar, and Peter L. White. Evading the cosmological domain wall problem. *Phys. Rev.*, D55:5129–5135, 1997.

[144] G.D. Coughlan, W. Fischler, Edward W. Kolb, S. Raby, and G.G. Ross. Cosmological problems for the polonyi potential. *Physics Letters B*, 131(1):59 – 64, 1983.

[145] O. Bertolami and Graham G. Ross. Inflation as a Cure for the Cosmological Problems of Superstring Models With Intermediate Scale Breaking. *Phys. Lett.*, B183:163–168, 1987.

[146] Orfeu Bertolami. Cosmological Difficulties of $N = 1$ Supergravity Models With Sliding Scales. *Phys. Lett.*, B209:277–282, 1988.

[147] Ian Affleck and Michael Dine. A New Mechanism for Baryogenesis. *Nucl. Phys.*, B249:361–380, 1985.

[148] Michael Dine, Lisa Randall, and Scott D. Thomas. Baryogenesis from flat directions of the supersymmetric standard model. *Nucl. Phys.*, B458:291–326, 1996.

[149] Sam Bartrum, Mar Bastero-Gil, Arjun Berera, Rafael Cerezo, Rudnei O. Ramos, and Joao G. Rosa. The importance of being warm (during inflation). *Phys. Lett.*, B732:116–121, 2014.

[150] P. S. Bhupal Dev, Anupam Mazumdar, and Saleh Qutub. Constraining Non-thermal and Thermal properties of Dark Matter. *Front.in Phys.*, 2:26, 2014.